NTNU – Trondheim
Norwegian University of
Science and Technology

Advanced Temperature Model for HPHT Conditions

Knut Vegard Løbergsli

Petroleum Geoscience and Engineering
Submission date: June 2015
Supervisor: Sigbjørn Sangesland, IPT
Co-supervisor: Bjørn Astor Brechan, IPT

Norwegian University of Science and Technology
Department of Petroleum Engineering and Applied Geophysics

Summary

Temperature changes of wells are analyzed in this Thesis. Wells need to be designed for all planned operations in order to maintain well integrity for the well life. Well barriers need to be numerically assessed for worst-case scenarios to ensure well integrity. However, when moving into harsh environment with high pressure and high temperature, the conventional methods for estimating the temperature in the well may be conservative.

There are softwares on the market today that account for these harsh conditions but they are not open source and does not give insight into the calculation. To figure out the effects of the input data and to learn more about the computation of the temperature distribution, a model was build and programmed in a simulation software.

In production cases, heat transfer is calculated radially for small length increments upwards along the wellbore. Thereby assuming steady state in the wellbore and transient state in the formation. A temperature distribution profile is based upon the heat transfer and the geothermal gradient of the formation. The results from the model are compared with industry leading simulation softwares.

The results of the various simulation softwares were found to be different. Sensitivity analysis of the input variables was conducted. Conductivity in tubing and casing is high, resulting in that the conductivity can be neglected in the calculations. It also shows the variation between different approximations of the dimensionless formation temperature is large at short duration of production and quite like at longer duration of production.

The effect of duration of production, production rate and various geothermal gradients is investigated. It is clear that caution should be obtained when deciding the geothermal gradient. Accurate characterization of the reservoir fluid is important since it influence the kinetic energy term and J-T effect, which again influence the temperature distribution.

The impact of temperature on the thermal load is described. A high temperature at the wellhead gives a responding compression force, which can lead to higher risk of buckling.

Further improvements of the model are required. Pressure drops from friction and hydrostatic head as well as fluids phase behavior need to be added to make the model valid for multiphase flow.

Sammendrag

Temperaturendring i en brønn under ulike operative forhold er analyser i denne oppgaven. Brønner må være planlagt for alle operasjonene som skal utføres, for å sikre tilstrekkelig brønnintegritet gjennom levetiden. I brønner med høyt trykk og temperatur kan konvensjonelle metoder for temperaturberegning være for konservativ.

Det finnes programvarer på markedet, men som oftest vises ikke teorien som ligger til grunn for beregningene. For å sjekke ut eksisterende modeller som anvendes i industrien, er det utviklet en egen modell.

I produksjonsfasen blir varmeoverføring beregnet radielt. Det er antatt at varmeoverføringen er uavhengig av tid i brønnen og avhengig av tid i formasjonen. En temperaturfordelingsprofil blir beregnet basert på varmeoverføringskapasiteten til systemet og den geotermiske gradienten til formasjonen. Resultatet er sammenlignet med andre simuleringsprogram.

Resultatene fra de forskjellige simuleringsprogrammene er ulike. Det er derfor utført følsomhetsanalyser, for å se betydningen av de forskjellige inngangsverdiene. Varmeledningsevnen i produksjonsrøret og foringsrøret er høy, og resultatet viser at ledningsevnen kan neglisjeres i beregningen. Resultatene viser også at variasjonen mellom de forskjellige tilnærmelsene av den dimensjonsløse formasjons temperaturen i litteraturen er stor ved kort produksjonstid og relativt lik ved lengre produksjonstid.

Effekten av produksjonstid, produksjonsrate og forskjellige geotermiske gradienter er også undersøkt. Det kommer klart frem at man bør være nøyaktig i valg av geotermisk gradient. Nøyaktige reservoar data også helt nødvendig for å få en korrekt temperatur profil.

Det er også vist hvordan den termiske lasten påvirkes av temperatur profilen. En høy temperatur ved brønnhode gir en kompresjons kraft, som kan gi en høyere risiko for bukling.

Modellen trenger videre utvikling. Trykktap fra friksjon og hydrostatisk trykkforandring, samt faseoppførsel må inkluderes for å gjøre modellen gjeldene for flerfasestrømninger.

Acknowledgments

This Master Thesis has been prepared during the spring 2015 and is a result of the 30 credits (European Credit Transfer System) course "TPG4910 – Petroleum Engineering, Drilling Engineering, Master Thesis" at the Norwegian University of Science and Technology (NTNU), Department of Petroleum Engineering and Applied Geophysics. The main objective of the course has been to write a scientific paper on a topic within the students' specialization in Drilling Engineering. The course gives the student an opportunity to specialize with a specific topic, is chosen in cooperation between the student and supervisor.

Hence, I would thank my supervisor Sigbjørn Sangesland, NTNU, for providing me the opportunity to write this Master Thesis and also his support when needed. I would also like to thank my co-supervisor for Bjørn Astor Brechan, Statoil ASA, for the guidance, locating recourses and valuable support and motivation during the semester.

Additionally, I would like to thank Jesus De Andrade for valuable inputs and discussions during this Thesis. I also would like to thank my fellow students, Johan Holm Østvedt and Marie Tøien, for sharing knowledge, relevant discussions and for keeping the spirit high.

Finally, I would like to thank the rest of my fellow students, friends and family, especially my girlfriend Kamilla and daughter Natalie, for the support through the studies at NTNU. It has been quite a journey!

Regards,

Knut Vegard Løbergsli

June 2015

Table of Content

List of Figures

List of Tables

Chapter 1 Introduction

1.1 Background

The oil and gas industry is facing new challenges to fulfill the world´s increasing oil and gas demand, leading them into new and more difficult fields while also ensuring that the existing production is safe and feasible. With today's low oil price, high rig rates and the lack of standardization in planning and operations, the industry is struggling with cost reduction. The importance of cost reduction is reflected in development of new fields as well as during the production phase where intervention and possibly work-over is required.

Thus, going into rougher environment with high pressure and high temperature (HPHT) requires a more complex well design. This Master's Thesis focus on temperature variations in wells, and how heat is transferred into the annuli and the surrounding formation. Since, the packers, the tubing, the casings and the formation act as barriers for a lifetime in a well, it is essential to know the temperature at different stages and understand how it affects the equipment.

The well planning engineers are using simulation softwares during the design process. The problem, however, is that these simulation softwares are a closed source, like a black box, and give no insight into the calculations conducted. The design engineer may not be aware of all the calculations and assumptions made to provide the result, which means that the user spends a lot of time to review the results.

1.2 Motivation and Goal

The motivation is to create a modern and flexible program, so the design engineer could get an insight in how the calculations are carried out. The new software should be integrated with other softwares for better and easier workflow, more and faster experience transfer, and intelligent algorithm assisting planning and execution of operations. This would create a greater understanding among the engineers. Furthermore, this give the engineers more time to engineering work instead of quality controlling the results. It might also be a step further to standardize the planning process in the industry.

The goal of this Master's Thesis is to investigate the interactions between the surrounding temperature and the flowing temperature anywhere in the well. Further work would be to

complete the model to be applicablefor not just one-phase flow but also implement a two-phase flow accounting for pressure drop and phase behavior. The ultimate goal would be to fulfill a modern and flexible software, for well design purpose.

1.3 Literature Review

This Master's Thesis is based on written literature from the early 1960´s up until today. Ramey´s paper from 1962 was one of the first that enlighten and came up with an empirical expression for the transient heat transfer in the surrounding formation. Willhite (1967) followed up with a detailed description on how to calculate the overall heat transfer coefficient in the wellbore by taking account for the different heat transfer modes. Sagar, Doty, & Schmidt. (1991) took Ramey´s theory further by implementing two-phase flow and an empirical expression for the kinetic energy and the Joule-Thomson (J-T) coefficient. Hasan and Kabir have published a lot of work regarding heat transfer and temperature estimation in the wellbore in modern time.

Because the model developed in this Thesis is based on few references and empirical expressions and correlations, the author recommends the model to be calibrated with real log data from producing wells.

1.4 Studies and Work

This Thesis is an extension of the autumn project, focusing on production loads on tubing and other production equipment. In the work to establish the load cases, it was found that the stress from temperature is significant and therefor a precise prediction of the temperature in any point in the well is important. The work to establish this model has been the main focus in this Thesis.

Chapter 2 Well Integrity

NORSOK D-010 defines well integrity as: *"Application of technical, operational and organizational solutions to reduces risk of uncontrolled release of formation fluids throughout the life cycle of a well*" (NORSOK-D-010, 2004).

Following from the definition of well integrity, the personnel planning drilling and completion operations needs to identify solutions that meets the requirements to the standard. Thus, the planning personnel needs to design the well so the barriers can withstand any situation. This requires investigation into temperature and pressure profiles as well as load calculations.

2.1 Well Barriers

To keep the well safe in all operation, it needs well barriers. NORSOK D-010 defines well barriers as: *"Envelope of one or several well barrier elements preventing fluids from flowing unintentionally from the formation into the wellbore, into another formation or to the external environment"* (NORSOK-D-010, 2004). The main objective of a well barrier is to prevent any uncontrolled flow of hydrocarbons during, drilling, production or shut-in operations.

Figure 2-1 shows a well barrier schematic for a production well. Blue color indicates primary barrier and red color indicates secondary barrier. NORSOK D-010 distinguishes between primary and secondary barriers. The primary barrier is closest to the pressurized hydrocarbons, and is able to contain them. The secondary barrier is designed so that if the primary barrier fails, the secondary will prevent outflow of the well. (Torbergsen et al., 2012).

2.2 Well Barrier Element

A well barrier has one or more well barrier elements. NORSOK D-010 defines well barrier element as: *"A physical element which in itself does not prevent flow but in combination with other well barrier elements forms a well barrier"* (NORSOK-D-010, 2004).

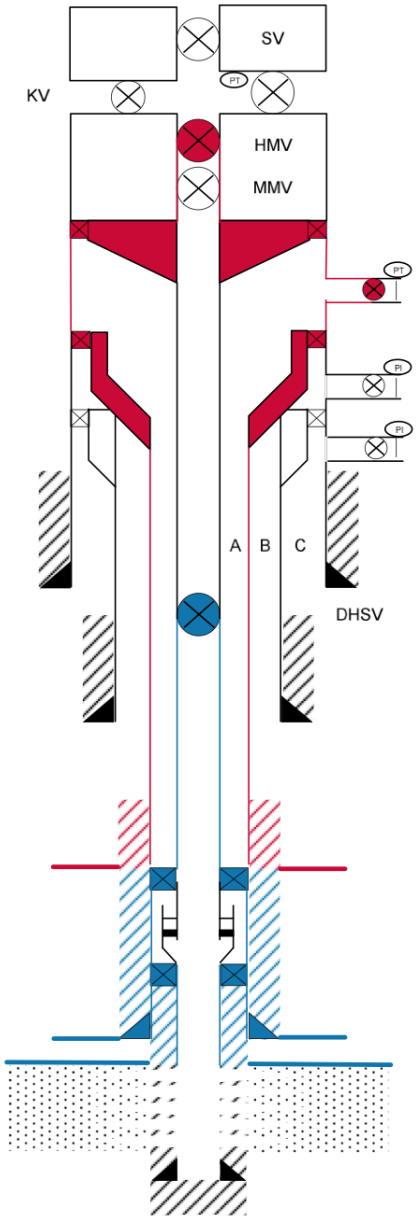

Figure 2-1 Primary and secondary barriers in production mode (Torbergsen et al., 2012)

Chapter 3 Thermal Effects

Applications such as HPHT field, deepwater developments and viscous crude have stressed the important role that temperature plays in safe and efficient well design. Tubing and casing stress analysis is fundamental for a well design. The requirements and the complexity increase when the industry is moving into deeper water, hotter reservoirs and more complex completions. According to Chapter 2, the well barriers must be designed to be intact in the whole lifetime of the well, to ensure well integrity. For design purpose, temperature and thermal effects need to be taken into consideration.

3.1 Temperature Effect on Material Properties

Several materials are used in the wellbore and elevated temperature can affect those materials. General background theory for stress, strain, yield point and ultimate stress can be found in appendix Appendix A.

3.1.1 Thermal Properties

Thermal conductivity of material usually decreases with temperature, and should be taken in account when considering thermal elongation and thermal stresses.

3.1.2 Sealing Elements and Elastomers

The effect of temperature on sealing elements and elastomers are one of the most aspects of concern in HP/HP fields (Berckenhoff & Wendt, 2005). Elastomers are affected by temperature. At low temperatures, the elastomers become hard and resistant to deformation. At high temperature, they become soft and mobile. (Aadnøy, 2009). Elastomers are easily deformed but are virtually incompressible. By squeezing elastomers in one direction it will create expansion in the other direction, with the elastomer volume remaining unchanged.

If thermoplastic seals are exposed to high temperature, they will soften and then melt. Thermosetting plastics will decompose at high temperature. Oilfield plastics are less resilient than elastomers, meaning that they will deform plastically. (Bellarby, 2009). Although, metal-to-metal (M-M) seals can be used, but they are rather expensive (Aadnøy, 2009). M-M seals are often required through operators governing documentation.

3.2 Temperature Effect on Fluid Properties

Temperature does also affect the properties of the different fluids in a well.

3.2.1 Reservoir Fluids

HPHT conditions affect the properties of the reservoir fluids. Typically, HPHT conditions increase the volatility of heavy compounds, which results in heavier compounds in gas condensate. Furthermore, volatility of water also increases with temperature. Water increases the viscosity and the heat capacity of the fluid. Therefore, water should also be taken into account when considering HPHT reservoir fluids. (Aadnøy, 2009).

3.2.2 Drilling Fluids

Drilling fluids are complex fluids that contain chemical additives. High temperature causes the fluid to expand, while high pressure causes fluid compression. These two situations have opposite effect to the equivalent circulation density (ECD) and also the bottom hole temperature. The rheology of the drilling fluid needs to be controlled, since it may lead to poor hole cleaning, barite sag and a non-uniform density profile in the annulus. (Skalle, 2013).

3.2.3 Cements

Accurate prediction of bottomhole circulating temperatures is important to ensure that the cement sets at the right time. High temperature increases the hydration of cement, which decreases the thickening time. Other factors such as rheology, fluid loss, stability and compressive strength are influenced by temperature (Skalle, 2013).

3.3 Temperature Effect on Loads

Original load cases are used in HPHT design. In addition, special cases concerning temperature effects are added to complete the full picture of resulting loads.

3.3.1 Thermal Elongation

Metal expands when it is heated, and contracts when it is cooled. The length change, ΔL_T, (specified positive for expansion) is given by equation (3.1),

$$\Delta L_T = C_T \Delta T L_T \tag{3.1}$$

Where

- ΔL_T = metal expansion or contraction (ft)
- C_T = coefficient of thermal expansion ($°F^{-1}$)
- ΔT = averange change in temperature from the base case to the load case (°F)
- L_T = length of the tubing or the uncemented section of casing (ft)

The coefficient of thermal expansion, C_T, is a material property and varies with different metallurgies and can itself be temperature dependent. C_T has a value around $5{,}5x10^{-6}$ to $6x10^{-6}$ $°F^{-1}$ Carbon steels and 13Cr, and around $6{,}5x10^{-6}$ to $6{,}9\ x10^{-6}$ $°F^{-1}$ for steel.

If the tubing is fixed in both ends, heating will cause compressive force and cooling a tensile force. The tubing is fixed in the tubing hanger and the production packer. The casing is fixed in the casing hanger and the cement. Equation (3.2) gives the change in axial force due to temperature change,

$$F_T = -C_T E \Delta T (A_o - A_i) \tag{3.2}$$

Where

- F_T = force in tubing or casing (lbf)
- E = Young's modulus (psi)
- A_o = outer area of tubing or casing (in^2)
- A_i = inner area of tubing or casing (in^2)

Equation (3.2) expressed as stress is given by equation (3.3),

$$\sigma_z = -C_T E \Delta T \tag{3.3}$$

Where

- σ_z = axial stress (psi)

The Young's modulus for steel is usually taken to be $3x10^7$ psi. Both E and C_T are functions of temperature, but a rule of thumb in field units is that their product is close to 200 psi/°F (Aadnøy, 2009). The axial stress is taken into consideration when calculating the triaxial stress, found in equation (A.4).

3.3.2 Wellhead Movement

Tubulars are terminated at the wellhead. As mentioned in chapter 3.3.1, temperature change can lead to change in tubular length. The tubulars are then forced to move such that their axial displacement at the wellhead (WH) is the same. This phenomenon is known as wellhead movement (WHM). WHM usually occurs during production. It is a response to the thermal forces from expansion of the tubulars, and to the forces in the annular space. The axial stiffness of the strings and the resistance where the WH is installed countering the response. (Aadnøy, 2009).

3.3.3 Annular Pressure Build-up

Annular pressure build-up (APB) is a result of the difference between the volume change of annular fluid and the volume change of tubing or casing that forms the annulus. To maintain mechanical equilibrium the annulus changes its volume in response to fluid pressure and temperature changes. (Aadnøy, 2009). Fixed platforms and jack-ups allow access to any annulus. Therefore, APB can be maintained by bleeding off the pressure build-up in annulus. However, in subsea wells, the A-annulus is often the only annulus where pressure build-up can be bled off. Thus, the B- and C-annulus can often not be bled off. (Landmark, 2013).

3.4 Software Calculation of Temperature Distribution

There are simulation softwares on the marked today that considers load case calculations for well design purpose. Two programs are picked as reference. Their temperature distribution during production is shown in the following sections.

3.4.1 Industry Leading Software for Conventional Design

The industry-leading software for conventional wellbore design is generally over conservative when temperature leads to major loads. It is assuming that the temperature distribution profile during production is the maximum undisturbed reservoir temperature at the perforation from the total depth (TD) to surface (Landmark, 2008).Therefore, the conventional design software is not used in HPHT well design. Figure 3-1 shows an example of a temperature distribution during production applied for load calculations, for the conventional wellbore design software.

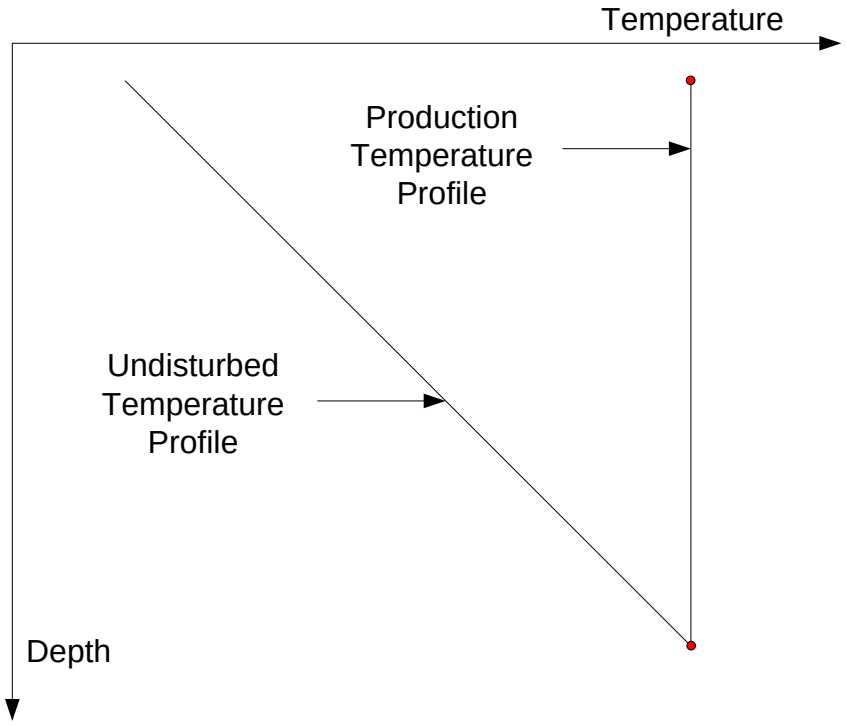

Figure 3-1 Temperature profile during production for the conventional design software

3.4.2 Industry Leading Software for HPHT Design

The industry-leading software for HPHT wellbore design takes account for transient and steady state conditions in the wellbore, by including the radial heat transfer in the annuli at all times (Landmark, 2013). During load calculation, the software accounts for initial conditions and final conditions of the operations. The temperature can change rapidly, during different operations, which may lead to a significant contribution to the loads. (Landmark, 2001) Figure 3-2 shows an example of a temperature distribution profile during production applied for load calculations, for the HPHT wellbore design software.

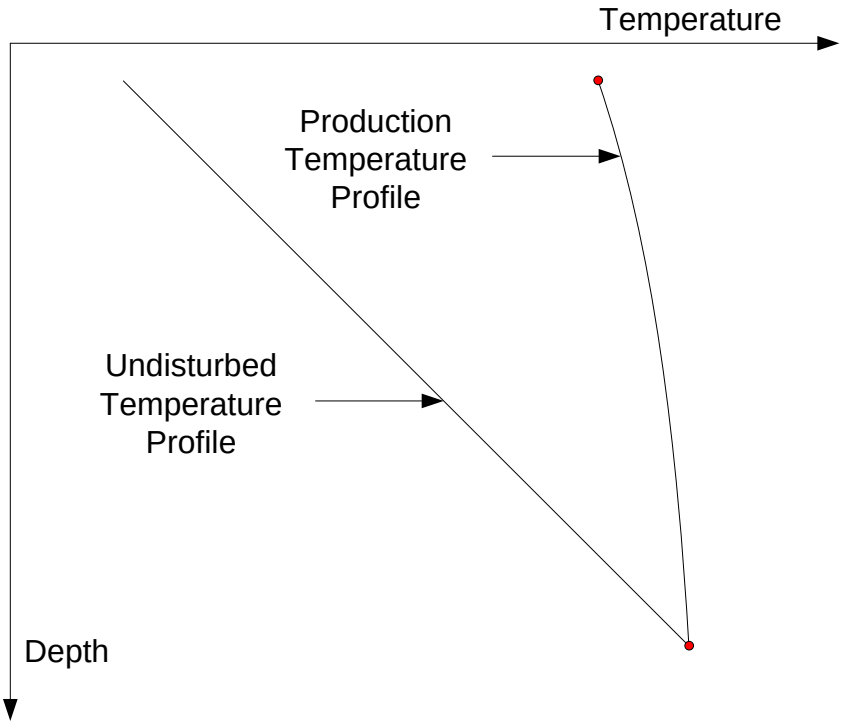

Figure 3-2 Temperature profile during production for the HPHT design software

Chapter 4 General Heat Transfer

4.1 Heat Transfer

"Heat transfer is thermal energy in transit due to spatial temperature difference" (Incropera, 2007) Heat transfer occur whenever there exist a temperature difference in a medium or between media. The driving mechanism of heat flow is the cooling of the thermal gradients within our universe (Incropera, 2007). Heat transfer describes the exchange of thermal energy between systems, depending on pressure and temperature. Like our blood stream continuously exchange heat with the air around us. "*An imaging system without heat flow would be isothermal and totally isolated from any other region, will be considered as dead*" (Lienhard, 2003, pp. 4-6).

4.2 Modes of Heat Transfer

Conduction, convection and radiation are fundamental modes of heat transfer in nature. They are independent mechanisms, despite that; the total heat transferred in a system is often a combination all three modes.

4.2.1 Conduction

Thermal conduction is the transfer of kinetic and potential energy, known as internal energy, by microscopic diffusion and collisions of particles within a body. In 1822, Joseph Fourier published his book (translated by Freeman in 1878), *Théorie Analytique de la Chaleurin,* were he formulated theory of heat conduction, today known as Fourier's law. The empirical law is stated as follows; "*the heat flux, resulting from thermal conduction is proportional to the magnitude of the temperature gradient and opposite to it in sign"* (Fourier, 1878).

$$Q_x^{''} = -k\frac{dT}{dx} \tag{4.1}$$

Where

- Q_x'' = heat flux in x-direction per unit area (Btu/hr ft^2)
- k = thermal conductivity (Btu/hr ft °F)
- dT/dx = temperature gradient (°F/ft)

The heat flux moves from higher temperatures to lower temperatures. Equation (4.1) shows that if temperature decreases with x, Q_x'' will be positive, the heat flux will flow in the x-direction. If the temperature increases with x, Q_x'' will be negative, the heat flux will flow the opposite of the x-direction. This is shown in Figure 4-1.

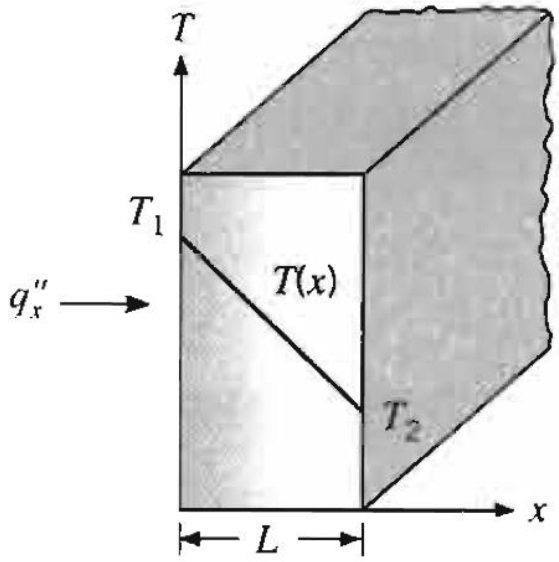

Figure 4-1 One dimensional heat transfer by conduction (Incropera, 2007, p. 4)

The thermal conductivity of the body in concern is required to use equation (4.1). The thermal conductivity is referred to a transport property, which provides an indication of transferred energy rate by the diffusion process.

Equation (4.1) provides a heat flux, which is the rate of heat transfer per unit area. The heat flow by conduction, Q_x, through a plane of area, A, is then the product of the area and the flux given in equation (4.2),

$$Q_x = Q_x'' A \tag{4.2}$$

Where

- Q_x = heat flow in x-direction (Btu/hr)
- A = area of wall (ft^2)

4.2.2 Convection

Convection comprises two mechanisms of heat flow. In addition to microscopic diffusion, macroscopic bulk motion of the fluid also transfers heat. If the heat transport is a combination of both microscopic diffusion and macroscopic bulk motion it is customary to use the term convection, and the term advection when referring to transport because of bulk fluid motion (Incropera, 2007). Natural convection occurs when convection is natural driven, which means that the fluid motion is only driven by buoyancy forces and not by any external source i.e. just by density difference with temperature variations in the fluid (Bai & Bai, 2005).

Figure 4-2 shows a typical convective cooling situation, where cool gas flows past a warm body. Heat is conducted from the boundary layer of the body, and mixes into the stream beyond the body. (Lienhard, 2003, p. 19).

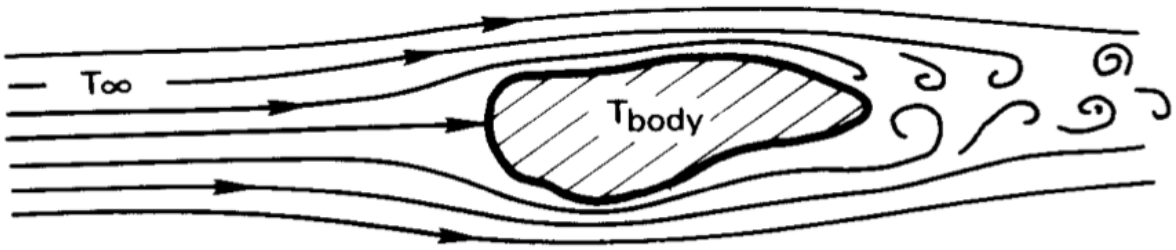

Figure 4-2 – The convective cooling of a heated body (Lienhard, 2003, p. 19)

In 1701, Isaac Newton formulated a theory of convection related to the cooling process named Newton's law of cooling,

$$Q_x^{''} = h(T_{body} - T_{\infty}) \tag{4.3}$$

Where

- h = average film coefficient or average heat transfer coefficient (Btu/ hr ft^2 °F)
- T_{body} = temperature of the body (°F)
- T_{∞} = temperature of the flowing fluid (°F)

The film coefficient depends on the temperature difference, the physical properties of the fluids, the physical situation where convection occurs and the geometry. This means that the film coefficient has a ”local” value at each point on the surface being considered. The local value of the coefficient is viewed as the problem of convection, as it has influence the boundary layers for the heat flux (Incropera, 2007, p. 355).

4.2.3 Radiation

Thermal radiation is heat transfer in form of waves. Therefore, radiation is the only way to transfer heat without presence of a material medium. The intensity of the heat flux depends on the temperature of the body and the nature of its surface. In fact, radiation transfer occurs most efficiently in a vacuum (Incropera, 2007). Thermal radiation often plays a significant role in heat transfer at high temperatures. A perfect emitter is called a *black-body*, since the body absorbs all the energy and reflects nothing (Burmeister, 1993). Thermal radiation of a *black-body* has an upper limit, prescribed by the Stefan-Boltzmann law,

$$E_b = A_s \sigma_{SB} {T_s}^{*4} \tag{4.4}$$

Where

- E_b = emissive power for a black-body (Btu/hr)
- σ_{SB} = Stefan-Boltzmann constant (0,1714 * 10^{-8} Btu/hr ft^2 °R^4)
- A_s = surface area of the body in concern – heat transfer surface (ft^2)
- ${T_s}^*$ = emitter absolute temperature (°R)

A nonblack-body emits less heat relative to a *black-body*. The efficiency of the surface is expressed with a multiplicative emissivity, ε, (Burmeister, 1993) which gives,

$$E = \varepsilon A_s \sigma {T_s}^{*4} \tag{4.5}$$

$$0 \leq \varepsilon \leq 1$$

Where

- E = emissive power (Btu/hr)
- ε = emissivity (dimensionless)

Radiation may also be "incident" on the surface from its surroundings. The radiation may originate from other surfaces to which the surface of interest is exposed, such as the sun or other close surfaces. Figure 4-4a shows, irrespective of the source, the rate of the incident radiation affecting the surface unit area is expressed as the irradiation, *G*, (Incropera, 2007). Absorbed irradiation is given by equation (4.6).

$$G_{abs} = aG \tag{4.6}$$

$$0 \leq a \leq 1$$

Where

- G_{abs} = absorbed irradiation (Btu/hr)
- a = absorptivity (dimensionless)
- G = irradiation (Btu/hr)

The absorptivity, *a*, is the surface radiant heat property, which in turn evaluates the rate at which radiant energy is absorbed per unit surface area.

Figure 4-3 shows an incident radiation for a non-black body. Determination of the transmitted, reflected and absorbed irradiation is often complex. For engineering purpose, the medium can be considered as opaque, which gives no transmission, and the remaining absorption and reflection may be treated as surface phenomena. Meaning, they are controlled by processes occurring within a fraction of a micrometer from the irradiated surface. It is therefore appropriate to speak of irradiation being absorbed and reflected by the surface, depending on the wavelength and the surface material. (Incropera, 2007)

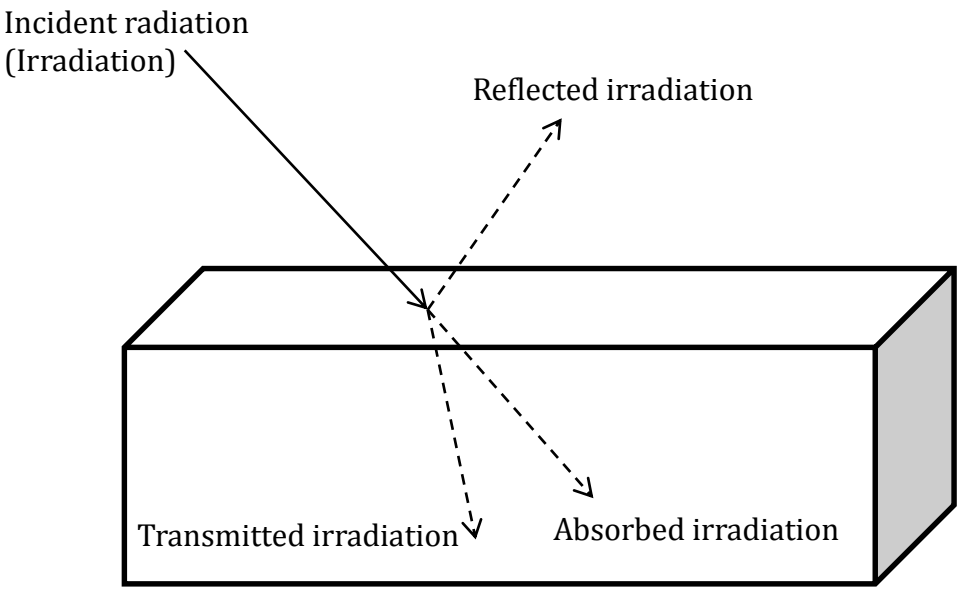

Figure 4-3 Irradiation

If the rate of radiation absorption is greater than the rate of radiation emission, the surface is said to be gaining energy by radiation. Otherwise, the surface is said to be losing energy by radiation.

Figure 4-4b shows a special case that occurs frequently, where a small surface at T_s is completely enclosed by much larger surface at absolute temperature of T_{sur}, separated by a gas that does not intervene with the radiation. For such conditions, where the system is assumed to be one, Kirchhoff's law of radiation gives,

$$\varepsilon = a \tag{4.7}$$

$$Q'' = \varepsilon\sigma({T_s}^{*4} - {T_{sur}}^{*4}) \tag{4.8}$$

Equation (4.8) provides the difference between the thermal energy that is released because of radiation emission and which is gained, because of radiation absorption. Expressed as heat exchange,

$$Q = h_r A({T_s}^{*4} - {T_{sur}}^{*4}) \tag{4.9}$$

Where

- h_r = heat transfer coefficient for radiation (Btu/hr ft^2 °F)

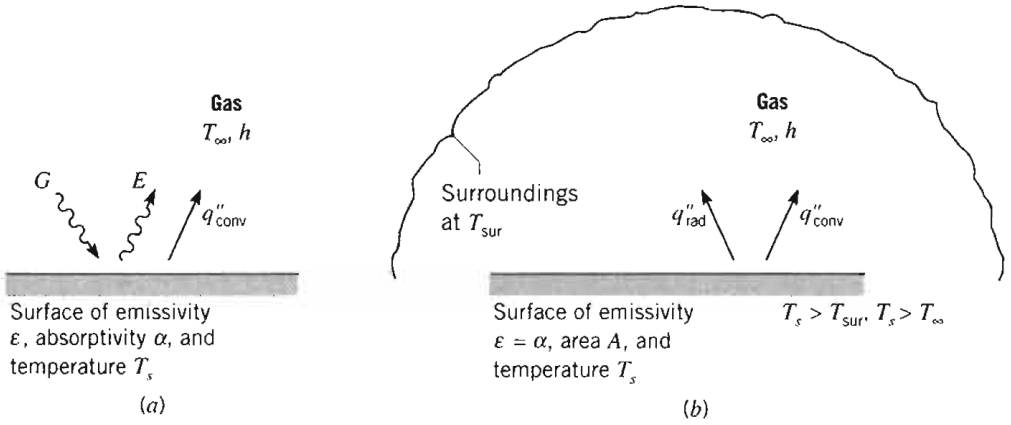

Figure 4-4 Radiation exchange: (a) at a surface and (b) between a surface and large surroundings (Incropera, 2007, p. 9)

4.2.4 Summation

The three mechanisms of heat transfer mentioned do not exist simultaneously in a medium, but they can act as a combination in a system. For example, heat transfer occurs only by conduction in opaque solids and by conduction and radiation in semitransparent solids. Thus, a solid may involve conduction and radiation, but not convection. However, a solid that is exposed to a fluid or other surfaces may involve heat transfer by convection and radiation on its surface.

Convection can also be viewed as combination of conduction and fluid motion, and conduction in a fluid can be viewed as a special case of convection in the absence of any fluid motion (Incropera, 2007).

Table 4-1Typical values of thermal properties of formation and wellbore material

Formation/Material	Thermal Conductivity, *k* (Btu/hr ft °F)	Specific Heat, *Cp* (Btu/lbm °F)
Formation	1,3-3,33	0,2-0,625
Cement	0,38-0,5	0,4771
Formation oil	0,08-0,1	0,4-0,5
Formation gas	0,1-0,3	0,25
Water	0,36	0,997
Steel	30	0,09542
Packer fluid	0,35	0,9

Chapter 5 Wellbore Heat Transfer

5.1 Heat Transfer Mechanisms in the Wellbore

Initially, the wellbore fluid is considered to have a geothermal temperature distribution. During production, fluid enters the wellbore with a temperature equal to the initial formation temperature. This means that the temperature in the well soon becoming significantly higher than the surroundings, because the formation temperature reduces with decreasing depth. By assuming steady state and turbulence fluid flow, which ensures a constant fluid temperature at a given depth. This leads to heat loss in radial direction from the fluid to the formation. The temperature distribution of the tubing fluid is dependent on the heat transfer properties of each well component in the well completion and the formation.

Figure 5-1 describes a typical temperature profile in an annular completion. The three modes of heat transfer mechanisms mentioned in Chapter 4.2, radiation, natural convection and conduction represents the overall heat flow. The main heat transfer mechanism from the producing fluid and the inside tubing is forced convection. The main mechanism through the casing and tubing itself is conduction. In a closed annulus filled with fluid the main mechanism is convection. If the temperature is large enough, radiation could also be a mayor mechanism in the annuli.

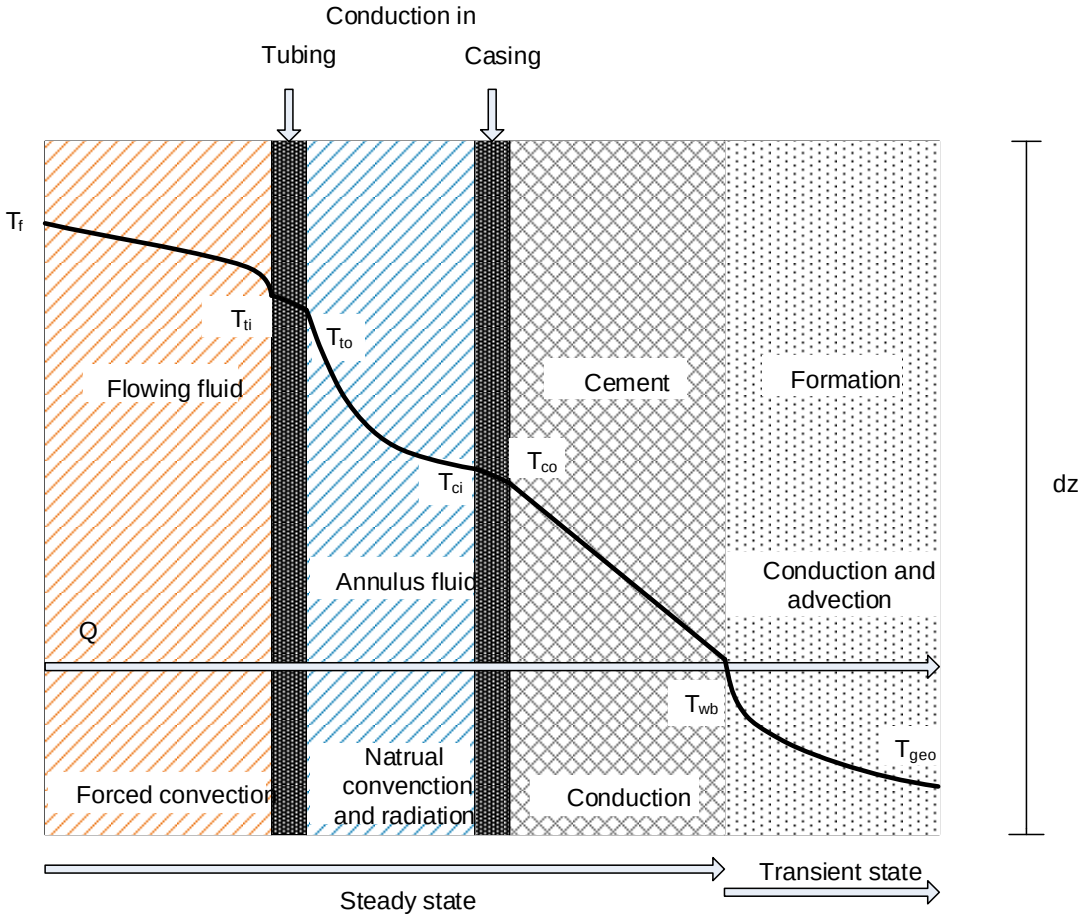

Figure 5-1 Temperature profile in an annular completion

5.1.1 Radial Heat Transfer Mechanisms in the Wellbore

The steady-state rate of heat flow through a wellbore, Q, is proportional to the temperature difference between the fluid and formation, and the cross-sectional area perpendicular to the direction of heat flow. The overall heat transfer coefficient, U_{to}, accounts for the net resistance to the heat flow in the flowing fluid(s), the tubing, the casing(s), the fluid filled annulus and the cement (Willhite, 1967).

An equation for the heat flow during production is developed, by first identifying a body of concern that is convenient to work with and a characteristic temperature difference. During production, the natural reference area is the outside surface area of the tubing, and the temperature difference between the flowing fluid and the temperature at cement-formation interface. Then the overall heat transfer coefficient is defined by an expression analogous to Newton´s law of cooling,

$$Q = 2\pi r_{to} U_{to} (T_f - T_{wb}) \Delta z \tag{5.1}$$

Where

- Q = heat flow rate (Btu/hr)
- r_{to} = outside radius of tubing (ft)
- U_{to} = overall heat transfer coefficient based on the outside tubing surface and the temperature difference between fluid and cement-formation interface (Btu/hr ft^2 °F)
- T_f = temperature of flowing fluid (°F)
- T_{wb} = temperature at cement-formation interface (°F)
- Δz = increment of tubing length (ft)

The following equations describe the heat transfer for each well element.

Heat transfer between the flowing fluid and the inside tubing wall is given by forced convection in equation (5.2)

$$Q = 2\pi r_{ti} h_f (T_f - T_{ti}) \Delta z \tag{5.2}$$

Where

- r_{ti} = tubing inside radius (ft)
- h_f = forced-convection heat transfer coefficient for the tubing fluid (Btu/hr ft^2 °F)
- T_{ti} = temperature of inside tubing surface (°F)

Heat flow through the tubing wall, casing wall and the cement sheath occurs by conduction. By rearranging Fourier's law to apply to a radial system, including the thermal conductivity of the mediums and the term $Q = Q'' * A$ gives,

$$Q_i = -2\pi r_i k_i \frac{dT}{dr} \Delta z \tag{5.3}$$

Where

- Q_i = heat flow rate (Btu/hr)
- r_i = radius (ft)

- k_i = thermal conductivity (Btu/hr ft °F)
- dT/dr = temperature gradient (°F/ft)

By integrating equation (5.3) with constant a Q gives the conduction through the tubing, the casing and the cement as follows.

Tubing,

$$Q = \frac{2\pi k_{tub}(T_{ti} - T_{to})\Delta z}{ln\frac{r_{to}}{r_{ti}}} \tag{5.4}$$

Where

- k_{tub} = thermal conductivity of the tubing material at average tubing temperature (Btu/hr ft °F)
- T_{to} = temperature of outside tubing surface (°F)

Casing,

$$Q = \frac{2\pi k_{csg}(T_{ci} - T_{co})\Delta z}{ln\frac{r_{co}}{r_{ci}}} \tag{5.5}$$

Where

- k_{csg} = thermal conductivity of the casing material at average tubing temperature (Btu/hr ft °F)
- T_{ci} = temperature of inside casing surface (°F)
- T_{co} = temperature of outside casing surface (°F)
- r_{ci} = casing inside radius (ft)
- r_{co} = casing inside radius (ft)

Cement,

$$Q = \frac{2\pi k_{cem}(T_{co} - T_{wb})\Delta z}{ln\frac{r_{wb}}{r_{co}}} \quad (5.6)$$

Where

- k_{cem} = thermal conductivity of the casing material at average tubing temperature (Btu/hr ft °F)
- r_{wb} = wellbore radius (ft)

Figure 5-1 shows that the annulus, between the tubing and casing, is filled with fluid. The annulus fluid can either be gas or liquid. Typical gases are air, N_2, CO_2 that contains hydrocarbons. Typical liquids are water, seawater, completion fluid and drilling mud. The tubing wall is hot, leading to less dens fluid at the tubing surface compared to the fluid in the center of the annulus. Similarly, the fluid at the casing surface is colder than the fluid in the center of the annulus. Fluid motion caused by density variation with temperature is called natural convection as mentioned in Chapter 4.2.2. When a body is heated, radiant energy is emitted at a rate, dependent on the temperature of the body itself. Which means that in HPHT radiation could have an influence on the heat flow. The amount of radiant energy transported between the tubing and casing depends on the emitting and absorbing characteristics of their surfaces and the view the surfaces have on each other. (Willhite, 1967).

Since the total heat flow through the annulus is the sum of conduction, convection and radiation. It is convenient to define the heat transfer rate in terms of the heat transfer coefficients for convection and natural convection, h_c, and for radiation, h_r (Willhite, 1967). The body of concern that these coefficients are based on are chosen to be the tubing outside surface area, and the temperature difference between the outside tubing surface and the inside casing surface. Thus,

$$Q = 2\pi r_{to}(h_c + h_r)(T_{to} - T_{ci})\Delta z \quad (5.7)$$

Where

- h_c = heat transfer coefficient for natural convection and conduction (Btu/hr ft^2 °F)
- h_r = heat transfer coefficient for radiation (Btu/hr ft^2 °F)

5.1.2 Establishing the Overall Heat Transfer Coefficient

From Figure 5-1 it is seen that the resistance is given in series

$$(T_f - T_{wb}) = (T_f - T_{ti}) + (T_{ti} - T_{to}) + (T_{to} - T_{ci}) + (T_{ci} - T_{co}) + (T_{co} - T_{wb}) \tag{5.8}$$

The value of heat flow, Q, does not change in the well completion, because it is assumed to be steady state at any time. Solving for the respective temperature difference in equation (5.8) for equation (5.2) and equation (5.4) through equation (5.7), gives equation (5.9).

$$(T_f - T_{wb}) = \frac{Q}{2\pi\Delta z}\left[\frac{1}{r_{ti}h_f} + \frac{ln\frac{r_{to}}{r_{ti}}}{k_{tub}} + \frac{1}{r_{to}(h_c + h_r)} + \frac{ln\frac{r_{co}}{r_{ci}}}{k_{csg}} + \frac{ln\frac{r_{wb}}{r_{co}}}{k_{cem}}\right] \tag{5.9}$$

An expression for U_{to} based on the outside tubing surface area is derived by setting the heat flow equation (5.1) into equation (5.9) and solve for U_{to},

$$U_{to} = \left[\frac{r_{to}}{r_{ti}h_f} + \frac{r_{to}ln\frac{r_{to}}{r_{ti}}}{k_{tub}} + \frac{1}{(h_c + h_r)} + \frac{r_{to}ln\frac{r_{co}}{r_{ci}}}{k_{csg}} + \frac{r_{to}ln\frac{r_{wb}}{r_{co}}}{k_{cem}}\right]^{-1} \tag{5.10}$$

In the literature simplifications are made when estimating the overall heat transfer coefficient. Willhite (1967) and Hasan and Kabir (1994) assume that the heat transfer coefficient for the tubing fluid is high, which gives the assumption $T_f = T_{ti}$. Further they assume the high value of conductivity of metals with relatively thin tubing and casing walls gives negligible temperature drop across the tubing and the casing, i.e. $T_{ti} = T_{to}$ and $T_{ci} = T_{co}$. Depending on the temperature profile of the wellbore they may also assume zero radiation in the annulus filled with liquid or gas. (Willhite, 1967) and (A. R. Hasan & Kabir, 1994).

5.1.3 Radiation in the Annulus

Using equation (4.5) for a nonblack-body and correlating the equation for a radial system for the annulus between the tubing and casing,

$$Q_r = 2\pi r_{to}\sigma F_{tci}(T_{to}^{*4} - T_{ci}^{*4})\Delta z \tag{5.11}$$

Where

- Q_r = heat flow in the annulus due to radiation (Btu/hr)
- F_{tci} = view factor based on outside tubing and inside casing surface (dimensionless)
- T_{to}^* = temperature of outside tubing surface (°R)
- T_{ci}^* = temperature of inside casing surface (°R)

The view factor, F_{tci}, depends on the emittances of the bodies involved, as well as the geometry for both the emitter and the absorber. In this case, radiation is emitted from the external surface area of the tubing, which is absorbed at the internal casing surface area. Equation (5.12) correlates for the geometry of the wellbore and account for the emitting property of the tubing and the casing. The emitting property of both the tubing and the casing depends on the emissivity of their surfaces. (Willhite, 1967).

$$\frac{1}{F_{tci}} = \frac{1}{\overline{F_{tci}}} + \left(\frac{1}{\varepsilon_{to}} - 1\right) + \frac{A_{to}}{A_{ci}}\left(\frac{1}{\varepsilon_{ci}} - 1\right) \tag{5.12}$$

Where

- $\overline{F_{tci}}$ = overall interchange factor between the outside tubing and inside casing surfaces (dimensionless)
- ε_{to} = emissivity of outside tubing surface (dimensionless)
- ε_{ci} = emissivity of inside casing surface (dimensionless)

$\overline{F_{tci}}$ is usually set to be 1,0 for wellbore heat transfer (Willhite, 1967), and equation (5.12) reduces to

$$\frac{1}{F_{tci}} = \frac{1}{\varepsilon_{to}} + \frac{r_{to}}{r_{ci}}\left(\frac{1}{\varepsilon_{ci}} - 1\right) \tag{5.13}$$

Defining h_r by factoring equation (5.11) and using the expressions shown in equation (5.15) and (5.16)

$$Q_r = 2\pi r_{to}\sigma F_{tci}\left(T_{to}^{*2} + T_{ci}^{*2}\right)\left(T_{to}^* + T_{ci}^*\right)\left(T_{to}^* - T_{ci}^*\right)\Delta L \tag{5.14}$$

$$Q_r = 2\pi r_{to} h_r\left(T_{to}^* - T_{ci}^*\right)\Delta L \tag{5.15}$$

$$= 2\pi r_{to} h_r (T_{to} - T_{ci})\Delta L \tag{5.16}$$

Gives,

$$h_r = \sigma F_{tci}\left(T_{to}^{*2} + T_{ci}^{*2}\right)(T_{to}^{*} + T_{ci}^{*}) \tag{5.17}$$

The expression for F_{tci} in equation (5.13) is set into equation (5.17). Finally,

$$h_r = \frac{\sigma\left(T_{to}^{*2} + T_{ci}^{*2}\right)(T_{to}^{*} + T_{ci}^{*})}{\frac{1}{\varepsilon_{to}} + \frac{r_{to}}{r_{ci}}\left(\frac{1}{\varepsilon_{ci}} - 1\right)} \tag{5.18}$$

5.1.4 Natural Convection in the Annulus

Unfortunately, no work on natural convection in vertical annular geometry is reported in the literature (A. R. Hasan & Kabir, 1994). Although, natural convection between two vertical plates has been studied. By neglecting the effect of curvature, results of vertical plates studies can be used to correct the boundary conditions to the heat transfer coefficient for natural convection, h_c.

Heat transfer by conduction and natural convection between the outside tubing surface and the inside casing surface is given by equation (5.19)

$$Q_c = \frac{2\pi k_{hc}(T_{to} - T_{ci})\Delta z}{ln\frac{r_{ci}}{r_{to}}} \tag{5.19}$$

Where

- Q_c = heat flow in the annulus by natural convection and conduction (Btu/hr)
- k_{hc} = equivalent thermal conductivity of the annular fluid with natural convection effects (Btu/hr ft °F)

When natural convection is small,

$$k_{hc} = k_{ha} \tag{5.20}$$

Where

- k_{ha} = thermal conductivity for fluid in annulus (Btu/hr ft °F)

Since,

$$Q_c = 2\pi r_{to} h_c (T_{to} - T_{ci}) \tag{5.21}$$

Equate equation (5.19) and equation (5.21), gives an expression for h_c,

$$h_c = \frac{k_{hc}}{r_{to} ln \frac{r_{ci}}{r_{to}}} \tag{5.22}$$

Dropkin and Somerscales (1965) measured the thermal conductivity of fluids with natural convection effects, k_{hc} between two vertical plates. They suggested a correction factor for the heat transfer coefficient based on a function of the Grashof number, Gr, and the Prandtl number, Pr. Equation (5.23) is the Dropkin and Somerscales correlation factor for h_c, expressed for the geometry, (Dropkin & Somerscales, 1965),

$$\frac{k_{hc}}{k_{ha}} = Nu = C(GrPr)^{1/3} Pr^{0,074} \tag{5.23}$$

$$for\ \theta = 90°\ and\ 5 * 10^4 < GrPr < 7{,}17 * 10^8$$

$$C = 0{,}049$$

Where

- Nu = Nusselt number (dimensionless)
- Gr = Grashof number (dimensionless)
- Pr = Prandtl number (dimensionless)

For different angels of inclinations with respective correlation constants, see Table B-1.

The Grashof number is given by equation (5.24),

$$Gr = \frac{(r_{ci} - r_{to})^3 g_{hr} \rho_{an} \beta (T_{to} - T_{ci})}{\mu_{an}^2} \tag{5.24}$$

Where

- g_{hr} = acceleration due to gravity (4,17 x 10^8 ft/hr^2)
- ρ_{an} = density of the fluid present in the annulus at T_{an} and pressure P_{an} (lb/ft^2)
- β = thermal volumetric expansion coefficient of the fluid in annulus (1/°R)
- μ_{an} = viscosity of the fluid present in the annulus at T_{an} and pressure P_{an} (lbm/ft hr)

$$\beta = \frac{1}{T_{an}^*} \tag{5.25}$$

Where

- T_{an}^* =absolute temperature of annulus fluid (°R)

And,

$$T_{an} = \frac{T_{to} + T_{ci}}{2} \tag{5.26}$$

Where

- The temperatures in equation (5.26) are given in °F.

The Prandl number is given by equation (5.27),

$$Pr = \frac{c_{an} \mu_{an}}{k_{ha}} \tag{5.27}$$

Where

- c_{an} = heat capacity of the fluid present in the annulus at the average annulus temperature (Btu/lbm °F)

Finally, an expression for the correlated heat transfer coefficient for natural convection, h_c, is,

$$h_c = \frac{0{,}049(GrPr)^{1/3}Pr^{0{,}074}k_{ha}}{r_{to}ln\frac{r_{ci}}{r_{to}}} \tag{5.28}$$

The Grashof number reflects the extended motion of the annulus fluid caused by natural convection i.e. the ratio of buoyancy force to viscous force. The Prandtl number is a measure of the interaction between the hydrodynamic and the thermal boundary layers, i.e. the ratio of momentum and thermal diffusivities.

Chapter 6 Temperature Model Establishment

This chapter explains the physics and the equations behind a temperature model made in MATLAB. The purpose of the model is to compute the temperature distribution profile from the reservoir to the WH.

6.1 Mathematical Model

The wellbore schematic for the heat transfer and temperature computation in this Thesis is shown in Figure 6-1. All the different cases are presented with the correspondingly different surroundings. The letters A and B denotes the different annuluses.

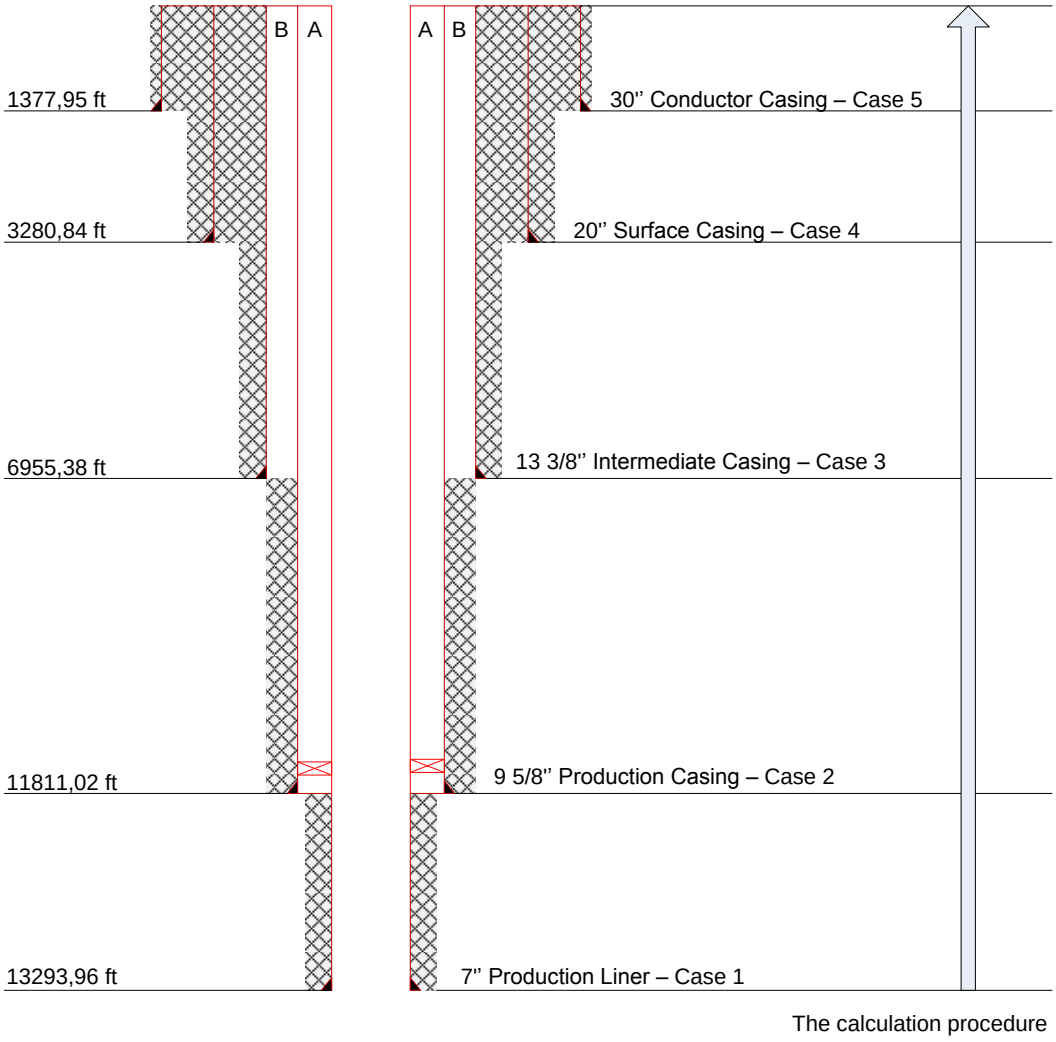

Figure 6-1 Wellbore schematic

Figure 6-2 explains the sign convection for the development of the programing model, during production. Measured Depth, MD, is the length from a reference point at surface, typical the Rotary Kelly Brushing (RKB), to the bottom. True Vertical Depth (TVD) is the vertical depth from the same reference point. The differential elements, *dz*, start- and end points are expressed by $z_{(i-1)}$ and z_i, respectively. They starting from bottom and goes along the wellpath towards surface. The inclination, θ_i, of the well seen from the horizontal, and the geothermal gradient, g_{Ti}, follows the same procedure. Note that the subsribt, *i*, denotes the current point in the wellbore, and subsribt, *i -1*, denotes the previous point.

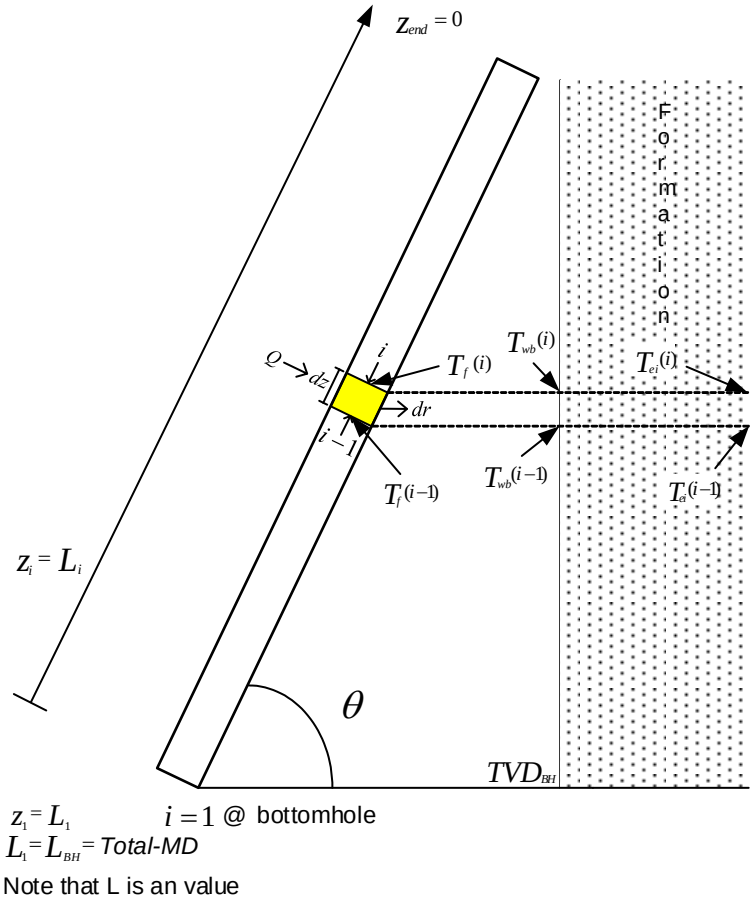

Figure 6-2 Sign convection during production

6.1.1 Assumptions

To calculate the temperature distribution some assumptions has been made. The assumptions are listed below.

- One-dimensional steady state flow – pressure and temperature are equal to each other within the cross section area of the tubing.
- Pressure drop and phase behavior to the production fluid is excluded.
- Production fluid assumed to be seawater.
- Steady state heat transfer in radial direction in the wellbore. Transient in formation.
- Forced convection inside tubing is neglected, gives $T_f = T_{ti}$.
- Conduction in vertical direction is neglected.
- Assuming homogeneous rock properties in every differential element *dz.*
- Rheology of annulus fluid is not investigated.
- Pressure and phase behavior of annulus fluid is excluded.
- Annulus is sealed with production packer.

6.1.2 Formation Temperature Distribution

The heat transfer from the wellbore to the surroundings is a three-dimensional problem, but because of symmetry in the wellbore and the surroundings it can be simplified to a two-dimensional problem for mathematical purpose. In addition, when considering very short sections in the vertical direction, vertical heat diffusion can be ignored because of relatively small vertical temperature gradients. (A. R. Hasan & Kabir, 1991).

Considering a short time interval, the heat flux density from the wellbore can be assumed as constant (A. R. Hasan & Kabir, 1991). An energy balance on the formation then leads to a partial-differential equation, derived in cylindrical coordinates, for the variation of formation temperature, with radial distance from the well and time of production.

6.1.2.1 Diffusivity Equation

$$\frac{\partial^2 T_e}{\partial r^2} + \frac{1}{r}\frac{\partial T_e}{\partial r} = \frac{c_e \rho_e}{k_e}\frac{\partial T_e}{\partial t} \tag{6.1}$$

Where

- T_e = formation temperature at any given depth (°F)
- r = radius, measured from the center of the wellbore (ft)
- c_e = heat capacity of formation (Btu/lbm °F)
- ρ_e = density of formation (lbm/ft^3)
- k_e = thermal conductivty of formation (Btu/hr ft °F)

6.1.2.2 Boundary Conditions

The thermal diffusivity equation is analogous to the equation used in pressure diffusion while solving pressure-transient problems (A. R. Hasan & Kabir, 1991). Initially, formation temperature equals the undisturbed formation temperature,

$$\lim_{t \to 0} T_e = T_{ei} \tag{6.2}$$

Where

- T_{ei} = undisturbed formation temperature (°F)

At the outer boundary the formation temperature does not change with radial distance, i.e.

$$\lim_{r \to \infty} \frac{\partial T_e}{\partial r} = 0 \tag{6.3}$$

From Fourier's law in chapter 4.2.1, the interface of the wellbore and formation is given as heat flow per unit mass of wellbore fluid, per unit length of the well, *dq/dz*.

$$\frac{dq}{dz} = -\frac{2\pi k_e}{W} \frac{r \partial T_e}{\partial r}\Big|_{r=r_{wb}} \tag{6.4}$$

Where

- W = total mass flow rate (lbm/hr)

6.1.2.3 Dimensionless Temperature

Rearranging equation (6.1) by applying dimensionless variables. This gives a more applicable solution.

$$r_D = \frac{r}{r_{wb}} \tag{6.5}$$

$$\alpha = \frac{k_e}{\rho_e c_e} \tag{6.6}$$

$$t_D = \frac{\alpha t}{r_{wb}^2} \tag{6.7}$$

Where

- r_D = radial distance (dimensionless)
- α = thermal diffusivity of formation (ft^2/hr)
- t_D = time (dimensionless)

$$\frac{\partial^2 T_e}{\partial r_D^2} + \frac{1}{r_D}\frac{\partial T_e}{\partial r_D} = \frac{\partial T_e}{\partial t_D} \tag{6.8}$$

And the boundary conditions from equation (6.3) and (6.4) changes to,

$$\lim_{r_D \to \infty} \frac{\partial T_e}{\partial r_D} = 0 \tag{6.9}$$

And,

$$\left.\frac{\partial T_e}{\partial r_e}\right|_{r_D=1} = -\frac{W(dq/dz)}{2\pi k_e} \tag{6.10}$$

Where

- q = heat flow from wellbore (Btu/lbm)

The best solution of equation (6.8) is carried out using Laplace transform (A. R. Hasan & Kabir, 1991), resulting in,

$$T(r_D, t_D) = T_{ei} + \frac{W(dq/dz)}{\pi^2 k_e} I' \tag{6.11}$$

Where

$$I' = \int_0^\infty \frac{1 - e^{-u^2 t_D}}{u^2} \frac{Y_1(u)J_0(ur_D) - J_1(u)Y_0(ur_D)}{J_1^2(u) + Y_1^2(u)} du \tag{6.12}$$

Where

- Y_0 = Zero-order modified Bessel function of the first kind.
- J_0 = Zero-order Bessel function of the first kind
- Y_1 = First-order modified Bessel function of the first kind
- J_1 = First-order Bessel function of the first kind

When $r_D = 1$, the temperature at the wellbore and formation interface is,

$$T_{wb} = T_{ei} + \frac{W(dq/dz)}{\pi^2 k_e} I \tag{6.13}$$

Where

$$I' = \int_0^\infty \frac{1 - e^{-u^2 t_D}}{u^2} \frac{Y_1(u)J_0(u) - J_1(u)Y_0(u)}{J_1^2(u) + Y_1^2(u)} du \tag{6.14}$$

Defining a dimensionless temperature, T_D, analogous to the dimensionless pressure used in pressure transient analysis as,

$$T_D = -\frac{2\pi k_e}{W(dq/dz)} (T_{wb} - T_{ei}) \tag{6.15}$$

Where

- T_D = temperature (dimensionless)

Thus,

$$T_D = -\frac{2I}{\pi} \tag{6.16}$$

At start of production, when the temperature difference is large, the heat flux from the wellbore to the formation would be high. After some time the heat flux will decrease due to increased resistance in the well completion. Equation (6.15) is valid only for constant heat flow from the wellbore. If the time is portioned into a series of sufficiently small time intervals, in each of which heat flow is assumed to remain constant, the superposition principle can be used to arrive the interface temperature between the wellbore and formation.

$$T(wb, t_n) = T_{ei} + \frac{1}{\pi^2 k_e} \sum_{i=1}^{n} [W(dq/dz)]_i \Delta I \tag{6.17}$$

Where

- $W(dq/dz)_I$ = heat flow the wellbore per unit time per unit length a ith time step, and,

$$\Delta I = \int_0^\infty \frac{1 - e^{-u^2 \Delta t_D}}{u^2} \frac{Y_1(u)J_0(u) - J_1(u)Y_0(u)}{J_1^2(u) + Y_1^2(u)} du \tag{6.18}$$

When the time intervals are equal to each other, equation (6.17) can be rewritten as,

$$T_D = -2\pi k_e \frac{(T_{wb} - T_{ei})}{\sum [W(dq/dz)]_j}$$

$$= -\frac{2\Delta I}{\pi} \tag{6.19}$$

Where

- ΔI is given by equation (6.18), and is the same as equation (6.14), but with dimensionless time step, Δt_D, instead of dimensionless time, t_D.

Equation (6.13) allows the wellbore temperature to be calculated from the undisturbed formation temperature if the heat flow rate from the wellbore fluid is known.

6.1.2.4 Approximate Dimensionless Temperature

Equation (6.13) and (6.14) are time consuming to solve for T_D, since it requires to solve the integral from zero to infinity and the integrand includes the Bessel functions. However, since equation (6.14) and (6.18) are just dependent upon the dimensionless production time, t_D, it is worth taking a closer look at the relationship between t_D and T_D. Some authors have made an approximation based on statistics,

1. Ramey's equation (Ramey, 1962),

$$T_D = ln\frac{2\sqrt{\alpha t}}{r_{wb}} - 0{,}29, \qquad t \geq 7\ days \tag{6.20}$$

2. Hasan and Kabir's equations (A. R. Hasan & Kabir, 1991),

$$T_D = 1{,}1281\sqrt{t_D}\left(1 - 0{,}3\sqrt{t_D}\right), \qquad 10^{-10} \leq t_D \leq 1{,}5 \tag{6.21}$$

$$T_D = (0{,}4063 + 0{,}5lnt_D\ )\left(1 + \frac{0{,}6}{t_D}\right), \qquad t_D > 1{,}5 \tag{6.22}$$

Equation (6.21) and (6.22) is used in the further calculation process. A comparison of the two approximations made by Ramey and Hasan and Kabir is shown in section 7.1.3.5.

An equation for T_{wb} is derived with respect form the approximated solution of T_D from equation (5.1) and (6.15). First by rearing equation (5.1) to yield for heat flow, Q, for each differential element, dz,

$$\frac{dQ}{dz} = -2\pi r_{to} U_{to}(T_f - T_{wb}) \tag{6.23}$$

By rearranging the units in equation (6.15) ,

$$\frac{dQ}{dz} = W\frac{dq}{dz} \tag{6.24}$$

Equalizing equation (6.15) and (6.23) and solving for T_{wb} gives,

$$-\frac{2\pi k_e}{T_D}(T_{wb} - T_{ei}) = -2\pi r_{to} U_{to}(T_f - T_{wb}) \tag{6.25}$$

$$T_{wb} = \frac{T_D T_f + \frac{k_e}{r_{to} U_{to}} T_{ei}}{T_D + \frac{k_e}{r_{to} U_{to}}} \tag{6.26}$$

6.1.3 Initial Formation Temperature

The undisturbed formation temperature, T_{ei}, is generally assumed as a linear function of depth.

$$T_{ei} = T_{eibh} - g_T(L_1 - z)sin\theta_i \tag{6.27}$$

$$T_{ei} = T_{eiwh} + g_T z sin\theta \tag{6.28}$$

Where

- T_{eibh} = undisturbed formation temperature at bottomhole (°F)
- T_{eiwh} = undisturbed formation temperature at wellhead (°F)
- g_T = geothermal gradient,(°F/ft)
- z = variable well depth, form surface – MD (ft)
- L_1 = Total length of wellbore – TMD (ft)
- θ = inclination angel from horizontal (degrees)

If the geothermal gradient varies with the formation depth due to different geologic zones, the undisturbed formation temperature can be suited to change for each differential length element *dz*.

$$T_{ei,i} = T_{ei,(i-1)} - (z_{(i-1)} - z_i) g_{T,(i-1)} sin\theta_{(i-1)} \tag{6.29}$$

6.1.4 Heat Transfer in the Wellbore

As mentioned in 0 the heat transfer can be considered as steady state in radial direction, if the length of the well is divided into small differential length element *dz*.

6.1.4.1 Wellbore Fluid Energy Balance

The model is derived from the total-energy-balance equation. By assuming steady-state conditions, and no work done by or to the flowing fluid the equation (Sagar, Doty, & Schmidt, 1991), gives the reduced total-energy equation as,

$$\frac{dH}{dz} = \frac{dq}{dz} - \frac{v}{Jg_c}\frac{dv}{dz} - \frac{g\sin\theta}{g_c J} \tag{6.30}$$

Where

- H = fluid enthalpy (Btu/lbm)
- v = specific volume (ft^3/lbm)
- J = mechanical equivalent of heat (778 ft-lbf/Btu)
- g_c = conversion factor (32,2 lbm ft /lbf sec^2)
- g = acceleration of gravity (32,2 ft/sec^2)

Basic thermodynamic principles give the specific enthalpy as,

$$\frac{dH}{dz} = \left(\frac{\partial H}{\partial T_f}\right)_p \frac{dT_f}{dz} + \left(\frac{\partial H}{\partial p}\right)_{T_f} \frac{dp}{dz} \tag{6.31}$$

Where

$$\left(\frac{\partial H}{\partial T_f}\right)_p = c_{pm} \tag{6.32}$$

$$\left(\frac{\partial H}{\partial p}\right)_{T_f} = -C_J c_{pm} \tag{6.33}$$

Where

- c_{pm} = heat capacity of wellbore fluid (Btu/lbm °F)
- C_J = Joule-Thopmson (J-T) coefficient

Gives,

$$\frac{dH}{dz} = c_{pm}\frac{dT_f}{dz} - C_J c_{pm}\frac{dp}{dz} \tag{6.34}$$

The radial heat transfer between the fluid and cement-formation interface can be expressed in terms of an overall heat transfer coefficient as equation (5.1), leading to the following expression for heat transfer rate, *dq/dz*, (A. R. Hasan & Kabir, 1994),

$$\frac{dq}{dz} = -\frac{2\pi r_{to} U_{to}}{W}(T_f - T_{wb}) \tag{6.35}$$

The radial heat transfer from the cement-formation interface to the formation can be described with the definition of T_D,

$$\frac{dq}{dz} = -\frac{2\pi k_e}{W T_D}(T_{wb} - T_{ei}) \tag{6.36}$$

Eliminating T_{wb} by combining equation (6.35) and (6.36),

$$\frac{dq}{dz} = -\frac{2\pi}{W}\left(\frac{r_{to} U_{to} k_e}{k_e + T_D r_{to} U_{to}}\right)(T_f - T_{ei}) \tag{6.37}$$

6.1.4.2 Overall Heat Transfer Coefficient

The overall heat transfer coefficient is established in chapter 5.1.2 and is given by equation (5.10). Equation (5.10) accounts for conduction, natural convection and radiation in the establishment of the overall heat transfer coefficient.

6.1.4.3 Temperature of Wellbore Fluid

An equation for the fluid temperature, dT_f / dz, is derived by rearranging equation (6.30) with the expression from equation (6.34) and (6.36). Thus,

$$\frac{dT_f}{dL} = \frac{T_{ei} - T_f}{A} - \frac{g\sin\theta}{g_c J c_{pm}} + C_J\frac{dp}{dL} - \frac{v dv}{g_c J c_{pm}} \tag{6.38}$$

Where

$$A = \frac{c_{pm}W}{2\pi}\left(\frac{k_e + T_D r_{to} U_{to}}{r_{to} U_{to} k_e}\right) \tag{6.39}$$

Assuming that the sum of the two last terms in equation (6.38) does not vary with depth (A. R. Hasan & Kabir, 1994).

$$\frac{dT_f}{dL} = \frac{T_{ei} - T_f}{A} - \frac{g sin\theta}{g_c J c_{pm}} + \phi \tag{6.40}$$

Where the variable ϕ denotes the kinetic-energy term and the J-T coefficient term,

$$\phi = \frac{dp}{dL} - \frac{v dv}{g_c J c_{pm}} \tag{6.41}$$

Sagar et al. (1991) proposed an empirical expression for ϕ.

$$\phi = -0{,}002978 + 1{,}006 * 10^{-10} p_{wh} + 1{,}906 * 10^{-4} W^* - 1{,}047 * 10^{-6} F_{gL} + 3{,}229 * 10^{-5} API + 0{,}004009 \gamma_g - 0{,}3551 g_T \tag{6.42}$$

$$\phi = 0{,}0, when\ W^* \geq 5\ lbm/sec$$

Where:

- p_{wh} = wellhead pressure (psig)
- W^* = total mass flow rate (lbm/sec)
- F_{gL} = gas/liquid ratio
- API = oil gravity (°API)
- γ_g = gas specific gravity (air=1)

Finally, an expression for the wellbore fluid is solved by the first order differential equation (6.40) by assuming all variables except T_f , to be constant in the well depth, *z*, for the particular section,

$$T_{f,i} = T_{ei,i} + A\left(1 - e^{\frac{z_{(i-1)} - z_i}{A}}\right)\left(-\frac{g sin\theta_i}{g_c J c_{pm}} + \phi + g_{T,i} sin\theta_i\right) + e^{\frac{z_{(i-1)} - z_i}{A}}\left(T_{f,(i-1)} - T_{ei,(i-1)}\right) \quad (6.43)$$

For a producing well, the first step *(i=1)*, has the following values for *z*, T_f and T_{ei},

$$z_1 = z_{bh} \quad (6.44)$$

$$T_{f_1} = T_{f_{bh}} \quad (6.45)$$

$$T_{ei_1} = T_{ei_{bh}} \quad (6.46)$$

6.2 The Calculation Procedure

To calculate the fluid temperature inside the tubing, T_f , from equation (6.43) it is necessary to calculate the overall heat transfer coefficient, U_{to}, from equation (5.10). The overall heat transfer coefficient is depending on the natural convection, h_c, and the radiation, h_r, from the annulus fluid, calculated from equation (5.22) and (5.18), respectively. The calculation of the natural convection and the radiation requires an evaluation of the temperature difference ($T_{to} - T_{ci}$), which in turn requires knowledge of T_{wb} from equation (6.26), T_f and $U_{to.}$ Hence, an iterative solution is required for each differential element of the well. The iterative solution assumes a value of T_f and U_{to} to calculate T_{wb} and T_{ci}, which again is used to calculate h_c and h_r. Then a new value of U_{to} is calculated and evaluated again the assumed value. This is done until convergence is obtained. Then a new value of T_f is calculated.. Figure 6-3 shows a flowdiagram on how the iterative process is done.

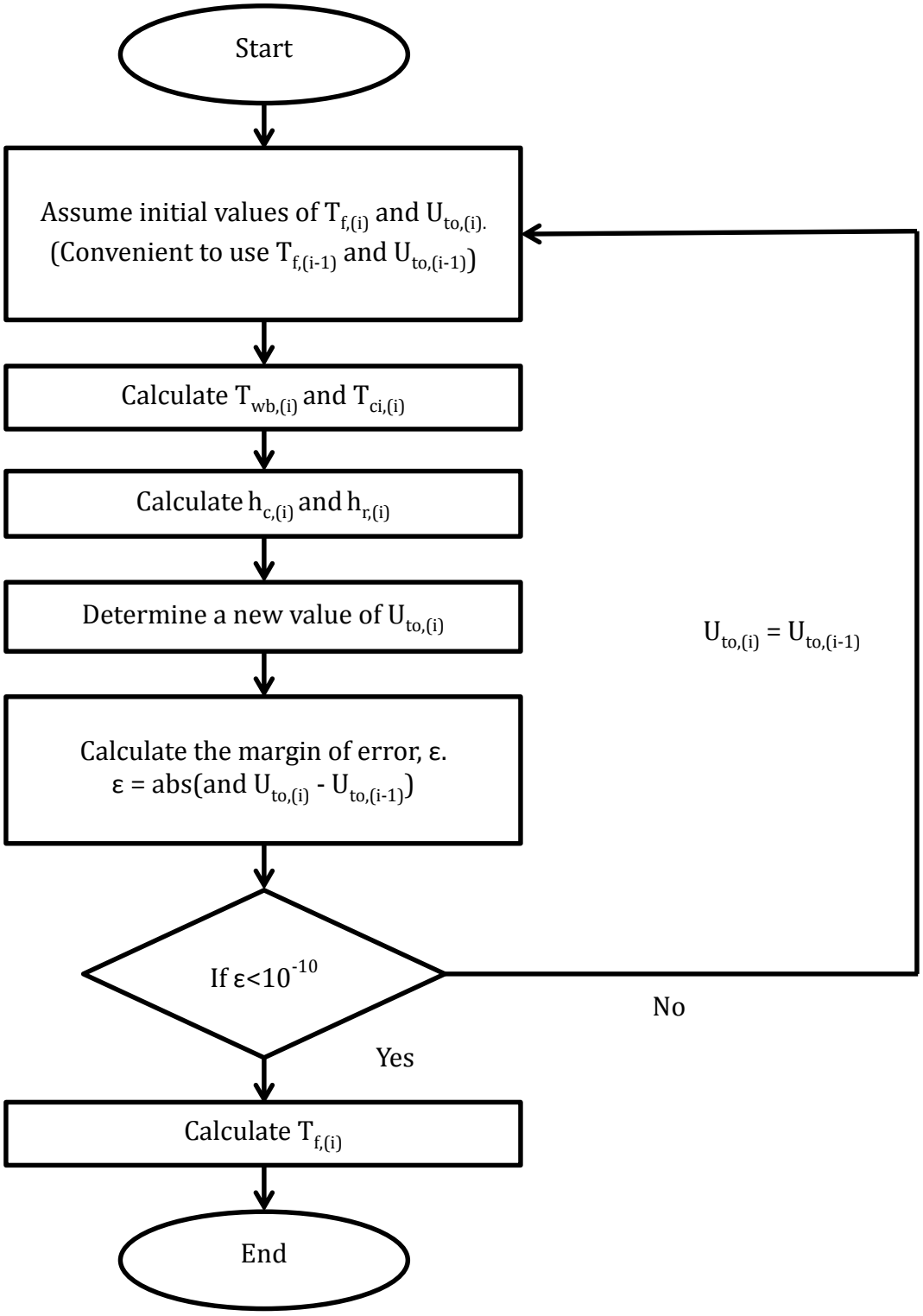

Figure 6-3 Flowdiagram

Chapter 7 Results

Results of the temperature model are shown in the following Chapter. Temperature effects are widely known in the industry. However, the results of the introduced model is compared with the result from ILS, due to the uncertainties in the calculation process in the ILS. Results of thermal loads affected by different temperature predictions are also presented.

7.1 Temperature Model Result

The temperature model is programmed in MATLAB. This chapter presents the most important results graphically.

7.1.1 Variables and Assumptions

The wellbore schematic shown in Figure 6-1 represents a graphical overview of the well trajectory and the well design presented in Table 7-1 and Table 7-2, respectively. The well design is based on pore pressure gradients, fracture pressure gradients and design criteria stated in the governing documentation from an operator.

Table 7-1 Well trajectory

Sections # 	Start MD (ft) 	End MD (ft) 	Inclination deg 	Inclination from horizontal deg
1	1072,83	1377,95	0	0
2	1377,95	3280,84	0	0
3	3280,84	6955,38	0	0
4	6955,38	11811,02	0	0
5	11811,02	13293,96	0	0

Table 7-2 Well design

	Name	Type	OD	ID	MD (ft)			Hole size	Grade	Weight
#			(in)	(in)	Hanger	TOC	Base	(in)	#	(ppf)
1	Conductor	Casing	30,000	28,000	1073	1073	1378	36,00	X-52	309,7
2	Surface	Casing	20,000	18,730	1073	1073	3281	26,00	X-56	133
3	Intermediate	Casing	13,375	12,347	1073	1073	6955	17,50	P-110	72
4	Production	Casing	9,625	8,535	1073	6955	11811	12,25	P-110	53,5
5	Production	Liner	7,000	6,004	11811	11811	13294	8,50	P-110	35
6	Production	Tubing	7,000	6,094	1073		11811		P-110	30

The input data needed to calculate the temperature distribution in the wellbore is presented in Table 7-3. Values found in ILS are thermal conductivity of steel (tubing and casing), thermal conductivity of cement, thermal conductivity of the formation and the densities of wellbore and annulus fluid. The geothermal gradient and the mudline temperature gives the reservoir temperature by equation (6.28). The author has selected the mass rate and production time, according to reservoir data and the flow capacity of the 7 inches production tubing. The thermal diffusivity of earth (formation) and the heat capacity, thermal conductivity, density and viscosity of the fluids are not found in the ILS. Thus, leads to uncertainties in the input variables. The fluid variables are depending on the composition of the fluid, the pressure and the temperature. The variations of the properties are not included in the temperature distribution model as listed in chapter 6.1.1.

Table 7-3 Input variables for temperature distribution calculation

Input variables		
Description	Value	Unit
Tubing		
Thermal conductivity, *k*	26,2	Btu/hr ft °F
Emissivity outside tubing, *e*	0,9	Dim.less
Casing		
Thermal conductivity, *k*	26,2	Btu/hr ft °F
Emissivity inside casing, *e*	0,9	Dim.less
Emissivity outside casing, *e*	0,9	Dim.less
Cement		
Thermal conductivity, *k*	0,568	Btu/hr ft °F
Formation		
Thermal conductivity, *k*	0,92	Btu/hr ft °F
Thermal diffusivity, α	0,04	ft^2/hr
Mudline temperature	39,2	°F
Geothermal gradient	1,44	°F/100ft
Annulus		
Density, ρ	64,37	lbm/ft3

Plastic viscosity, μ	2,63	lbm/ft hr
Thermal conductivity, *k*	0,35	Btu/hr ft °F
Heat capacity, *Cp*	0,95	Btu/lbm °F
Reservoir and Production data		
Reservoir temperature	215,35	°F
Heat capacity wellbore fluid	0,95	Btu/lbm °F
Production time	2000	hr
Total mass flow rate	131,54	lbm/sec

7.1.2 Results of the Temperature Model Simulation

Figure 7-1 shows the temperature distribution, in blue, and the overall heat transfer coefficient, in red, through the wellbore for the given well design in Table 7-2 and the input variables in Table 7-3. The interface between each case, highlighted in Figure 6-1, gives a large change in the overall heat transfer coefficient. In case 2 and 3, where the annulus is filled with completion fluid and only one cement layer presented outside. The trend in case 2 and 3 shows that the overall heat transfer coefficient is increasing towards the surface.

Seeing the result of the overall heat transfer coefficient, from Figure 7-1, as a result of the whole system, the coefficient decrease towards the surface.

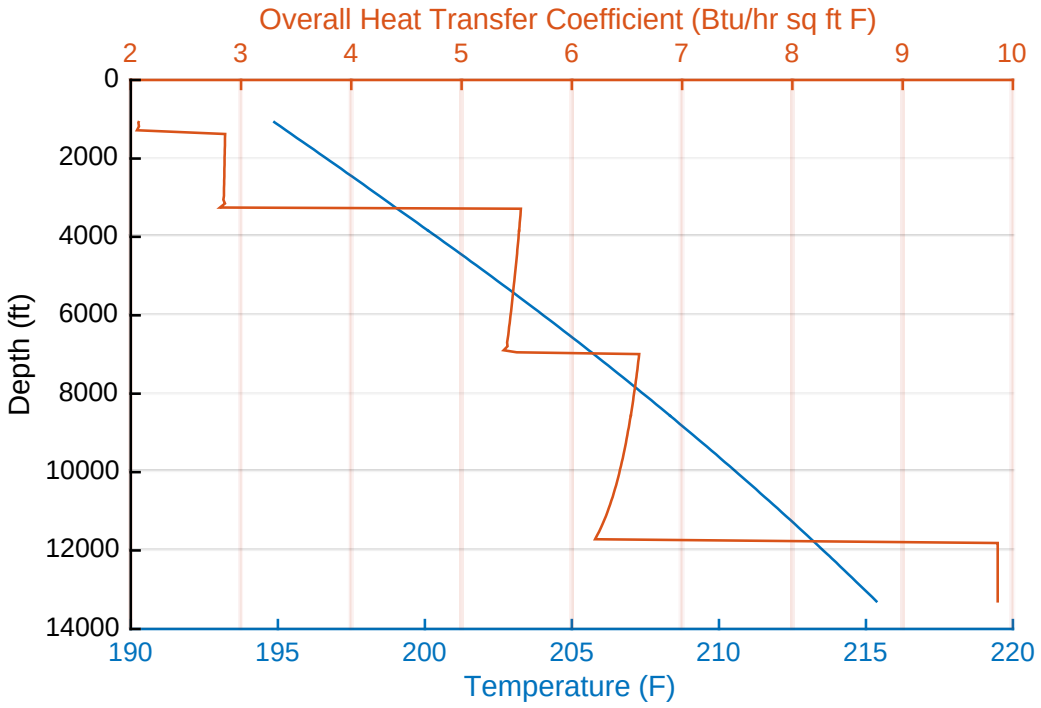

Figure 7-1 Temperature and Overall Heat Transfer Coefficient

The computed temperature distribution of the undisturbed formation temperature and the simulated temperature of wellbore fluid, of both the temperature model and ILS is presented in Figure 7-2. Where the red line is the undisturbed formation temperature, the blue line is the temperature profile from the temperature model and the yellow line is temperature profile from the ILS software. The difference between the temperature model and ILS is 14 degrees Fahrenheit.

This gives the temperature model an error of 6,7% in relation to the ILS. Unfortunately, no real data from a water-producing well has been available for comparison. However, Harald Rostad, daily user of the ILS, stated that the ILS accounts for heat tansfer about 1,64 ft into the formation (Rostad, 2015).

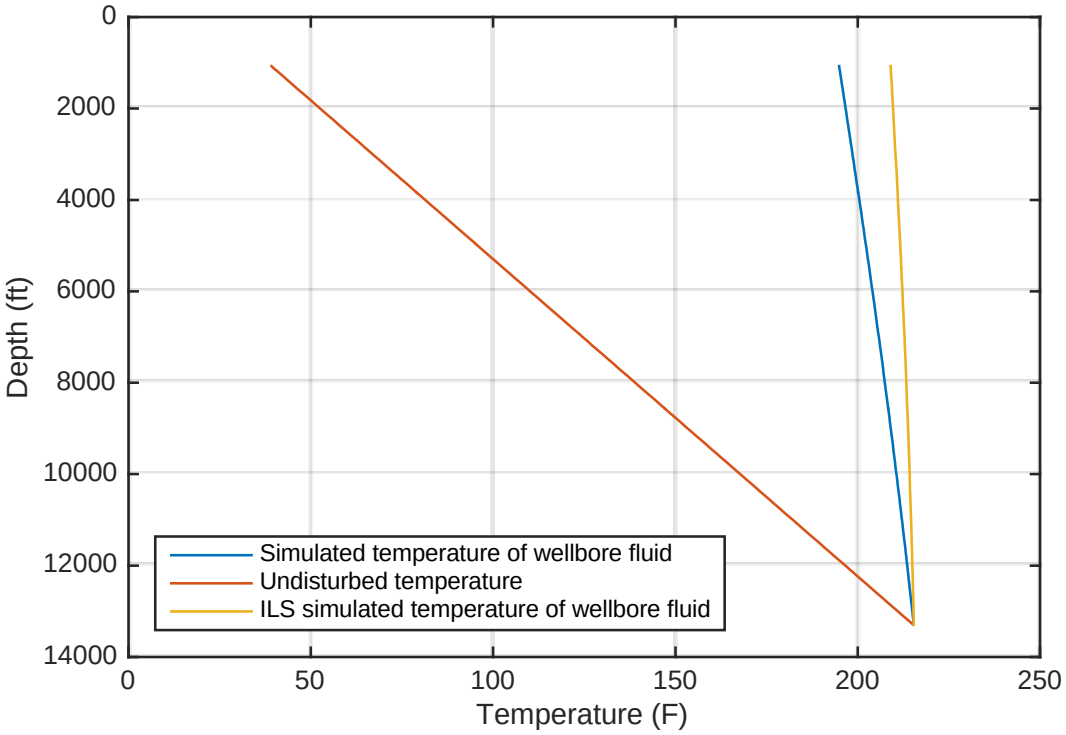

Figure 7-2 Temperature distribution

7.1.3 Sensitivity Analysis of the Unknown Input Data for ILS

The ILS does not give a full insight of all the input variables used in the computation of the temperature distribution. Sensitivity analysis has been conducted on the unknown variables.

7.1.3.1 Emissivity of the Inside of the Tubing

Figure 7-3 and Figure 7-4 shows that the change of emissivity inside the tubing hardly affects the temperature distribution profile. The emissivity inside the tubing is only taken into consideration when calculating the heat transfer coefficient for radiation. This may also mean that radiation is less significant when calculating the overall heat transfer coefficient.

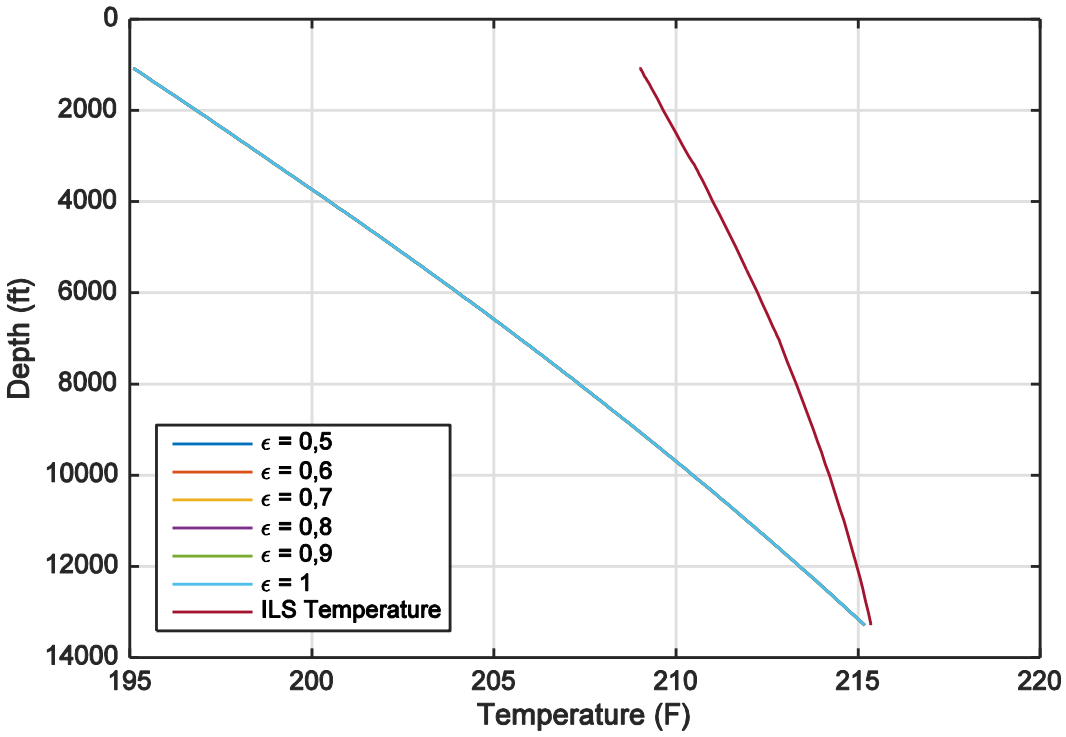

Figure 7-3 Temperature distribution with various emissivity's

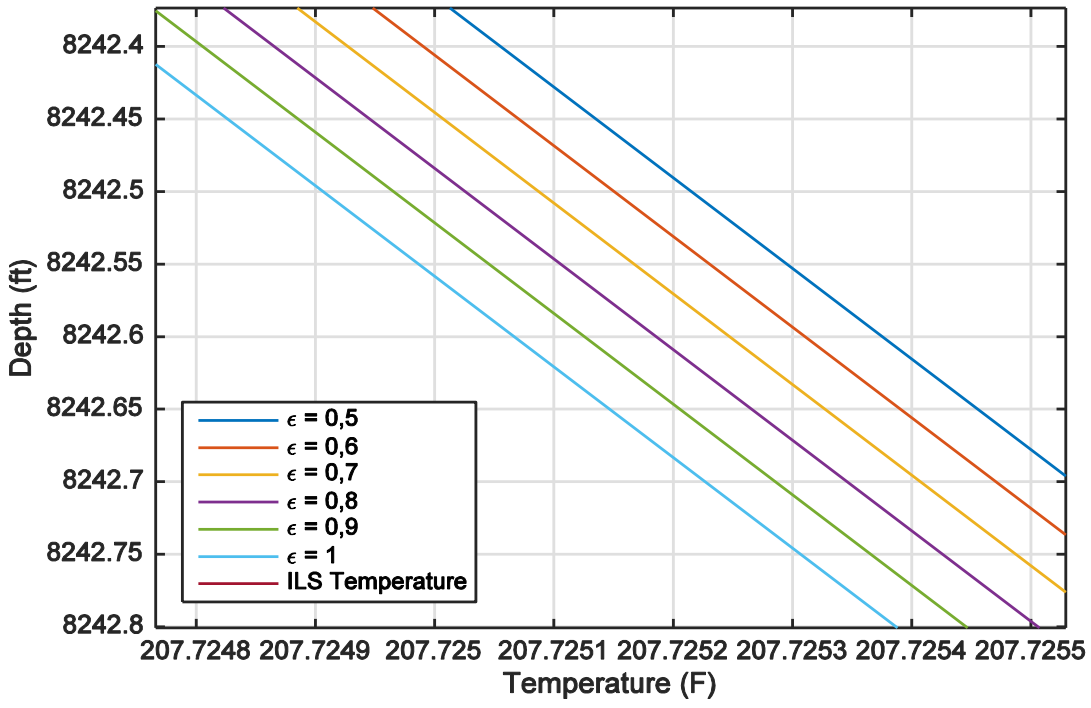

Figure 7-4 Zoomed temperature distribution with various emissivity's

7.1.3.2 Thermal Diffusivity of Formation

The thermal diffusivity of the formation can vary from the seafloor to the reservoir. It is applied in the calculation process of the dimensionless time, equation (6.7), which is applied when calculating the dimensionless temperature either by Ramey's method or Hasan and Kabir's method.

According to Figure 7-5 it is clear that the thermal diffusivity of the formation has a very low impact on the temperature of the wellbore fluid at high temperatures and some influence at lower temperatures. However, the influence is not enough to explain the difference between the temperature model and ILS.

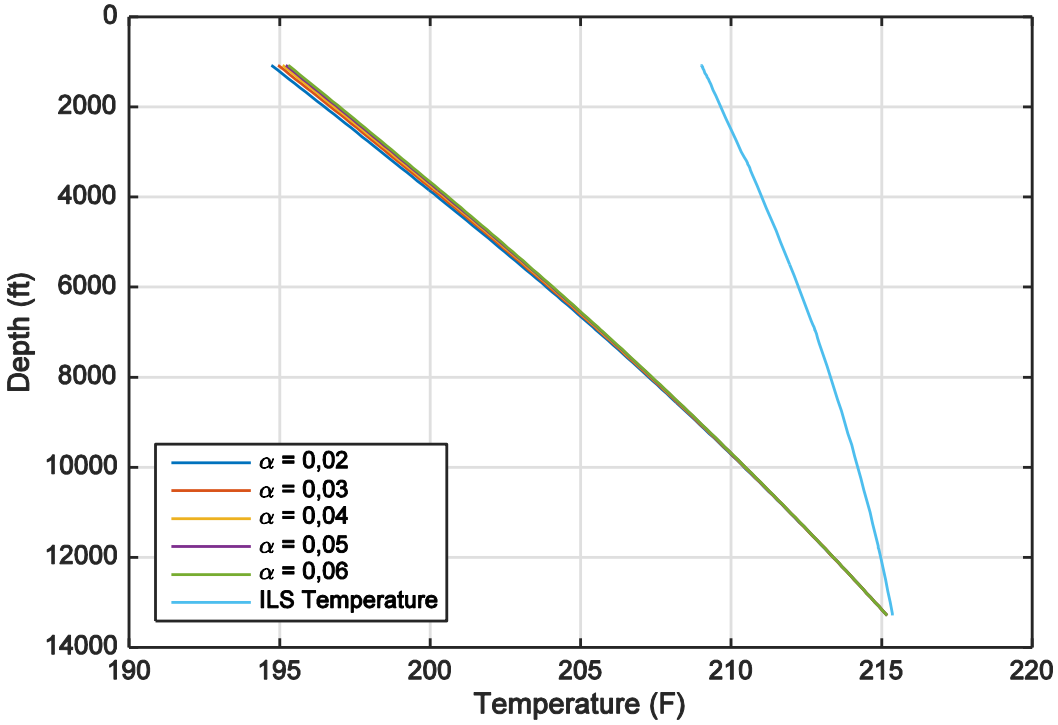

Figure 7-5 Temperature distribution with various thermal diffusivities of the formation

7.1.3.3 Heat capacity of Wellbore and Annulus Fluid

The well is completed with seawater in the annulus and for simplicity the well is set to produce seawater. This is done on purpose to exclude uncertainties in the comparison between the temperature model and ILS. Since the heat capacity of water changes with pressure and temperature, a simulation for various heat capacities was carried out. Figure 7-6 indicates that

the various heat capacities for seawater does not change the temperature distribution profile significantly.

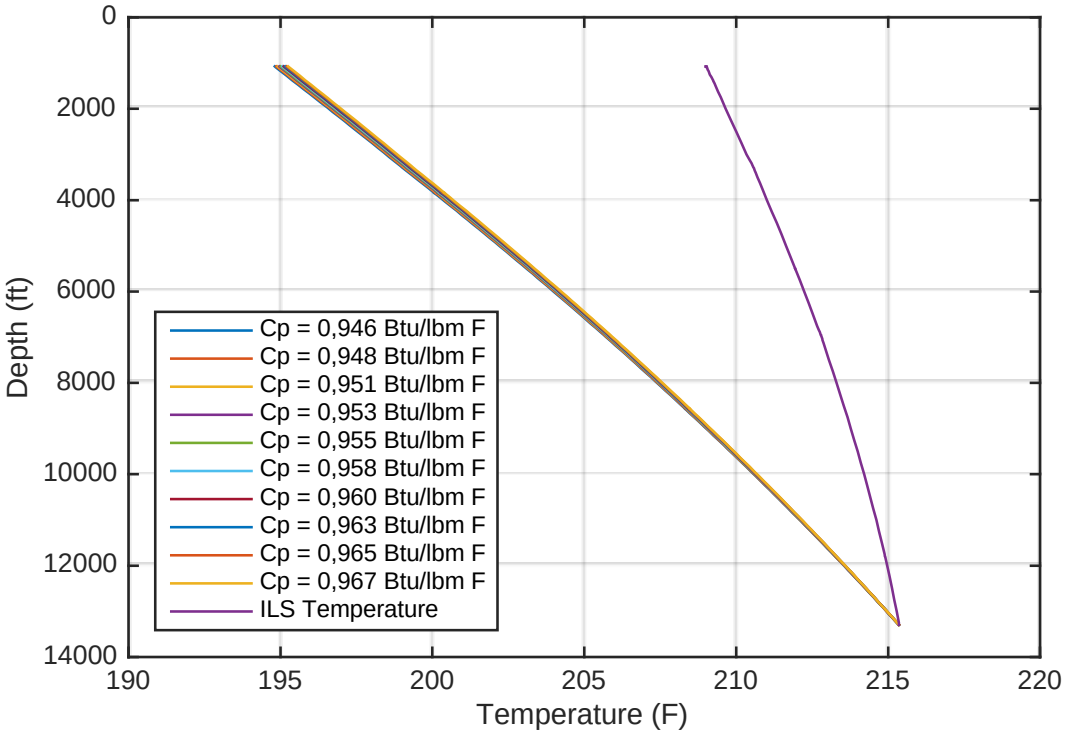

Figure 7-6 Temperature distribution with various heat capacities

7.1.3.4 Assuming no Thermal Resistance in Tubing and Casing

Willhite's paper from 1967 is found as a reference in the temperature calculation to the ILS. Willhite excluded the thermal conductivity of the tubing and casing, since it is considerably higher than the other materials in the wellbore. The statement was mentioned in chapter 5.1.2. Since the conductivity is high in metals, the temperature drop across the tubing and casings can be neglected. Figure 7-7 and Figure 7-8 indicates that the lower conductivity of the annulus and cement is the dominating resistance to heat flow and the assumption is valid for the case simulated in this Thesis.

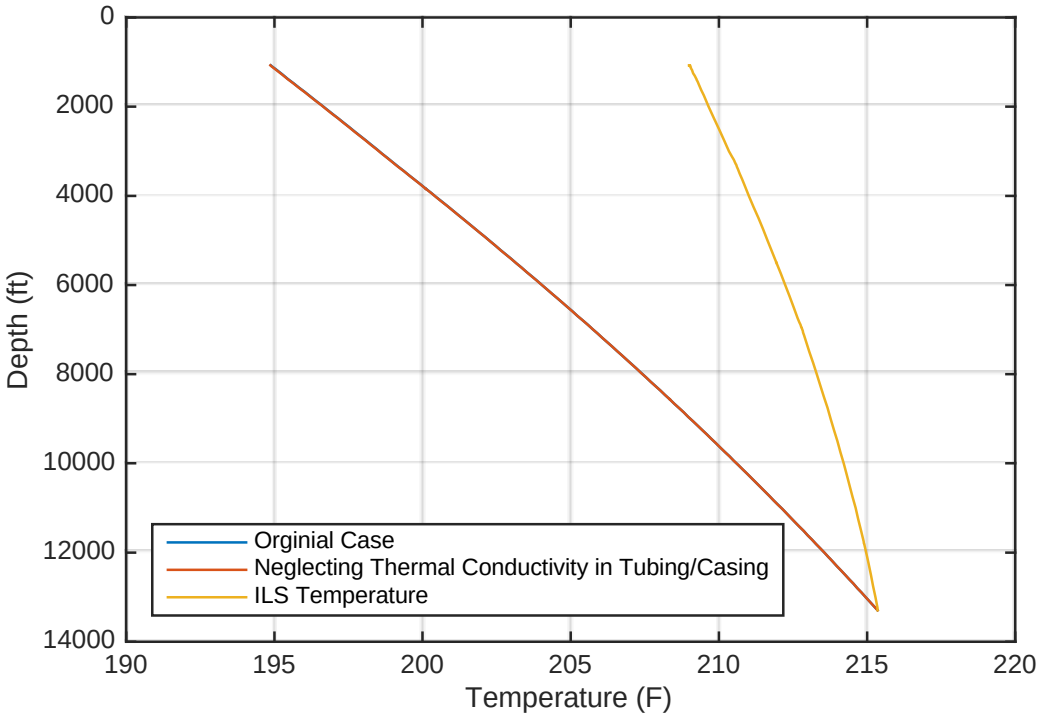

Figure 7-7 Temperature distribution by neglecting the thermal conductivity for metals

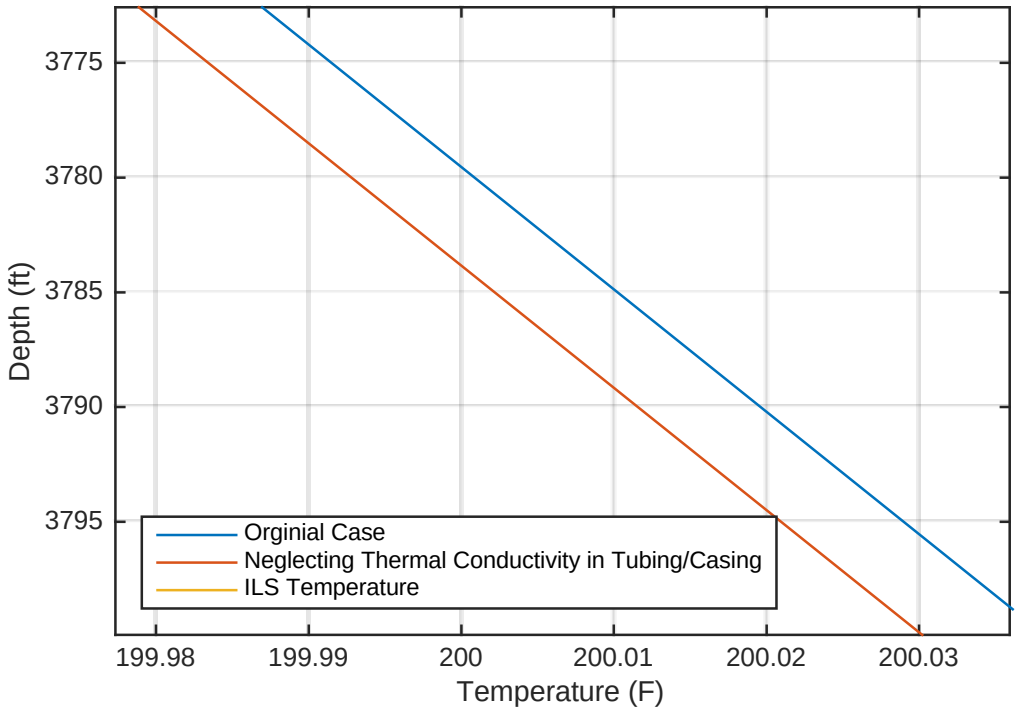

Figure 7-8 Zoomed temperature distribution by neglecting the thermal conductivity for steel

7.1.3.5 Comparison of the Dimensionless Temperature from Ramey and Hasan and Kabir

Chapter 6.1.2.4 highlights the approximation of the dimensionless temperature from both Ramey and Hasan and Kabir. In the literature it is stated that Ramey's method is only valid for durations greater than a week, whereas Hasan and Kabir's method is valid at all times. Figure 7-9 through Figure 7-13 demonstrate the difference between the two methods at different production durations.

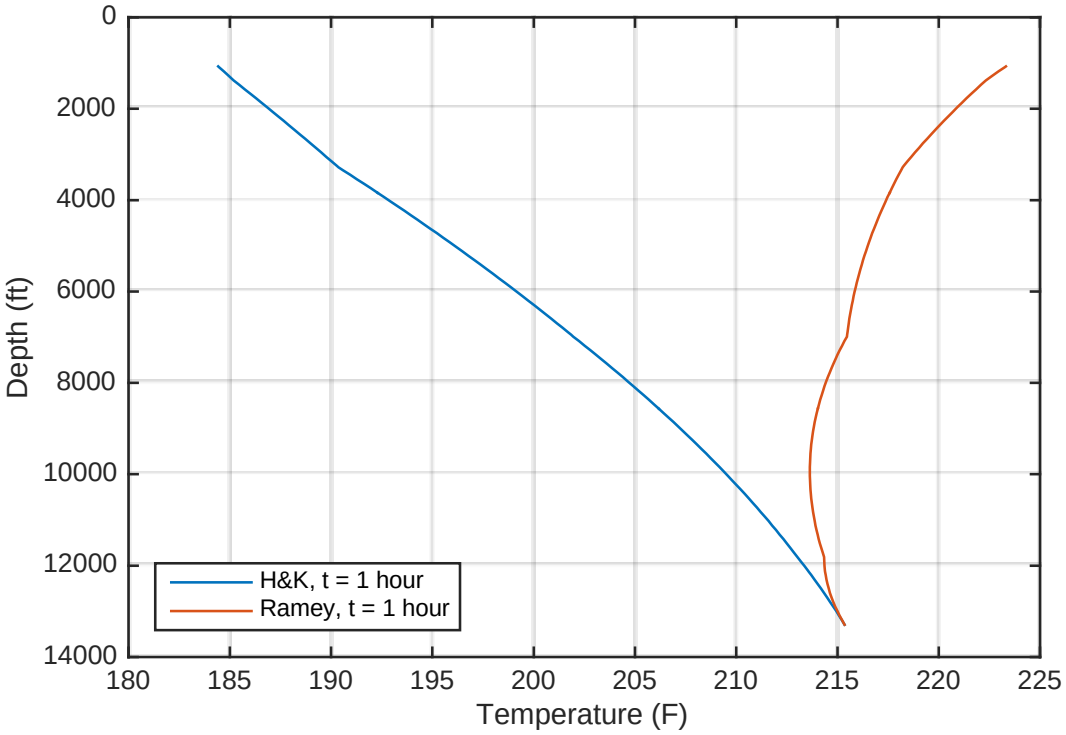

Figure 7-9 Temperature distribution after 1 hour with both methods

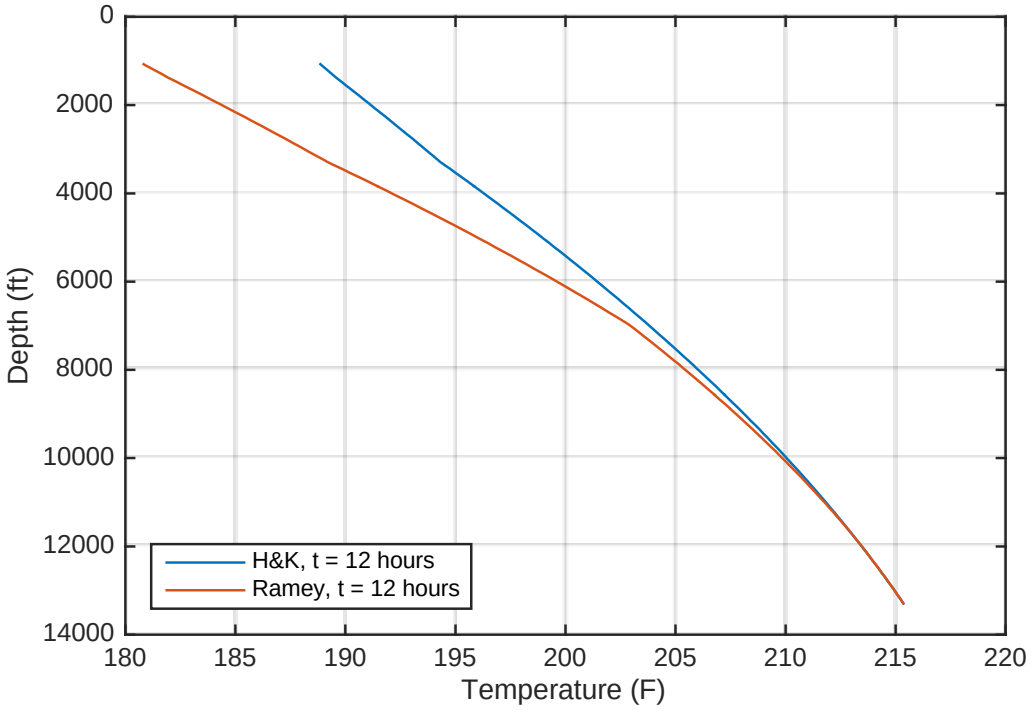

Figure 7-10 Temperature distribution after 12 hours with both methods

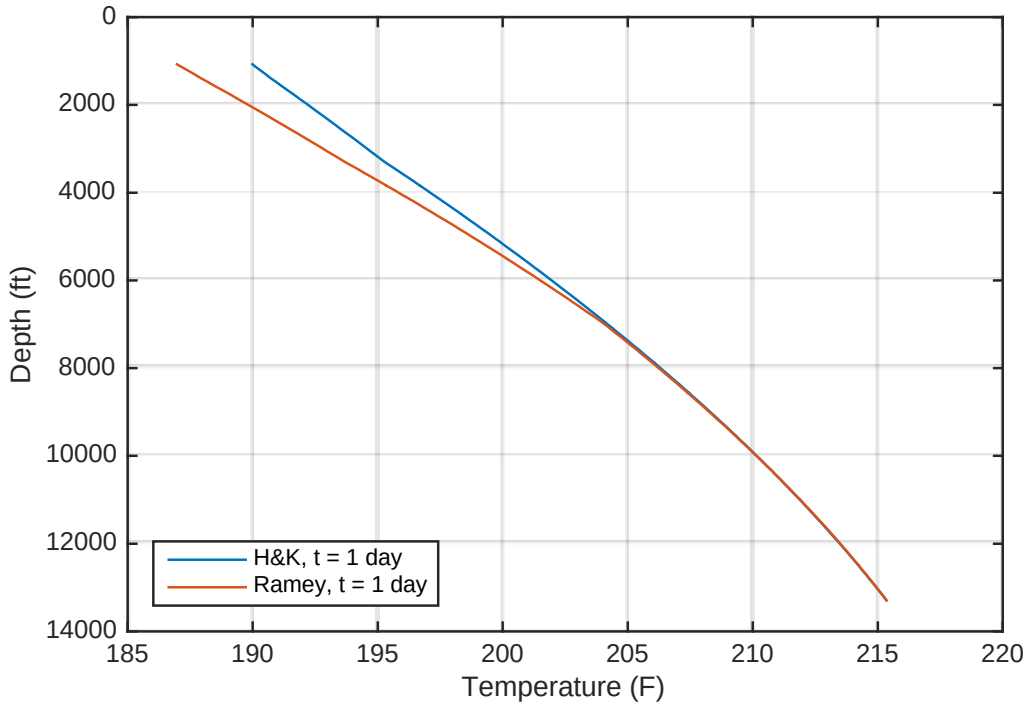

Figure 7-11 Temperature distribution after 1 day with both methods

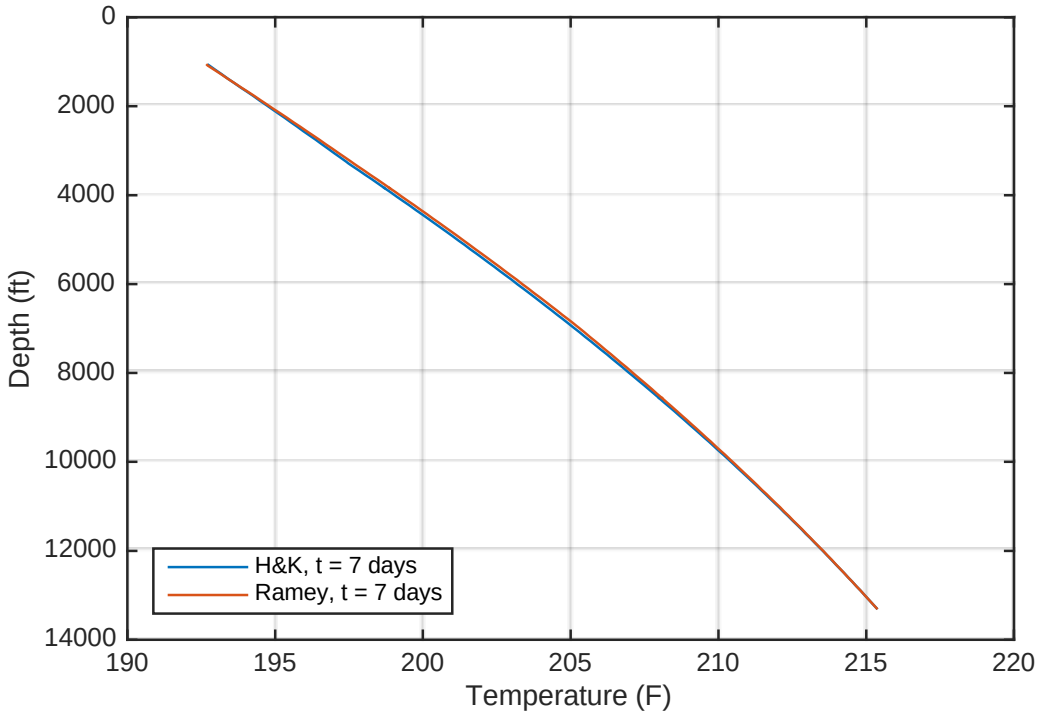

Figure 7-12 Temperature distribution after 7 days with both methods

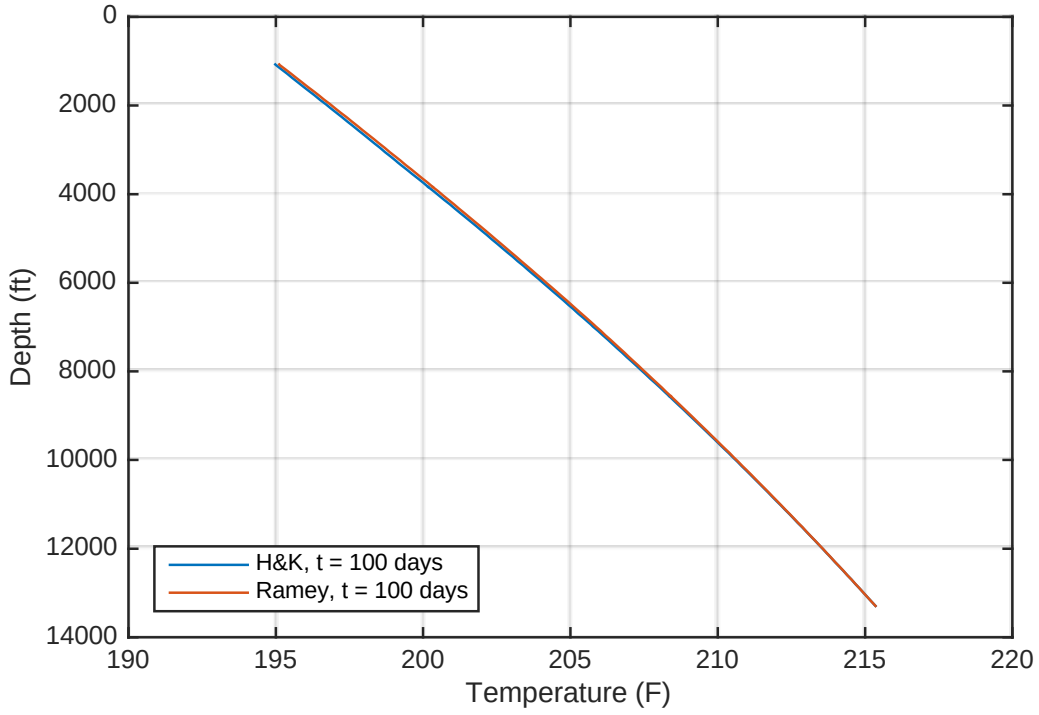

Figure 7-13 Temperature distribution after 100 days with both methods

7.1.4 Sensitivity Analysis of Known Input Parameters

Parameters such as duration of production, mass flow and the geothermal gradient are important parameters that affect the heat transfer and the temperature in the wellbore. The results of a sensitivity analysis in respect to those variables are shown in the following sections.

7.1.4.1 Production Time

Figure 7-14 shows the temperature distribution at different production durations. As mentioned, the model is not valid for transient conditions. It is reasonable to say that after 1 hour of production the well is in transient condition and that this model does not apply for that stage. In addition, the wellbore heats up rapidly from 1 to 12 hours. The transition zone is from 12 hours to 10 days before steady stage condition is reached. From 50 days to 2000 days, the production time does not change the temperature distribution significantly, thereby assumed to be steady state conditions.

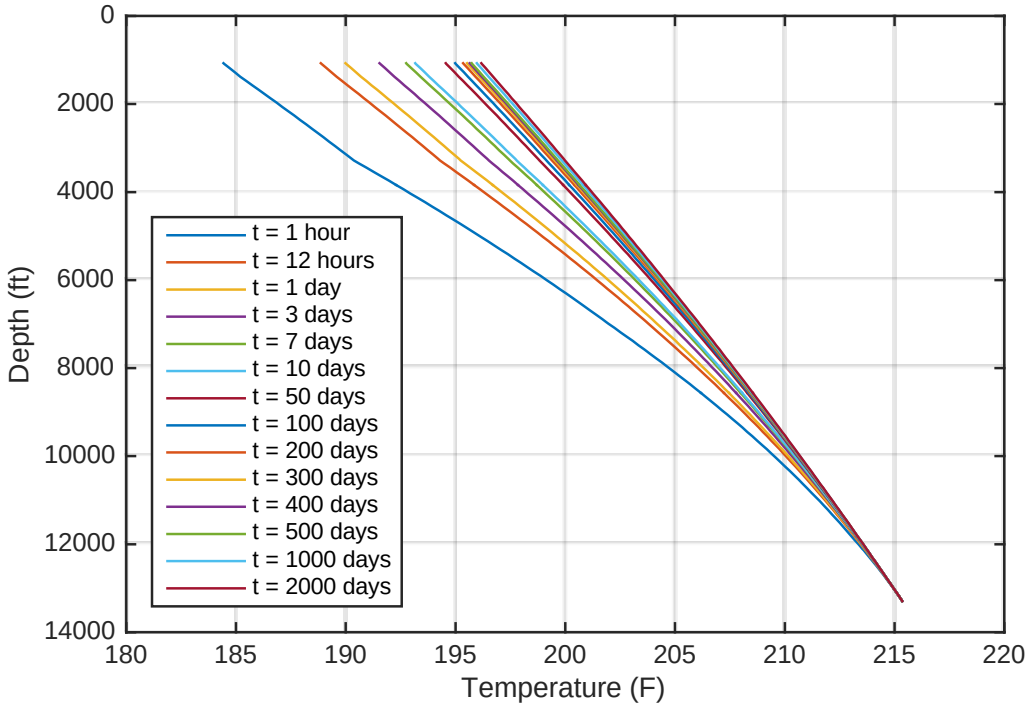

Figure 7-14 Temperature distribution with different production durations

7.1.4.2 Mass Flow

Mass flow affects the temperature distribution, especially at low rates, as seen on Figure 7-15. The mass rate is applied when calculating the constant, A, in equation (6.39). The constant is further used in the computation of the temperature distribution profile in equation (6.43).

Figure 7-15 demonstrates at low mass rate the influence on the temperature distribution profiles is high. When reaching 100 lbm/sec the influence on the temperature stabilizes. Thus, high mass rates gives less heat loss of the flowing fluid and higher temperature at the WH, but the heat loss will stabilize at certain point

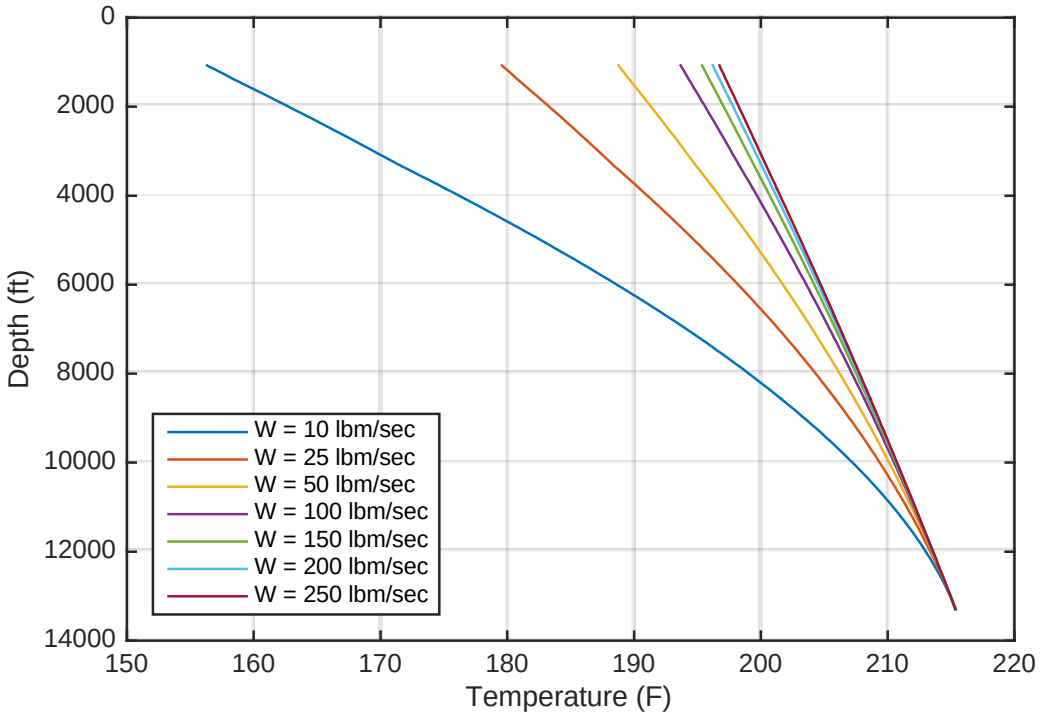

Figure 7-15 Temperature distribution with various production rates

7.1.4.3 Geothermal Gradient

The geothermal gradient is the base for the model, since the reservoir temperature and the surroundings temperature is a function of it. Figure 7-16 exhibits the temperature distribution for various geothermal gradients. 1,44 °F/100ft is the geothermal gradient used in the computation of the base case. The other values are 10% and 5% below the base case and 5% and 10% above the base case, respectively.

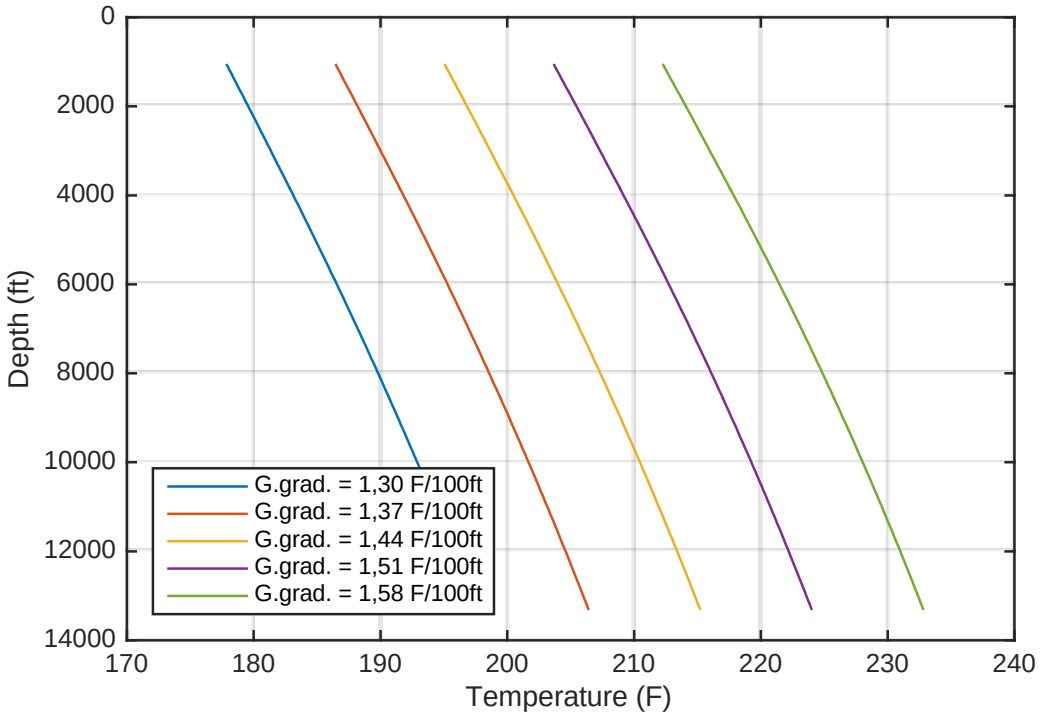

Figure 7-16 Temperature distribution with various geothermal gradients

7.2 Change in Loads due to Temperature

During production, the wellbore heats up. The high temperature leads to axial compressive force acting on the tubing. During injection of cold water, the opposite occurs. The wellbore cools down, leading to axial tensile force acting on the tubing. The axial forces also affect the triaxial stress that could be a major stress in HPHT conditions.

Figure 7-17 indicates the change in axial load for the 7 inches tubing due to temperature. The ILS for HPHT conditions gives the lowest compression force, followed by the temperature simulation model, and the ILS for conventional design, which is the most conservative of the lot. The temperature may also influence other axial loads such as buckling and ballooning effect, since enhanced temperature leads to compressive load. It also affects the pressure in the wellbore and the annulus, hereby also the burst and collapse loads. The purpose of wellbore design is to ensure well integrity for the lifetime of the well. To ensure that the wellbore design is trustworthy, it is important to compute the correct relationship of pressure and temperature based on the planned operations.

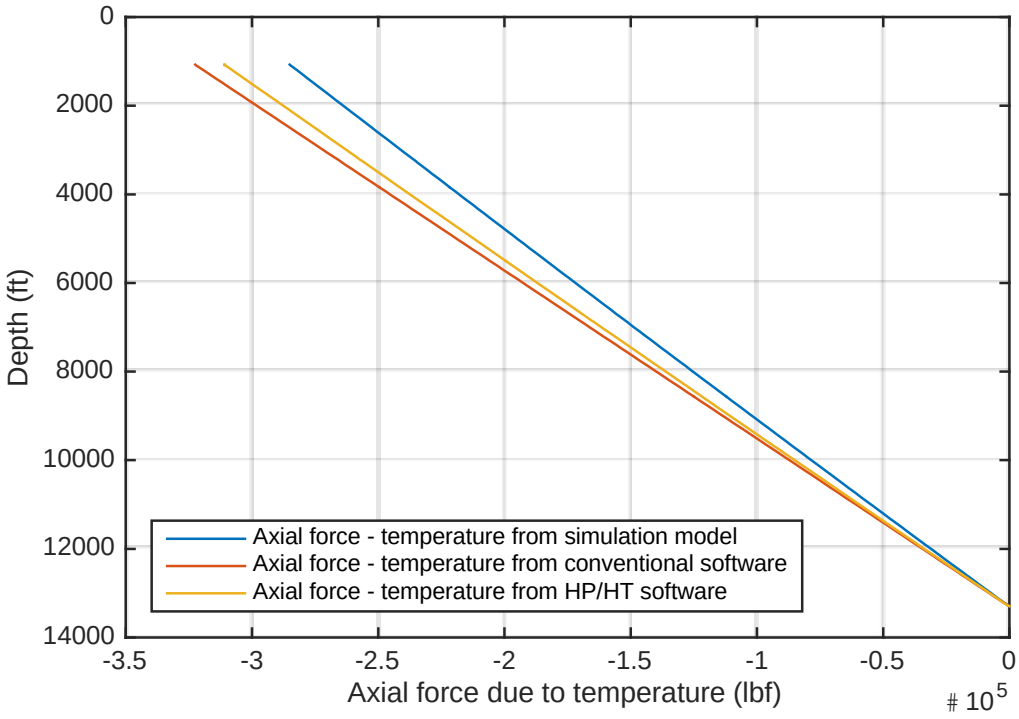

Figure 7-17 Axial load due to temperature difference

Chapter 8 Discussion

The foundation of this Master's Thesis was to investigate how the ILS computed the temperature distribution. A temperature model was built in MATLAB based on the most recognized theory in the industry, for comparison purpose. After the verification of the model behavior, the model in MATLAB was used to perform a sensitivity study on selected parameters.

8.1 Simulation Results

Figure 7-1 shows the temperature distribution and the overall heat transfer coefficient through the wellbore. By looking at the overall heat transfer coefficient as a result of the whole system, it decreasing towards surface due to increased resistivity in the surrounding well completion. Cement has low thermal conductivity, and act as a good isolator. As the number of cement layer increases towards surface, the resistivity also increases. However, in case 2 and 3 the overall heat transfer coefficient tends to increase from the start of their interval towards the end of their interval. This phenomenon occurs because the completion fluid in the annulus heats up towards the end of the interval, which leads to a higher contribution of convection and radiation that again leads to decreased thermal resistivity.

Heat loss to the formation is depending on the overall heat transfer coefficient. Thus, decreasing overall heat transfer coefficient leads to reduced heat loss to the formation. This indicates that the heat loss is high close to the reservoir in terms of low resistivity, and it is decreases towards the surface due to the increased number of cement layers.

Comparing the result from the temperature model with the HPHT ILS software gives a difference of 6,7% as seen in Figure 7-2. Unfortunately, no real data were available to compare or correct the temperature simulation model. Rostad's statement needs further investigation, since a boundary conditions of just 1,64 ft into the formation could have significant effect on the heat loss to the formation.

The HPHT ILS software is a black-box system, which gives no insight into the calculations performed. Though some input variables are known, there are still some input variables that remain unknown. Again, leading to uncertainties in the comparison of the two systems.

8.2 Sensitivities of Unknown Input Variables in the ILS

Sensitivity analysis of the unknown input variables are done in order to see how they affect the temperature distribution. The results of the analysis is presented graphically in chapter 7.1.3.

8.2.1 Emissivity of Inside Tubing

The effect of inside tubing emissivity changes is at a magnitude of a thousandth. The low difference indicates that the "view factor" does not influence the heat transfer coefficient for radiation enough to be a parameter of concern. Thus, heat transfer by radiation in annuli is most likely dominated by natural convection in this case. However, equation (5.18) shows that the heat transfer coefficient for radiation is strongly dependent on temperature. By moving in to hotter reservoirs, the magnitude of heat transfer contributed from radiation will increase.

8.2.2 Thermal Diffusivity of Formation

The thermal diffusivity of formation is used in the calculation of the transient temperature in the formation. Equation (6.7) indicates how the dimensionless time is computed. The dimensionless time is dependent on the thermal diffusivity of formation, time and the wellbore radius. At long duration of production, the thermal diffusivity has a low impact on the temperature distribution shown in Figure 7-5. At lower duration of production, the thermal diffusivity of formation has a higher impact on the temperature distribution shown in Figure C-1. Thus, the thermal diffusivity needs to be investigated for the particular surrounding formation. Early life production and shut-in cases are usually considered to be transient conditions, meaning that the thermal diffusivity could have a great impact on the temperature computation.

8.2.3 Heat Capacity of Wellbore and Annulus Fluid

Temperature and pressure change the heat capacity of a fluid. Despite that, the heat capacity of seawater, in liquid phase, changes little due to temperature and pressure. Figure 7-6 shows marginal effect of the temperature distribution with different heat capacities of seawater. Although, the heat capacity of the fluid should be calculated for each differential length element, especially when considering multiphase flow or gas filled annulus.

8.2.4 Comparison of the Dimensionless Temperature

The results from Figure 7-9 through Figure 7-13 gives some interesting result about the approximated dimensionless temperature. Clearly, Ramey's approximation does not give a valid solution of the dimensionless temperature approximation after 1 hour. While, the approximation developed by Hasan and Kabir is found valid after 1 hour.

Ramey's approximation gives a lower temperature than Hasan and Kabir's method, in the time range from 12 hours to 1 day. As the time increases, the difference between the methods also reduces. Hasan and Kabir stated that Ramey's solution was obtained by assuming vanishingly small well radius as boundary conditions, which affect the solution at small times (A. R. Hasan & Kabir, 1991).

After 7 days the temperature distribution from the two methods is almost similar to each other. This indicates that for the production time for the base case, 2000 hours, the choice of model barely affect the result.

8.3 Sensitivities of Known Input Variables in the ILS

Even though duration of production, production rate and the geothermal gradients are known input parameters in both the temperature model and ILS, they also affect the results.

8.3.1 Production time and production rates

Production duration and production rates will affect the temperature. The temperature model does not consider the temperature distribution in the well completion as function of time, only depth. Hence, the temperature model is not valid for transient conditions in the wellbore. However, it is useful to see how the overall temperature distribution profile is affected by the production time, seen in Figure 7-14.

According to the literature, heat flow in the wellbore is rapid compared to the heat flow in the formation. This leads to, relatively short after start of production, the heat flow in the wellbore reaches steady state. It is reasonable to assume steady state conditions between 7-50 days for this case, according to Figure 7-14. After reaching steady state, the transient heat flow in the formation contribute to increased temperature in the wellbore. However, the greatest temperature difference will give the highest load condition. So short periods of production is not the most important aspects of the model during production.

The production rate or mass flow is a measure on how much fluid is transported in the wellbore at the length of time. Higher production rates leads to higher temperature at the WH. This is seen in Figure 7-15. From 100 lbm/sec and higher, the production rate has low influence on the temperature distribution compared to lower rates. High turbulent flow transport heat with high efficiency.

8.3.2 Geothermal Gradient

The geothermal gradient is the base for the whole model, and the accuracy of the calculated temperature profile is dependent on the accuracy of the geothermal gradient. Therefore, care must be taken to obtain accurate temperature data of the formation. The reservoir pressure is the geothermal temperature at the specific depth of the reservoir. Also equation (6.43) shows that the fluid temperature at each point where the fluid temperature is calculated is depending on the geothermal gradient in that particular point. Figure 7-16 shows that if the geothermal data change with 5 or 10% the whole simulated temperature distribution also change by 5 or 10%, meaning that the model is highly driven by this boundary condition. Thus, the geothermal gradient should be estimated based on wells close to the wellbore being considered or data from an exploration well in the same area.

8.4 Model Verification

The radial heat transfer model is verified by programing Willhite's example from 1967. The results establish a base of the heat transfer calculation in the temperature model. Results of the verification are presented in Table 8-1.

Table 8-1 Comparison of Willhite and the simulation model

	Assumed, U_{to}	**Calculated, U_{to}**	**Iterations to convergence**	**Final wellbore temperature, T_{wb}**
Unit	(Btu/hr ft^2 °F)	(Btu/hr ft^2 °F)	#	(°F)
Willhite	4,05	3,15	3	364
Simulation model	4,05	3,13	11	363,3

Willhite calculated the iterative process by hand, since his work was done in 1967. The simulation model does the process by using computer power, which gives higher accuracy. Table 8-1 shows that the margin of error between the two models is low, which indicates that the simulation model for heat transfer computation is built correctly.

8.5 Model Evaluation

The model excludes the forced convection of the flowing fluid, due to low heat transfer resistance. The resistance from the production fluid to the tubing wall is often not very significant, but it depend on the conductivity, heat capacity and the flow regime. Most production and injections flow is turbulent, which reduces the resistance. (Bellarby, 2009). This leads to a uniform temperature at the cross section area of the fluid at the point being considered. This is a valid assumption stated by Willhite in 1967. Heat transfer in vertical direction is not considered. This leads to errors close to the seabed at large heat flow areas, due to the big temperature difference at the interface between the seabed and the WH. The heat transfer computation accounts for transient conditions in the formation and is therefore considered to be accurate according to Table 8-1.

The temperature model is a simplified solution and does not include a pressure drop model or a phase behavior model. However, Sagar, Doty, & Schmidt's (1991) empirical expression for ϕ, given in equation (6.42), denotes for the kinetic energy and J-T effect at low flow rates. The expression for ϕ is a constant for the whole computation process. It is only valid for two-phase mixtures with high liquid holdups or high wellhead pressure, Sagar, Doty, & Schmidt (1991) assumes little effect from J-T cooling and heating.

A. Rashid Hasan, Kabir, and Wang (2009) pointed that since ϕ is a function of the kinetic energy and the J-T terms, the empirical expression could lead to unacceptable errors. Since, deepwater wells often produce at high rates, it implies a significant contribution to the kinetic energy term. Also, high production rates and large pressure gradient affects the J-T effect. The J-T effect causes the temperature of a real gas to decrease as the pressure decreases in low-pressure systems. Whereas the opposite happens in liquids. Therefore, in a well producing two-phase fluids, the fraction of each phase present in a given discretized wellbore cell, *dz*, can see a increase or decrease in temperature with pressure reduction because of the J-T effect. Thus, knowing the fluid properties is critical to obtain an accurate temperature predictions. When

phase transfers are included and the heat energy required or extracted during evaporation or condensation, the importance of an accurate fluid model is increased further.

There will also be a temperature effect on the pressure, although this would be less pronounced (Bellarby, 2009). To have sustainable temperature model it should iterate both on pressure and temperature, and then find the proper fluid composition.

Liquids expand when heat is applied and are compressed by pressure. Therefore, the density of the fluid decreases with increasing temperature, but increases with increasing pressure. As fluid is produced, injected or pumped and circulated, the temperature and pressure effect change the density of the fluid. It should also include viscosity, heat capacity and thermal conductivity as function of pressure and temperature.

Chapter 9 Conclusion

The main objective of this Thesis was to build a temperature model for a production case, compare it with ILS and analyze the different inputs parameters used in the model. The analysis has identified some important aspects regarding of temperature modeling in wells:

- It is important to have the correct geothermal gradient, since the temperature model is highly driven by this boundary condition. Accuracy in measuring or modeling the geothermal gradient should therefore be applied. Other input variables as emissivity of tubing, heat diffusivity of the formation and change in heat capacity due to temperature had little effect on the temperature distribution.
- The cement-formation interface temperature should be calculated by using Hasan and Kabir's approximation of the dimensionless temperature for the formation.
- Duration of production and mass flow affects the temperature distribution significantly, and should be specific values for the case taken into consideration.
- Accurate characterization of the reservoir fluid is important since it influence the kinetic energy term and the J-T effect, which again influence the temperature distribution.
- The heat transfer approach followed is sufficient for temperature profile computation, according to the literature. The heat transfer approach is validated against Willhite's approach. Moreover, it is found out that the thermal conductivity of the tubing and casing can be neglected in the calculations.
- The temperature model needs improvements, to taken account for pressure drop and phase behavior. However, it is accurate enough to get a good estimate of the temperature for a one-phase production case.
- In HPHT wells, the temperature variations along the wellpath have shown to be highly relevant for the axial tubing load, APB and WHM.

Chapter 10 Further Work

The author has divided the further work in three phases, executed in ascending order.

1. **Pressure Drop, Phase Behavior and Heat Transfer Optimization**
    - Implement a model for pressure drop, which include friction in the flowing fluid and hydrostatic head. Begs and Brill or Zhang mechanics are examples of models.
    - Modified black-oil phase behavior for a generalized reservoir composition. For specific field hydrocarbons, input from lab work and Equation of State should be used.
    - Include the cooling effect of the riser in offshore wells.
    - Investigate the boundary conditions for heat transfer into the formation used in the ILS.
    - Compare the result of the model with actual data from a specific well.
2. **Transient Conditions and Circulation**
    - Early stage production and shut-in short are transient conditions. Implement transient conditions by applying an implicit solution using for example backwards Euler and and Newton-Raphson iteration.
    - Circulation during drilling, stimulation and workover leading to vertical heat transfer in the wellbore as well as radial. For example, during drilling where the depth of circulation and the wellbore thermal resistance change as the well is drilled and casing is set. Implement behavior of heat transfer during circulation. Also behavior of non-Newtonian fluids need to be accounted for, since the properties change with depth and time.
3. **Establish an User Friendly Platform**
    - Increase the user friendliness by establishing an open source program on an intuitive app form.

Abbreviations

APB	Annular Pressure Build-up
ECD	Equivalent Circulating Density
HPHT	High Pressure, High Temperature
ILS	Industry Leading Software
MD	Measured Depth
M-M	Metal to Metal
NTNU	Norwegian University of Science and Technology
RKB	Rotary Kelly Brushing
TVD	True Vertical Depth
WH	Wellhead
WHM	Wellhead Movement

Nomenclature

$\overline{F_{tci}}$	overall interchange factor between the outside tubing and inside casing surfaces (dimensionless)
A	unit area (in^2)
a	absorptivity (dimensionless)
A_i	inner area of tubing or casing (in^2)
A_o	outer area of tubing or casing (in^2)
API	oil gravity (°API)
A_s	surface area of the body in concern - heat transfer surface (ft^2)
c_{an}	heat capacity of the fluid present in the annulus at the average annulus temperature (Btu/lbm °F)
c_e	heat capacity of foramtion (Btu/lbm °F)
C_J	Joule-Thopmson (J-T) coefficient
c_{pm}	heat capaity of wellbore fluid (Btu/lbm °F)
C_T	coefficient of thermal expansion ($°F^{-1}$)
dT/dr	temperature gradient (°F/ft)
dT/dx	temperature gradient (°F/ft)
E	Young's modulus (psi)

E	emissive power (Btu/hr)
E_b	emissive power for a black-body (Btu/hr)
F	force (lbf)
F_{gL}	gas/liquid ratio
F_T	force in tubing or casing (lbf)
F_{tci}	view factor based on outside tubing and inside casing surface (dimensionless)
G	irradiation (Btu/hr)
g	acceleration of gravity (32,2 ft/sec^2)
G_{abs}	absorbed irradiation (Btu/hr)
g_c	conversion factor (32,2 lbm ft /lbf sec^2)
g_{hr}	acceleration due to gravity (4,17 x 10^8 ft/hr^2)
Gr	Grashof number (dimensionless)
g_T	geothermal gradient,(°F/ft)
h	average film coefficient or average heat transfer coefficient (Btu/ hr ft^2 °F)
H	fluid enthalpy (Btu/lbm)
h_c	heat transfer coefficient for natural convection and conduction (Btu/hr ft^2 °F)
h_f	forced-convection heat transfer coefficient for the tubing fluid (Btu/hr ft^2 °F)

h_r	heat transfer coefficient for radiation (Btu/hr ft^2 °F)
J	mechanical equivalent of heat (778 ft-lbf/Btu)
J_0	Zero-order Bessel function of the first kind
J_1	First-order Bessel function of the first kind
K	thermal conductivity (Btu/hr ft °F)
k_{cem}	thermal conductivity of the casing material at average tubing temperature (Btu/hr ft °F)
k_{csg}	thermal conductivity of the casing material at average tubing temperature (Btu/hr ft °F)
k_e	thermal conductivty of formation (Btu/hr ft °F)
k_{ha}	thermal conductivity for fluid in annulus (Btu/hr ft °F)
k_{hc}	equivalent thermal conductivity of the annular fluid with natural convection effects (Btu/hr ft °F)
k_{tub}	thermal conductivity of the tubing material at average tubing temperature (Btu/hr ft °F)
L	length (ft)
ΔL	length change (ft)
L_1	Total length of wellbore – TMD (ft)
L_T	length of the tubing or the uncemented section of casing (ft)
ΔL_T	metal expansion or contraction (ft)
Nu	Nusselt number (dimensionless)

Pr	Prandtl number (dimensionless)
p_{wh}	wellhead pressure (psig)
Q	heat flow rate (Btu/hr)
q	heat flow from wellbore (Btu/lbm)
Q_c	heat flow in the annulus by natural convection and conduction (Btu/hr)
Q_r	heat flow in the annulus due to radiation (Btu/hr)
Q_x	heat flow in x-direction (Btu/hr)
Q_x''	heat flux in x-direction per unit area (Btu/hr ft^2)
r	radius, measured from the center of the wellbore (ft)
r_D	radial distance (dimensionless)
r_{ti}	tubing inside radius (ft)
r_{to}	outside radius of tubing (ft)
r_{wb}	wellbore radius (ft)
T_∞	temperature of the flowing fluid (°F)
T_{an}^*	absolute temperature of annulus fluid (°R)
T_{body}	temperature of the body (°F)
T_{ci}	temperature of inside casing surface (°F)

T_{ci}^*	temperature of inside casing surface (°R)
T_{co}	temperature of outside casing surface (°F)
t_D	time (dimensionless)
T_D	temperature (dimensionless)
T_e	formation temperature at any given depth (°F)
T_{ei}	undisturbed formation temperature (°F)
T_{eibh}	undisturbed formation temperature at bottomhole (°F)
T_{eiwh}	undisturbed formation temperature at wellhead (°F)
T_f	temperature of flowing fluid (°F)
T_{ti}	temperature of inside tubing surface (°F)
T_{to}	temperature of outside tubing surface (°F)
T_{to}^*	temperature of outside tubing surface (°R)
T_{wb}	temperature at cement-formation interface (°F)
ΔT	average change in temperature from the base case to the load case (°F)
U_{to}	overall heat transfer coefficient based on the outside tubing surface and the temperature difference between fluid and cement-formation interface (Btu/hr ft^2 °F)
W	total mass flow rate (lbm/hr)
W^*	total mass flow rate (lbm/sec)

Y_0	Zero-order modified Bessel function of the first kind.
Y_1	First-order modified Bessel function of the first kind
z	variable well depth, form surface - MD (ft)
Δz	increment of tubing length (ft)
α	thermal diffusivity of formation (ft^2/hr)
β	thermal volumetric expansion coefficient of the fluid in annulus (1/°R)
γ_g	gas specific gravity (air=1)
ε	strain (dimensionless)
ε	emissivity (dimensionless)
ε_{ci}	emissivity of inside casing surface (dimensionless)
ε_{to}	emissivity of outside tubing surface (dimensionless)
θ	inclination angel from horizontal (degrees)
μ_{an}	viscosity of the fluid present in the annulus at T_{an} and pressure P_{an} (lbm/ft hr)
ρ_{an}	density of the fluid present in the annulus at T_{an} and pressure P_{an} (lbm/ft hr)
ρ_e	density of formation (lbm/ft^3)
σ	stress (psi)

σ_{SB}	Stefan-Boltzmann constant (0,1714 * 10^{-8} Btu/hr ft^2 °R^4)
σ_z	axial stress (psi)
υ	specific volume (ft^3/lbm)

Subscripts

A	A - Annulus
B	B – Annulus
9 5/8	Casing size
13 3/8	Casing size
20	Casing size
30	Casing size

Reference

Bai, Y., & Bai, Q. (2005). Subsea Pipelines and Risers: Elsevier.

Bellarby, J. (2009). *Well completion design*. Amsterdam ; Oxford: Elsevier.

Berckenhoff, M., & Wendt, D. (2005). *Design and Qualification Challenges for Mudline Well Control Equipment Intended for HPHT Service*. https://www.onepetro.org:443/download/conference-paper/SPE-97563-MS?id=conference-paper%2FSPE-97563-MS

Burmeister, L. C. (1993). *Convective Heat Transfer*: Wiley.

Dropkin, D., & Somerscales, E. (1965). Heat Transfer by Natural Convection in Liquids Confined by Two Parallel Plates Which Are Inclined at Various Angles With Respect to the Horizontal. *Journal of Heat Transfer, 87*(1), 77-82. doi: 10.1115/1.3689057

Fourier, J. B. J. (1878). *The analytical theory of heat by Joseph Fourier ; translated, with notes, by Alexander Freeman ; edited for the Syndics of the University Press*. Cambridge [Eng.] :: University Press.

Hasan, A. R., & Kabir, C. S. (1991). *Heat Transfer During Two-Phase Flow in Wellbores; Part I--Formation Temperature*. https://www.onepetro.org:443/download/conference-paper/SPE-22866-MS?id=conference-paper%2FSPE-22866-MS

Hasan, A. R., & Kabir, C. S. (1994). Aspects of Wellbore Heat Transfer During Two-Phase Flow (includes associated papers 30226 and 30970). doi: 10.2118/22948-PA

Hasan, A. R., Kabir, C. S., & Wang, X. (2009). A Robust Steady-State Model for Flowing-Fluid Temperature in Complex Wells. doi: 10.2118/109765-PA

Incropera, F. P. (2007). *Fundamentals of heat and mass transfer*: John Wiley.

Landmark. (2001). WellCat (pp. 760). Huston, Texas: Halliburton.

Landmark. (2008). StressCheck - Training Manual (pp. 362). Huston, Texas: Halliburton.

Landmark. (2013). Well Integrity Analysis in Deepwater HP/HT Scenarios. Retrieved 29.05.2015, 2015, from https://www.landmarksoftware.com/Lists/DocumentRepository/2013-11-HPHT-Well-Integrity-Wellcat-white-paper.pdf

Lienhard, J. H. (2003). *A heat transfer textbook*: Phlogiston Press.

"Well integrity in drilling and well operations" Rev. 4, June 2013. (2004).

Ramey, H. J., Jr. (1962). Wellbore Heat Transmission. doi: 10.2118/96-PA

Rostad, H. (2015, 19.05.2015). [Information about ILS].

Sagar, R., Doty, D. R., & Schmidt, Z. (1991). Predicting Temperature Profiles in a Flowing Well. doi: 10.2118/19702-PA

Skalle, P. (2013). *Drilling Fluid Engineering* (pp. 159).

Torbergsen, H.-E. B., Haga, H. B., Sangesland, S., Aadnøy, B. S., Sæby, J., Johnsen, S., . . . Lundeteigen, M. A. (2012). An Introduction to Well Integrity (rv.0 ed., pp. 146).

Willhite, G. P. (1967). Over-all Heat Transfer Coefficients in Steam And Hot Water Injection Wells. doi: 10.2118/1449-PA

Aadnøy, B. S. (2009). Advanced drilling and well technology. XII, 876 s. : ill.

Appendix

Appendix A Stress and Strain

A.1 Stress, Strain, Yield Point and Ultimate Tensile Stress

The fundamental in stress analysis is to understand the behavior of metals under loads and the limits that tubing and casing material can withstand. The loads can come from sources as pressure, temperature and weight of the pipe. This Thesis focuses on the temperature. Equation (A.1) gives stress, σ, is defined as force, F, per unit area, A.

$$\sigma = \frac{F}{A} \tag{A.1}$$

Where

- σ = stress (psi)
- F = force (lbf)
- A = unit area (in^2)

When tubing is subjected to stress, it will elongate or stretch. Equation **(A.2)** gives strain, ε, is defined as the fractional length change.

$$\varepsilon = \frac{\Delta L}{L} \tag{A.2}$$

Where

- ε = strain (dimensionless)
- ΔL = length change (ft)
- L = length (ft)

Figure A-1shows a linear relationship between the stress and the strain at ambient conditions. This gives an expression for the modulus of elasticity indicated in equation (A.3)

$$E = \frac{\sigma}{\varepsilon} \tag{A.3}$$

Where

- E = Young's modulus (psi)

The straight-line assumption is an approximation for practical purpose. For some corrosion-resistant alloys, the relationship is non-linear throughout. A linear curve fitting is used where the relationship is non-linear. (Bellarby, 2009).

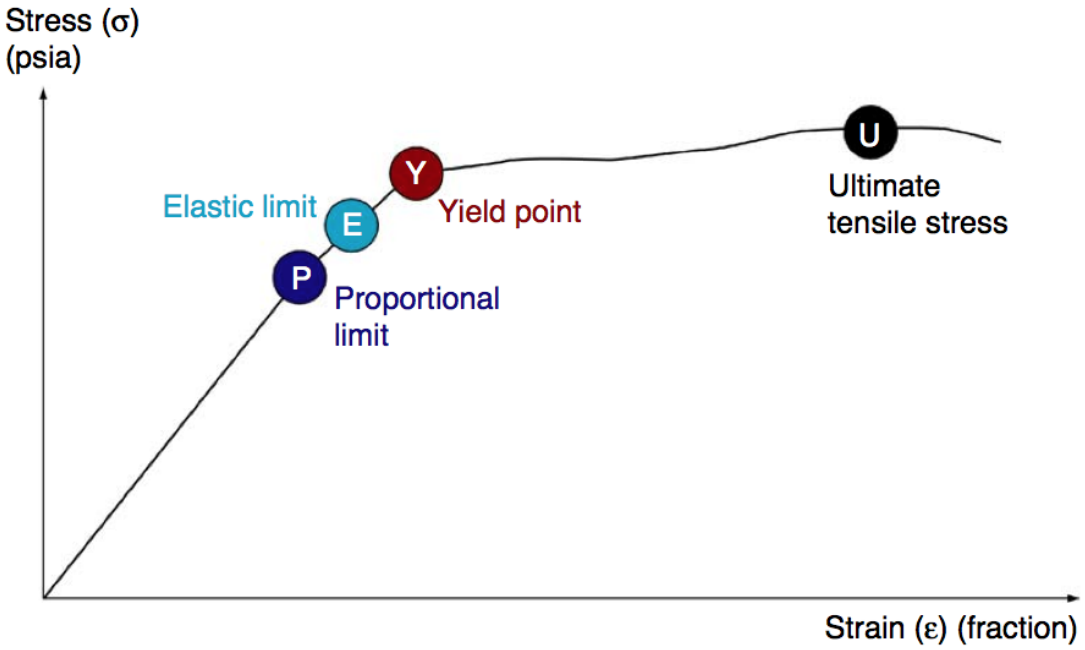

Figure A-1 Stress-strain relationship (Bellarby, 2009)

The material stress-strain curve is a function of temperature and material. Typical used linear deration of steel is approximately 0,02 to 0,05% per °F (Aadnøy, 2009). However, assuming ambient temperature derived Young's modulus will result in slight conservatism in the stress analysis (Bellarby, 2009). Temperature dependent yield is also manufacturing dependent. Therefore, specific values should be obtained directly form the vendor, that is found experimentally.

A.2 Triaxial Analysis

Triaxial stress is a combination of axial stress (σ_z), radial stress (σ_r) and tangential stress (σ_t). The most widely used yielding criterion is the Huber-Hencky-Mises yield condition. Huber-Hencky-Mises is abbreviated as Von Mises (VME), and is based on the maximum distortion energy theory. A simplified Von Mises equation, ignoring torque, is presented in equation (A.4). (Bellarby, 2009),

$$\sigma_{VME}^2 = (\sigma_z - \sigma_r)^2 + (\sigma_z - \sigma_t)^2 + (\sigma_r - \sigma_t)^2 \quad \text{(A.4)}$$

Where

- σ_{VME} = Huber-Henck Mises yield strength (psi)
- σ_z = axial stress (psi)
- σ_r = radial stress (psi)
- σ_t = tangential stress (psi)

Figure A-2 displays a triaxial illustration of the stress in combination.

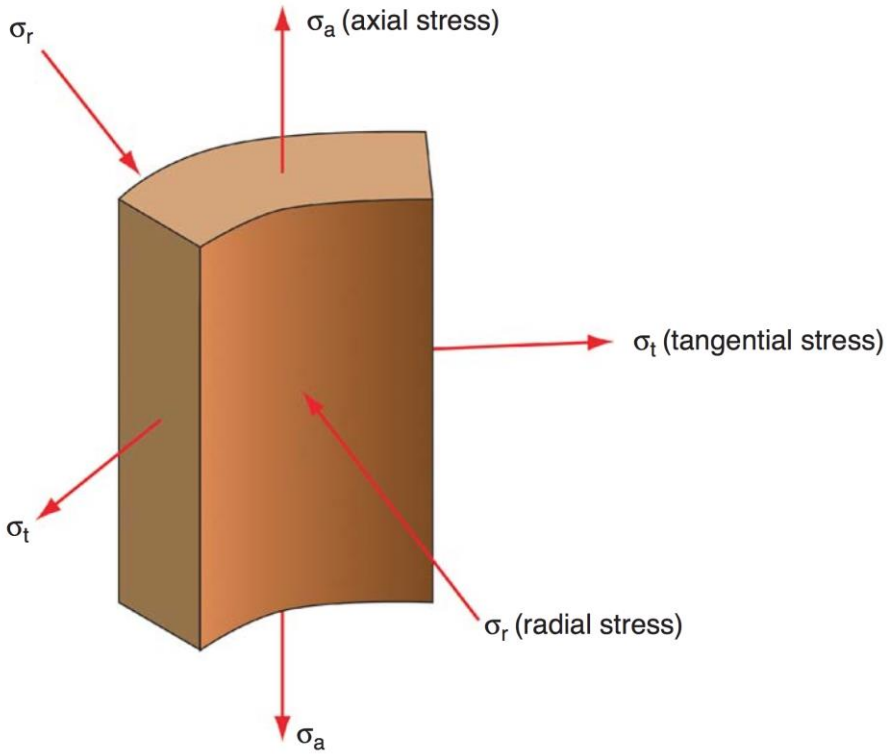

Figure A-2 Triaxial illustration (Bellarby, 2009)

Appendix B Temperature Model

Figure 6-1 shows the wellbore schematic for the wellbore considered in this Thesis. The figure shows the different cases, due to different surroundings. For each case there are different heat transfer scenarios leading to different temperature distribution, which again leading to different equations for the wellbore. The following equations are based on the wellbore schematic and chapter 5.1.

B.1.1 Case 1

B.1.1.1 Temperature from Flowing Fluid to Cement-Formation Interface for Case 1

$$\left(T_f - T_{wb}\right) = \left(T_f - T_{ti}\right) + \left(T_{ti} - T_{to}\right) + \left(T_{to} - T_{wb}\right) \tag{B.1}$$

B.1.1.2 Overall Heat Transfer Coefficient for Case 1

Excluding forced convection in tubing

$$U_{to} = \left[\frac{r_{to} ln \frac{r_{to}}{r_{ti}}}{k_{tub}} + \frac{r_{to} ln \frac{r_{wb}}{r_{to}}}{k_{cem}}\right]^{-1} \tag{B.2}$$

B.1.2 Case 2

B.1.2.1 Temperature from Flowing Fluid to Cement-Formation Interface for Case 2

$$\left(T_f - T_{wb}\right) = \left(T_f - T_{ti}\right) + \left(T_{ti} - T_{to}\right) + \left(T_{to} - T_{ci_{9\,5/8}}\right) + \left(T_{ci_{9\,5/8}} - T_{co_{9\,5/8}}\right) + \left(T_{co_{9\,5/8}} - T_{wb}\right) \tag{B.3}$$

B.1.2.2 Overall Heat Transfer Coefficient for Case 2

Excluding forced convection in tubing.

$$U_{to} = \left[\frac{r_{to} ln \frac{r_{to}}{r_{ti}}}{k_{tub}} + \frac{1}{(h_{c_A} + h_{r_A})} + \frac{r_{to} ln \frac{r_{co_{9\,5/8}}}{r_{ci_{9\,5/8}}}}{k_{csg}} + \frac{r_{to} ln \frac{r_{wb}}{r_{co_{9\,5/8}}}}{k_{cem}} \right]^{-1} \quad \text{(B.4)}$$

B.1.3 Case 3

B.1.3.1 Temperature from Flowing Fluid to Cement-Formation Interface for Case 3

$$\begin{aligned} (T_f - T_{wb}) = (T_f - T_{ti}) + (T_{ti} - T_{to}) + \left(T_{to} - T_{ci_{9\,5/8}}\right) + \left(T_{ci_{9\,5/8}} - T_{co_{9\,5/8}}\right) \\ + \left(T_{co_{9\,5/8}} - T_{ci_{13\,3/8}}\right) + \left(T_{ci_{13\,3/8}} - T_{co_{13\,3/8}}\right) + (T_{co_{13\,3/8}} - T_{wb}) \end{aligned} \quad \text{(B.5)}$$

B.1.3.2 Overall Heat Transfer Coefficient for Case 3

Excluding forced convection in tubing.

$$\begin{aligned} U_{to} = \left[\frac{r_{to} ln \frac{r_{to}}{r_{ti}}}{k_{tub}} + \frac{1}{(h_{c_A} + h_{r_A})} + \frac{r_{to} ln \frac{r_{co_{9\,5/8}}}{r_{ci_{9\,5/8}}}}{k_{csg}} + \frac{r_{to}}{r_{co_{9\,5/8}}(h_{c_B} + h_{r_B})} + \frac{r_{to} ln \frac{r_{co_{13\,3/8}}}{r_{ci_{13\,3/8}}}}{k_{csg}} \right. \\ \left. + \frac{r_{to} ln \frac{r_{wb}}{r_{co_{13\,3/8}}}}{k_{cem}} \right]^{-1} \end{aligned} \quad \text{(B.6)}$$

B.1.4 Case 4

B.1.4.1 Temperature from Flowing Fluid to Cement-Formation Interface for Case 4

$$\begin{aligned} (T_f - T_{wb}) = (T_f - T_{ti}) + (T_{ti} - T_{to}) + \left(T_{to} - T_{ci_{9\,5/8}}\right) + \left(T_{ci_{9\,5/8}} - T_{co_{9\,5/8}}\right) \\ + \left(T_{co_{9\,5/8}} - T_{ci_{13\,3/8}}\right) + \left(T_{ci_{13\,3/8}} - T_{co_{13\,3/8}}\right) + \left(T_{co_{13\,3/8}} - T_{ci_{20}}\right) \\ + \left(T_{ci_{20}} - T_{co_{20}}\right) + (T_{co_{20}} - T_{wb}) \end{aligned} \quad \text{(B.7)}$$

B.1.4.2 Overall Heat Transfer Coefficient for Case 4

Excluding forced convection in tubing.

$$U_{to} = \left[\frac{r_{to} ln \frac{r_{to}}{r_{ti}}}{k_{tub}} + \frac{1}{(h_{c_A} + h_{r_A})} + \frac{r_{to} ln \frac{r_{co_{9\,5/8}}}{r_{ci_{9\,5/8}}}}{k_{csg}} + \frac{r_{to}}{r_{co_{9\,5/8}}(h_{c_B} + h_{r_B})} + \frac{r_{to} ln \frac{r_{co_{13\,3/8}}}{r_{ci_{13\,3/8}}}}{k_{csg}} + \frac{r_{to} ln \frac{r_{ci_{20}}}{r_{co_{13\,3/8}}}}{k_{cem}} + \frac{r_{to} ln \frac{r_{co_{20}}}{r_{ci_{20}}}}{k_{csg}} + \frac{r_{to} ln \frac{r_{wb}}{r_{co_{20}}}}{k_{cem}} \right]^{-1} \quad \text{(B.8)}$$

B.1.5 Case 5

B.1.5.1 Temperature from Flowing Fluid to Cement-Formation Interface for Case 5

$$\begin{aligned} (T_f - T_{wb}) = {} & (T_f - T_{ti}) + (T_{ti} - T_{to}) + \left(T_{to} - T_{ci_{9\,5/8}}\right) + \left(T_{ci_{9\,5/8}} - T_{co_{9\,5/8}}\right) \\ & + \left(T_{co_{9\,5/8}} - T_{ci_{13\,3/8}}\right) + \left(T_{ci_{13\,3/8}} - T_{co_{13\,3/8}}\right) + \left(T_{co_{13\,3/8}} - T_{ci_{20}}\right) \\ & + \left(T_{ci_{20}} - T_{co_{20}}\right) + \left(T_{co_{20}} - T_{ci_{30}}\right) + \left(T_{ci_{30}} - T_{co_{30}}\right) + \left(T_{co_{30}} - T_{wb}\right) \end{aligned} \quad \text{(B.9)}$$

B.1.5.2 Overall Heat Transfer Coefficient for Case 5

Excluding forced convection in tubing.

$$U_{to} = \left[\frac{r_{to} ln \frac{r_{to}}{r_{ti}}}{k_{tub}} + \frac{1}{(h_{c_A} + h_{r_A})} + \frac{r_{to} ln \frac{r_{co_{9\,5/8}}}{r_{ci_{9\,5/8}}}}{k_{csg}} + \frac{r_{to}}{r_{co_{9\,5/8}}(h_{c_B} + h_{r_B})} + \frac{r_{to} ln \frac{r_{co_{13\,3/8}}}{r_{ci_{13\,3/8}}}}{k_{csg}} + \frac{r_{to} ln \frac{r_{ci_{20}}}{r_{co_{13\,3/8}}}}{k_{cem}} + \frac{r_{to} ln \frac{r_{co_{20}}}{r_{ci_{20}}}}{k_{csg}} + \frac{r_{to} ln \frac{r_{ci_{30}}}{r_{co_{20}}}}{k_{cem}} + \frac{r_{to} ln \frac{r_{co_{30}}}{r_{ci_{30}}}}{k_{csg}} + \frac{r_{to} ln \frac{r_{wb}}{r_{co_{300}}}}{k_{cem}} \right]^{-1} \quad \text{(B.10)}$$

B.2 Dropkin and Somercales Correlation

The Nusselt number is depending on the angel of inclination. Equation (5.23) is expressed with a constant, C, that depends on the angel of inclination, from horizontal. The correlation factors are shown in **Error! Reference source not found.**.

Table B-1Correlation factors with respect to angel of inclination (Dropkin & Somerscales, 1965)

Inclination from horizontal, θ	Correction factor, C
degrees	#
0	0,069
30	0,065
45	0,059
60	0,057
90	0,049

Appendix C Additional Results

C.1 Thermal Diffusivity of Formation at Short Duration of Production

By set the production time to 24 hours, assumed to be transient conditions, in order to see the influence of the thermal diffusivity of the formation. Although, the model does not yield for transient conditions in the wellbore, the interesting part is to see the relationship of the how thermal diffusivity versus the production time influence the temperature distribution.

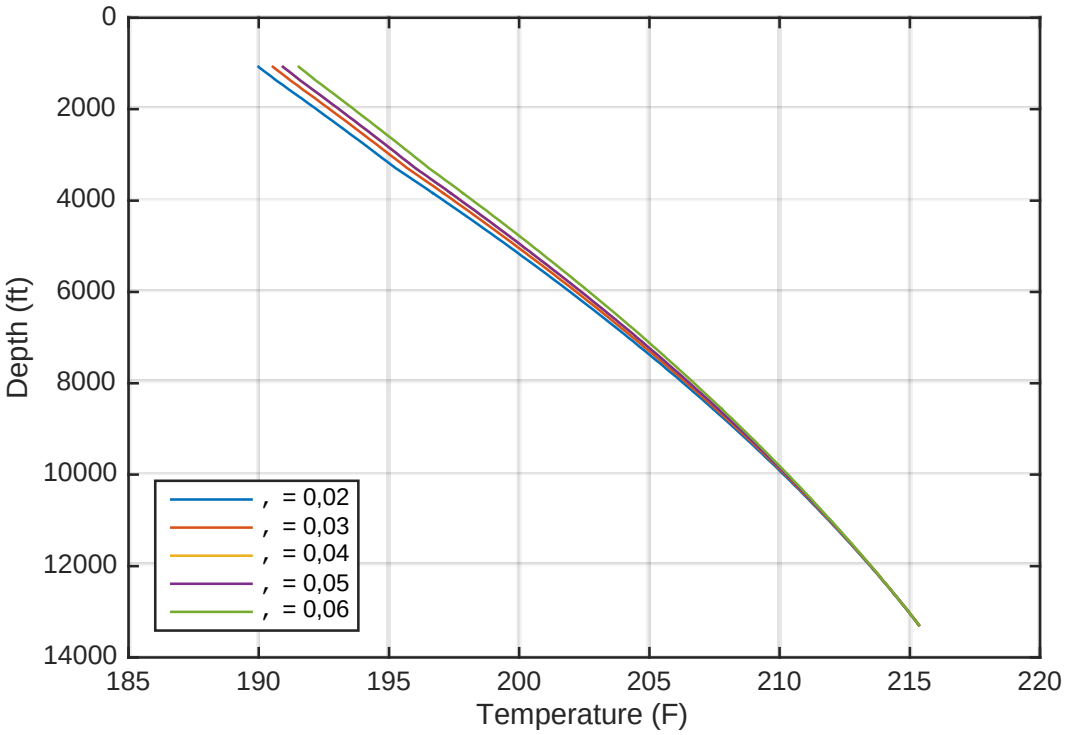

Figure C-1Temperature distribution with various thermal diffusivities of the formation. Production duration set to be 24 hours.

C.2 Calculated Temperature

The temperature distribution profile from the temperature mode, the conventional ILS and the HPHT ILS are presented in Table C-1.

Table C-1Temperature profile from the model an both ILS.

Temperature model		Conventional ILS		HPHT ILS	
MD (ft)	Temperature (°F)	MD (ft)	Temperature (°F)	MD (ft)	Temperature (°F)
327,00	195,10	327,00	215,35	327,00	208,99
330,00	195,11	330,00	215,35	327,15	209,01
360,00	195,30	360,00	215,35	327,30	209,01
390,00	195,48	390,00	215,35	327,46	209,01
420,00	195,66	420,00	215,35	327,61	209,01
450,00	195,85	450,00	215,35	327,91	209,02
480,00	196,03	480,00	215,35	328,22	209,02
510,00	196,22	510,00	215,35	328,83	209,02
540,00	196,40	540,00	215,35	329,44	209,02
570,00	196,59	570,00	215,35	330,35	209,02
600,00	196,77	600,00	215,35	331,88	209,03
630,00	196,95	630,00	215,35	333,09	209,03
660,00	197,13	660,00	215,35	334,92	209,03

690,00	197,32	690,00	215,35	336,75	209,04
720,00	197,50	720,00	215,35	339,52	209,05
750,00	197,68	750,00	215,35	342,28	209,05
780,00	197,86	780,00	215,35	347,82	209,06
810,00	198,04	810,00	215,35	358,88	209,09
840,00	198,22	840,00	215,35	381,00	209,13
870,00	198,40	870,00	215,35	397,45	209,18
900,00	198,58	900,00	215,35	405,68	209,20
930,00	198,75	930,00	215,35	413,90	209,22
960,00	198,93	960,00	215,35	420,00	209,24
990,00	199,11	990,00	215,35	426,10	209,25
1000,00	199,17	1000,00	215,35	433,87	209,27
1020,00	199,29	1020,00	215,35	441,65	209,29
1050,00	199,47	1050,00	215,35	457,20	209,32
1080,00	199,65	1080,00	215,35	495,30	209,40
1110,00	199,83	1110,00	215,35	533,40	209,49
1140,00	200,01	1140,00	215,35	609,60	209,65
1170,00	200,19	1170,00	215,35	685,80	209,82
1200,00	200,37	1200,00	215,35	762,00	210,00

1230,00	200,55	1230,00	215,35	838,20	210,17
1260,00	200,73	1260,00	215,35	914,40	210,34
1290,00	200,90	1290,00	215,35	952,50	210,44
1320,00	201,08	1320,00	215,35	971,55	210,50
1350,00	201,26	1350,00	215,35	981,08	210,52
1380,00	201,43	1380,00	215,35	985,84	210,53
1410,00	201,61	1410,00	215,35	990,60	210,54
1440,00	201,79	1440,00	215,35	993,90	210,55
1470,00	201,96	1470,00	215,35	1000,00	210,56
1500,00	202,13	1500,00	215,35	1006,10	210,58
1530,00	202,31	1530,00	215,35	1021,27	210,61
1560,00	202,48	1560,00	215,35	1036,45	210,64
1590,00	202,65	1590,00	215,35	1066,80	210,70
1620,00	202,83	1620,00	215,35	1104,90	210,78
1650,00	203,00	1650,00	215,35	1143,00	210,86
1680,00	203,17	1680,00	215,35	1219,20	211,01
1710,00	203,34	1710,00	215,35	1295,40	211,17
1740,00	203,51	1740,00	215,35	1371,60	211,33

1770,00	203,68	1770,00	215,35	1447,80	211,49
1800,00	203,85	1800,00	215,35	1524,00	211,64
1830,00	204,02	1830,00	215,35	1600,20	211,79
1860,00	204,19	1860,00	215,35	1676,40	211,94
1890,00	204,35	1890,00	215,35	1752,60	212,09
1920,00	204,52	1920,00	215,35	1828,80	212,24
1950,00	204,69	1950,00	215,35	1905,00	212,38
1980,00	204,86	1980,00	215,35	1981,20	212,52
2010,00	205,02	2010,00	215,35	2057,40	212,66
2040,00	205,19	2040,00	215,35	2085,65	212,72
2070,00	205,35	2070,00	215,35	2099,78	212,75
2100,00	205,52	2100,00	215,35	2113,90	212,77
2117,00	205,61	2117,00	215,35	2116,95	212,78
2130,00	205,68	2130,00	215,35	2120,00	212,79
2160,00	205,84	2160,00	215,35	2123,05	212,79
2190,00	206,01	2190,00	215,35	2126,10	212,80
2220,00	206,17	2220,00	215,35	2133,60	212,81
2250,00	206,33	2250,00	215,35	2143,13	212,83
2280,00	206,49	2280,00	215,35	2152,65	212,84

2310,00	206,65	2310,00	215,35	2171,70	212,87
2340,00	206,81	2340,00	215,35	2209,80	212,93
2370,00	206,97	2370,00	215,35	2286,00	213,05
2400,00	207,13	2400,00	215,35	2362,20	213,18
2430,00	207,29	2430,00	215,35	2438,40	213,30
2460,00	207,45	2460,00	215,35	2514,60	213,42
2490,00	207,61	2490,00	215,35	2590,80	213,54
2520,00	207,77	2520,00	215,35	2667,00	213,66
2550,00	207,92	2550,00	215,35	2743,20	213,77
2580,00	208,08	2580,00	215,35	2819,40	213,88
2610,00	208,24	2610,00	215,35	2895,60	214,00
2640,00	208,39	2640,00	215,35	2971,80	214,10
2670,00	208,55	2670,00	215,35	3048,00	214,21
2700,00	208,70	2700,00	215,35	3124,20	214,31
2730,00	208,85	2730,00	215,35	3200,40	214,41
2760,00	209,01	2760,00	215,35	3276,60	214,51
2790,00	209,16	2790,00	215,35	3352,80	214,61
2820,00	209,31	2820,00	215,35	3429,00	214,70

2850,00	209,47	2850,00	215,35	3505,20	214,79
2880,00	209,62	2880,00	215,35	3581,40	214,88
2910,00	209,77	2910,00	215,35	3592,90	214,89
2940,00	209,92	2940,00	215,35	3593,90	214,89
2970,00	210,07	2970,00	215,35	3599,00	214,90
3000,00	210,22	3000,00	215,35	3600,00	214,90
3030,00	210,37	3030,00	215,35	3605,10	214,91
3060,00	210,52	3060,00	215,35	3606,09	214,91
3090,00	210,67	3090,00	215,35	3657,60	214,97
3120,00	210,82	3120,00	215,35	3733,80	215,05
3150,00	210,96	3150,00	215,35	3810,00	215,13
3180,00	211,11	3180,00	215,35	3886,20	215,20
3210,00	211,26	3210,00	215,35	3962,40	215,28
3240,00	211,40	3240,00	215,35	4038,60	215,35
3270,00	211,55	3270,00	215,35	4045,90	215,35
3300,00	211,70	3300,00	215,35	4052,00	215,35
3330,00	211,84	3330,00	215,35		
3360,00	211,98	3360,00	215,35		
3390,00	212,13	3390,00	215,35		

3420,00	212,27	3420,00	215,35		
3450,00	212,42	3450,00	215,35		
3480,00	212,56	3480,00	215,35		
3510,00	212,70	3510,00	215,35		
3540,00	212,84	3540,00	215,35		
3570,00	212,98	3570,00	215,35		
3600,00	213,12	3600,00	215,35		
3630,00	213,26	3630,00	215,35		
3660,00	213,40	3660,00	215,35		
3690,00	213,54	3690,00	215,35		
3700,00	213,59	3700,00	215,35		
3720,00	213,68	3720,00	215,35		
3750,00	213,82	3750,00	215,35		
3780,00	213,96	3780,00	215,35		
3810,00	214,09	3810,00	215,35		
3840,00	214,23	3840,00	215,35		
3870,00	214,37	3870,00	215,35		
3900,00	214,50	3900,00	215,35		

3930,00	214,64	3930,00	215,35		
3960,00	214,77	3960,00	215,35		
3990,00	214,91	3990,00	215,35		
4020,00	215,04	4020,00	215,35		
4052,00	215,18	4052,00	215,35		

Appendix D MATLAB codes

D.1 Model Verification

The model is validated from Willhite's example in his paper from 1967 (Willhite, 1967). The input variables and the solution are included in the script. The function does an iterative process to find a proper value of the overall heat transfer coefficient based on the steam injection temperature.

D.1.1 Script

```
%%%-------------------------------------------------------------------------%%%
%%%-------------------------Model Verification-----------------------------%%%
%%%-----------------------Last updated 11.05.15----------------------------%%%
%%%-------------------------------------------------------------------------%%%
%%%------------------Testing Willhite's (1967) method-------------------%%%
%%%-------------------------------------------------------------------------%%%

%Steam at 600F is injected down 3 1/2in tubing set on a 9 5/8in packer,
%53.5 kb/ft, N-80 casing. The annulus contains a stagnant gas at 14.7 psia
%and the casing is cemented to surface in a 12in hole. A temperature survey
%in the well indicates a mean subsurface temperature of 100F. The reservoir
%is at 1,000 ft.

%Estimate the over-all heat transfer coefficient, averange
%casing and wellbore heat loss after 21 days of continuous injection.

%Input data
r_to=0.146;      %ft
r_ci=0.355;      %ft
r_co=0.400;      %ft
r_wb=0.500;      %ft
alpha=0.0286;    %sq-ft/hr
k_e=1.0;         %Btu/hr sg ft F/ft
e_to=0.9;
e_ci=e_to;
```

```
    k_cem=0.2;      %Btu/hr sg ft F/ft

SB=1.713e-9;    %Stefan-Boltzmann constant

t=21*24;    %Time in hr
T_geo=100;  %Geothermal temp, F
T_f=600;    %Steam injection temp

%Input to calculate h_c:
rho_an=0.0388;  %lb/cu ft
my_an=0.069;    %lb mass/ft hr
cp_an=0.245;    %Btu/lb F (Heat capasity of fluid in annulus)
k_ha=0.0255;    %Btu/hr sq ft F/ft (Thermal conductivity)
g=4.17e8;       %ft/hr^2 (Accelration due to gravity)

U_to=zeros(2,1);    %Make a matrix with zeros.
T_wb=zeros(size(U_to));

%Estimated U_to from Fig 3. / Guessed parameter
U_to(1)= 4.05;  %Btu/hr sg ft F/ft

for i=2:length(U_to)

    [U_to(i), T_wb(i)] = Uwillhite(U_to(i-1),r_wb,t,alpha,T_f,k_e,r_to,...
        T_geo,r_co,k_cem,e_to,r_ci,e_ci,SB,cp_an,my_an,k_ha,rho_an,g)

end
```

D.1.2 Function

```
%%%-------------------------------------------------------------------------%%%
%%%------------------Function for "Willhiteeexample"--------------------%%%
%%%-----------------------Last updated 11.05.15-------------------------%%%
%%%-------------------------------------------------------------------------%%%

%The function is used for an iterative solution to determine a proper
```

```
%combination of U_to and T_ci.

function [U_to_new, T_wb] = Uwillhite(U_temp,r_wb,t,alpha,T_f,k_e,r_to,...
    T_geo,r_co,k_cem,e_to,r_ci,e_ci,SB,cp_an,my_an,k_ha,rho_an,g)

f_t=log(2*sqrt(alpha*t)/r_wb)-0.29;

run_while=5;
Counter=0;

while run_while>4;
    Counter=Counter+1;
    T_wb=(T_f*f_t+(k_e/(r_to*U_temp)*T_geo))/(f_t+(k_e/(r_to*U_temp)));
    T_ci=T_wb+(r_to*U_temp*log(r_wb/r_co))/k_cem*(T_f-T_wb);

    F_tci=1/((1/e_to)+((r_to/r_ci)*(1/e_ci-1)));
    %Temperatures i Rankin (T(R)=T(F)+460)
    h_r=SB*F_tci*((T_f+460).^2+(T_ci+460).^2)*((T_f+460)+(T_ci+460));

    T_an=(T_f+T_ci)/2;      %Temp in Annulus, F
    betta=1/(T_an+460);     %Temp in R
    %Prandtl number, Pr
    Pr=(cp_an*my_an)/k_ha;
    %Grashof number, Gr
    Gr=((r_ci-r_to).^3*g*rho_an.^2*betta*(T_f-T_ci))/my_an.^2;
    h_c=((0.049*(Gr*Pr).^(1/3))*(Pr.^0.074)*k_ha)/(r_to*log(r_ci/r_to));

    %Overall heat transfer coefficient, Btu/hr sq ft F
    U_to_new=(1/(h_c+h_r)+(r_to*log(r_wb/r_co))/k_cem).^-1;

    %Margin of error in the iterative approach
    if abs(U_to_new-U_temp)<1e-10
        break
    else
        U_temp=U_to_new;
```

```
        end

end
disp(['Counter:' num2str(Counter)]);
end
```

D.2 Temperature Simulation Model

The input variables and the solutions for the temperature simulation model are presented in the script. The calculation of the overall heat transfer coefficient and the wellbore fluid temperature for each differential element for the different annuluses presented in Figure 6-1 are conducted with the different functions.

D.2.1 The Main Script

```
%%%-------------------------------------------------------------------------%%%
%%%-------------------------Master Thesis 2015------------------------------%%%
%%%-----------------------------Mainscript----------------------------------%%%
%%%------------------------Knut Vegard Loebergsli-------------------------%%%
%%%------------------Heat transfere during production-------------------%%%
%%%------------------------Last updated 05.06.15-------------------------%%%
%%%-------------------------------------------------------------------------%%%

% Main function: Calculate the temperature distribution profile

% The scipt defines input variables from the trajectory (readed from excel)
% and the well design.
% Other input data is specified:
% - Geothermal gradient
% - Thermal properties
% - Reservoir fluid data, production rate and production time
% - Annulus fluid properties

% The script gives input data to the 5 different function, one for each
% case, and retrieves the results.

%%%-------------------------------------------------------------------------%%%

close all

%Read the general MD, TVD and Inclination form Excel
input=xlsread('DepthKV.xlsx','general');
```

```
    %Flip matrix in input
    B=flipud(input);

%Sorting parameters in Excel file
MD=B(:,1)/.3048;
TVD=B(:,2)/.3048;
INC=B(:,3);
%Horizontal inclination
HOR=90-INC;

% %ft=in/12
% %ft=m/0.3048

%Defining shoe depth and top of cement for all sections. All given in ft.

%7in liner, 13Cr-110
shoe7=4052/.3048;
toc7=3600/0.3048;
%Assuming that the production tubing and the liner has same diameter.
%Tubing outside radius, ft
r_to=7/2/12;
%Thickness, ft
t_7=0.498/12;
%Tubing inside radius, ft
r_ti=r_to-t_7;
%Radius of drill hole, ft
r_wb_7=8.5/2/12;

%9 5/8in casing, P-110
shoe958=3600/.3048;
toc958=2120/.3048;
%Casing outside radius,ft
r_co_9=(9+5/8)/2/12;
%Thickness, ft
t_9=0.545/12;
```

```
%Casing inside radius, ft
r_ci_9=r_co_9-t_9;
%Radius of drill hole, ft
r_wb_9=12.25/2/12;

%13 3/8in casing, P-110
shoe1338=2120/.3048;
toc1338=327/.3048;
%Casing outside radius,ft
r_co_13=(13+3/8)/2/12;
%Thickness, ft
t_13=0.514/12;
%Casing inside radius, ft
r_ci_13=r_co_13-t_13;
%Radius of drill hole, ft
r_wb_13=17.5/2/12;

%20in casing, X-56
shoe20=1000/.3048;
toc20=327/.3048;
%Casing outside radius,ft
r_co_20=20/2/12;
%Thickness, ft
t_20=0.635/12;
%Casing inside radius, ft
r_ci_20=r_co_20-t_20;
%Radius of drill hole, ft
r_wb_20=26/2/12;

%30in casing, X-52
shoe30=420/.3048;
toc30=327/.3048;
%Casing outside radius,ft
r_co_30=30/2/12;
%Thickness, ft
```

```
    t_30=1/12;
    %Casing inside radius, ft
r_ci_30=r_co_30-t_30;
%Radius of drill hole, ft
r_wb_30=36/2/12;

%Mudline = ml, ft
ml=327/0.3048;
%Mudline temp = ml_t, F
ml_T=39.2;

%Geothermal gradient, F/ft
g_T=0.0144;
%Matrix, same size as MD/TVD
T_geo=zeros(size(MD));
%Geothermal temperature (F) given by:
T_geo(:,1) = ml_T+(TVD(:,1)-ml)*g_T;

%Thermal properties of tubing, casing and formation.
%Thermal conductivity of formation from ILS, Btu/(hr-ft-F)
k_e=0.92;
%Thermal conductivity of tubing from ILS, Btu/(hr-ft-F)
k_tub=26.2;
%Emissitvity of outside tubing surface, dimensionless
e_to=0.9;
%Thermal conductivity of casing from ILS, Btu/(hr-ft-F)
k_csg=26.2;
%Emissitvity of outside casing surface (for all csg), dimensionless
e_co=0.9;
%Emissitvity of inside casing surface (for all csg), dimensionless
e_ci=0.9;
%Thermal conductivity of cement from ILS, Btu/(hr-ft-F)
k_cem=0.568;
%Thermal diffusivity of formation/earth, sq ft/hr
alpha=0.04;     %From Hasan and Kabir
```

```
%Stefan-Boltzmann constant, Btu/sq ft hr R
SB=1.713e-9;

%Production and reservoir fluid data:
%Assumed to produce "seawater"
%Production time, hr
t=2000;
%Reservoir temperature, F
T_res=T_geo;
%Total mas flow rate, lbm/sec (5000 m3/day)
W_sec=131.54;
%Total mas flow rate, lbm/hr
W=W_sec*3600;
%Heat capacity of wellbore fluid, Btu/lbm F
cp_f=3974.1/4186.8;                 %from [J/kg K] to [Btu/lbm F]

%Annulus A data - ref nr.1. Seawater in annulus.
%Density of annular fluid from Wellcat, lbm/cu ft
rho_an1=1031.1/16.01846;            %from [kg/m3] to [lbm/cu ft]
%Platic viscosity of annular fluid from Wellcat, lbm/ft hr
my_an1=1.089/0.4133788732138;       %from [cp] to [lbm/ft hr]
%Thermal conductivity of annular fluid, Btu/hr ft F
k_an1=0.601/1.7307;                 %from [W/mK] to [Btu/hr ft F]
%Heat capasity of annular fluid, Btu/lbm F
cp_an1=3974.1/4186.8;               %from [J/kg K] to [Btu/lbm F]

%Annulus B data - ref nr.2 Seawater in annulus.
%Density of annular fluid from Wellcat, lbm/cu ft
rho_an2=1031.1/16.01846;            %from [kg/m3] to [lbm/cu ft]
%Platic viscosity of annular fluid from Wellcat, lbm/ft hr
my_an2=1.089/0.4133788732138;       %from [cp] to [lbm/ft hr]
%Thermal conductivity of annular fluid, Btu/hr ft F
k_an2=0.601/1.7307;                 %from [W/mK] to [Btu/hr ft F]
%Heat capasity of annular fluid, Btu/lbm F
cp_an2=3974.1/4186.8;               %from [J/kg K] to [Btu/lbm F]
```

```
    %Accelration due to gravity, ft/sec^2
g=32.2;
%Conversion factor, lbm ft/lbf sq sec
g_c=32.2;
%Accelration due to gravity, ft/hr^2
g_hr=32.2*3600.^2;
%Mechanical equivalent of heat, ft-lbf/Btu
J=778;

%Creating matrix of T_f and U_to with same size as MD/TVD
T_f = zeros(size(MD));
U_to = T_f;
T_co=zeros(size(MD));
T_wb=zeros(size(MD));

%Defining the first step for those variables were that is needed:
%First U_to - over-all heat transfer coefficient, Btu/hr sq ft F
U_to(1)=(r_to*log(r_to/r_ti)/k_tub + r_to*log(r_wb_7/r_to)/k_cem).^-1;
% %Assuming thermal conducitivty in tubing and casing is high;
% %T_ti=T_to
% %Neglecting resistance in the tubing.
% U_to(1)=(r_to*log(r_wb_7/r_to)/k_cem).^-1;

%First T_f is assumed to be like the reservoir temp, F.
T_f(1)=T_res(1);

Counter=0;
for i=2:length(MD)
   %Case 1
   if MD(i)<=shoe7 && MD(i)>=shoe958
        U_to(i)=U_to(1);
        [T_f(i), T_wb(i)] = TUpred1(T_f(i-1),U_to(i),MD(i-1),MD(i),...
            T_geo(i-1),T_geo(i),alpha,t,r_wb_7,cp_f,W,k_e,r_to,g,...
            HOR(i),g_c,J,g_T);
```

XXX

```
    %Case 2
    elseif MD(i)<shoe958 && MD(i)>=shoe1338
         [U_to(i),  T_f(i), T_co(i), T_wb(i)] = TUpred2(T_f(i-1),...
             U_to(i-1),MD(i-1),MD(i),T_geo(i-1),T_geo(i),HOR(i),alpha,...
             t,r_wb_9,k_e,r_to,r_co_9,k_cem,r_ci_9,k_csg,cp_an1,my_an1,...
             k_an1,g_hr,rho_an1,k_tub,r_ti,e_to,e_ci,SB,cp_f,W,g,g_c,J,g_T);
    %Case 3
    elseif MD(i)<shoe1338 && MD(i)>=shoe20
         [U_to(i), T_f(i), T_co(i), T_wb(i)] = TUpred3(T_f(i-1),...
             U_to(i-1),MD(i-1),MD(i),T_geo(i-1),T_geo(i),HOR(i),...
             T_co(i-1),alpha,t,r_wb_13,r_to,k_e,r_co_13,k_cem,r_ci_13,...
             k_csg,r_co_9,e_co,e_ci,SB,cp_an2,my_an2,k_an2,rho_an2,g_hr,...
             e_to,r_ci_9,cp_an1,my_an1,k_an1,rho_an1,r_ti,g,g_c,J,cp_f,...
             g_T,k_tub,W);
    %Case 4
    elseif MD(i)<shoe20 & MD(i)>=shoe30
         [U_to(i), T_f(i), T_co(i), T_wb(i)] = TUpred4(T_f(i-1),...
             U_to(i-1),MD(i-1),MD(i),T_geo(i-1),T_geo(i),HOR(i),...
             T_co(i-1),alpha,t,r_wb_20,r_to,k_e,r_co_13,k_cem,r_ci_13,...
             k_csg,r_co_9,e_co,e_ci,SB,cp_an2,my_an2,k_an2,rho_an2,g_hr,...
             e_to,r_ci_9,cp_an1,my_an1,k_an1,rho_an1,r_ti,g,g_c,J,cp_f,...
             g_T,k_tub,W,r_co_20,r_ci_20);
    %Case 5
    elseif MD(i)<shoe30 & MD(i)>=ml
        [U_to(i),  T_f(i), T_co(i), T_wb(i)] = TUpred5(T_f(i-1),...
            U_to(i-1),MD(i-1),MD(i),T_geo(i-1),T_geo(i),HOR(i),...
            T_co(i-1),alpha,t,r_wb_30,r_to,k_e,r_co_13,k_cem,r_ci_13,...
            k_csg,r_co_9,e_co,e_ci,SB,cp_an2,my_an2,k_an2,rho_an2,g_hr,...
            e_to,r_ci_9,cp_an1,my_an1,k_an1,rho_an1,r_ti,g,g_c,J,cp_f,...
            g_T,k_tub,W,r_co_20,r_ci_20,r_co_30,r_ci_30);
    end
end
```

```
    %Read "industry leading software" temperatures form Excel
    input2=xlsread('WCtemp.xls');
%Flip matrix in input2
WC=flipud(input2);
%Sorting parameters
MD2=WC(:,1)/.3048;
T_f_wc=WC(:,2);
T_ti_wc=WC(:,3);

Tliste=zeros(length(T_f),2); Tliste(:,1)=MD*0.3048;Tliste(:,2)=T_f;...
    Tliste(:,3)=T_geo;Tliste(:,4)=T_co;Tliste(:,5)=T_wb;Tliste(:,6)=U_to;

%Read "force due to temperature" form Excel
input3=xlsread('DepthKV.xlsx','force');
%Flip matrix in input
force=flipud(input3);
%Sorting parameters
F_ML=force(:,1);
F_SC=force(:,2);
F_WC=WC(:,14);
```

D.2.2 Functions

D.2.2.1 Function for Case 1

```
%%%-------------------------------------------------------------------%%%
%%%-------------------------Master Thesis 2015------------------------%%%
%%%---------------------------------Case 1----------------------------%%%
%%%------------------------Knut Vegard Loebergsli---------------------%%%
%%%--------------Calculation of wellbore fluid temperature------------%%%
%%%------------------------Last updated 05.06.15----------------------%%%
%%%-------------------------------------------------------------------%%%

% TUpred1 calculates the fluid temperature in case nr.1

%%%-------------------------------------------------------------------%%%
```

```
function [T_f, T_wb_7] = TUpred1(T_prev,U_i,MD_prev,MD,T_g_prev,T_g,...
    alpha,t,r_wb_7,cp_f,W,k_e,r_to,g,hor,g_c,J,g_T)

%Where:
%T_prev=T_f(i-1)
%U_i=U_to(i)
%MD_prev=MD(i-1)
%MD=MD(i)
%T_g_prev=T_geo(i-1)
%T_g=T_geo(i)
%hor=HOR(i)

%Transient time function, dimensionless. Devloped by Ramey (1962)
% f_t=log(2*sqrt(alpha*t)/r_wb_7)-0.29;

%Tranisent time function, dimensionless. Developed by Hasan and Kabir
%(1994)
t_D=alpha*t/r_wb_7;

if t_D>=1e-10 && t_D<=1.5
    f_t=1.1281*sqrt(t_D)*(1-0.3*sqrt(t_D));
else
    f_t=(0.4063+0.5*log(t_D))*(1+0.6/t_D);
end

%Temperature at cement-formation interface, F
T_wb_7=(T_prev*f_t + (k_e/(r_to*U_i)*T_g))/(f_t + (k_e/(r_to*U_i)));

%Inverse relaxation distance, ft
A=cp_f*W/(2*pi)*((k_e+(r_to*U_i*f_t))/(r_to*U_i*k_e));

%Temperature of flowing fluid, F
T_f=T_g + A*(1-exp((-MD_prev+MD)/A))*(-g*sin(degtorad(hor))/...
    (g_c*J*cp_f) + g_T*sin(degtorad(hor))) + exp((-MD_prev+MD)/A)*...
    (T_prev-T_g_prev);
```

```
    end
```

D.2.2.2 Function for Case 2

```
%%%-------------------------------------------------------------------------%%%
%%%-------------------------Master Thesis 2015------------------------------%%%
%%%--------------------------------Case 2-----------------------------------%%%
%%%------------------------Knut Vegard Loebergsli-------------------------%%%
%%%---------Calculation of the overall heat transfer coefficient--------%%%
%%%-----------------and the wellbore fluid temperature-------------------%%%
%%%-------------------------Last updated 05.06.15-------------------------%%%
%%%-------------------------------------------------------------------------%%%

% TUpred2 calculates the fluid temperature in case nr.2 by an iterative
% process until convergence is obtained with the guessed and calculated
% U_to.

%%%-------------------------------------------------------------------------%%%

function [U_new, T_new, T_co_9, T_wb_9] = TUpred2(T_prev,U_prev,...
    MD_prev,MD_i,T_g_prev,T_g,hor,alpha,t,r_wb_9,k_e,r_to,r_co_9,...
    k_cem,r_ci_9,k_csg,cp_an1,my_an1,k_an1,g_hr,rho_an1,k_tub,r_ti,...
    e_to,e_ci,SB,cp_f,W,g,g_c,J,g_T)

%Where:
%T_prev=T_f(i-1)
%T_new=T_f(i)
%U_prev=U_to(i-1)
%U_new=U_to(i)
%MD_prev=MD(i-1)
%MD_i=MD(i)
%T_g_prev=T_geo(i-1)
%T_g=T_geo(i))
%hor=HOR(i)
```

```
%Transient time function, dimensionless. Devloped by Ramey (1962)
% f_t=log(2*sqrt(alpha*t)/r_wb_9)-0.29;

%Tranisent time function, dimensionless. Developed by Hasan and Kabir
%(1994)
t_D=alpha*t/r_wb_9;

if t_D>=1e-10 && t_D<=1.5
    f_t=1.1281*sqrt(t_D)*(1-0.3*sqrt(t_D));
else
    f_t=(0.4063+0.5*log(t_D))*(1+0.6/t_D);
end



run_while=2;
Counter2=0;

while run_while>1;
    Counter2=Counter2+1;
    %Temperature at cement-formation interface, F
    T_wb_9=(T_prev*f_t + (k_e/(r_to*U_prev)*T_g))/...
        (f_t + (k_e/(r_to*U_prev)));
    %Temperature outside of 9 5/8 casing surface, F
    T_co_9=T_wb_9 + r_to*U_prev*(log(r_wb_9/r_co_9)/k_cem)*(T_prev-T_wb_9);
    %Temperature inside of 9 5/8 casing surface, F
    T_ci_9=T_co_9 + r_to*U_prev*log(r_co_9/r_ci_9)/k_csg*(T_prev-T_wb_9);

%     %Assuming thermal conducitivty in tubing and casing is high;
%     %T_ti=T_to and T_ci=T_co
%     %Temperature outside of 9 5/8 casing surface, F
%     T_co_9=T_wb_9+...
%          (r_to*U_prev*(log(r_wb_9/r_co_9)/k_cem)*(T_prev-T_wb_9));
%     %Temperature inside of 9 5/8 casing surface, F
%     T_ci_9=T_co_9;
```

```
    %View factor based on outside tubing and inside casing surfaces,
    %dimensionless
F_tci=1/((1/e_to)+((r_to/r_ci_9)*(1/e_ci-1)));
%Heat transfer for radiation, Btu/hr sq ft F
%Temperatures i Rankin (T(R)=T(F)+460)
h_r=SB*F_tci*((T_prev+460).^2 + (T_ci_9+460).^2)*...
    ((T_prev+460) + (T_ci_9+460));

%Temp in Annulus, F
T_an=(T_prev+T_ci_9)/2;
%Betta,temp in R
betta=1/(T_an+460);
%Prandtl number, Pr, dim.less
Pr=(cp_an1*my_an1)/k_an1;
%Grashof number, Gr, dim.less
Gr=((r_ci_9-r_to).^3*g_hr*rho_an1.^2*betta*abs(T_prev-T_ci_9))/...
    my_an1.^2;

%Heat transfet for natrual convection, Btu/hr sq ft F
h_c=((0.049*(Gr*Pr).^(1/3))*(Pr.^0.074)*k_an1)/(r_to*log(r_ci_9/r_to));

%Over-all heat transfer coefficient, Btu/hr sq ft F
U_new=1/(1/(h_c+h_r)+(r_to*log(r_wb_9/r_co_9))/k_cem+...
    (r_to*log(r_to/r_ti))/k_tub+(r_to*log(r_co_9/r_ci_9))/k_csg);

%     %For the assumption
%     %Over-all heat transfer coefficient, Btu/hr sq ft F
%     U_new=1/(1/(h_c+h_r)+(r_to*log(r_wb_9/r_co_9))/k_cem);

%Margin of error in the iterative approach
if abs(U_new-U_prev)<1e-10
       %Inverse relaxation distance, ft
        A=cp_f*W/(2*pi)*((k_e+r_to*U_new*f_t)/(r_to*U_new*k_e));
       %Temperature of flowing fluid, F
        T_new =  T_g + A*(1-exp((-MD_prev+MD_i)/A))*...
```

```
                (-g*sin(degtorad(hor))/(g_c*J*cp_f) +...
                g_T*sin(degtorad(hor))) + exp((-MD_prev+MD_i)/A)*...
                (T_prev-T_g_prev);
        break
    else
        U_prev=U_new;

    end

end
disp(['Counter for case 2:' num2str(Counter2(end))]);
end
```

D.2.2.3 Function for Case 3

```
%%%-------------------------------------------------------------------------%%%
%%%-------------------------Master Thesis 2015------------------------------%%%
%%%--------------------------------Case 3-----------------------------------%%%
%%%-----------------------Knut Vegard Loebergsli----------------------------%%%
%%%---------Calculation of the overall heat transfer coefficient--------%%%
%%%-----------------and the wellbore fluid temperature------------------%%%
%%%-------------------------Last updated 05.06.15---------------------------%%%
%%%-------------------------------------------------------------------------%%%

% TUpred3 calculates the fluid temperature in case nr.2 by an iterative
% process until convergence is obtained with the guessed and calculated
% U_to.

%%%-------------------------------------------------------------------------%%%


function [U_new, T_new, T_co_new, T_wb_13] = TUpred3(T_prev,U_prev,...
    MD_prev,MD_i,T_g_prev,T_g,hor,T_co_prev,alpha,t,r_wb_13,r_to,k_e,...
    r_co_13,k_cem,r_ci_13,k_csg,r_co_9,e_co,e_ci,SB,cp_an2,my_an2,...
    k_an2,rho_an2,g_hr,e_to,r_ci_9,cp_an1,my_an1,k_an1,rho_an1,r_ti,...
    g,g_c,J,cp_f,g_T,k_tub,W);
```

```
    %Where:
%T_prev=T_f(i-1)
%T_new=T_f(i)
%U_prev=U_to(i-1)
%U_new=U_to(i)
%MD_prev=MD(i-1)
%MD_i=MD(i)
%T_g_prev=T_geo(i-1)
%T_g=T_geo(i))
%hor=HOR(i)
%T_co_new=T_co(i)
%T_co_prev=T_co(i-1)

% Transient time function, dimensionless. Devloped by Ramey (1962)
% f_t=log(2*sqrt(alpha*t)/r_wb_13)-0.29;

% Tranisent time function, dimensionless. Developed by Hasan and Kabir
% (1994)
t_D=alpha*t/r_wb_13;

if t_D>=1e-10 && t_D<=1.5
    f_t=1.1281*sqrt(t_D)*(1-0.3*sqrt(t_D));
else
    f_t=(0.4063+0.5*log(t_D))*(1+0.6/t_D);
end



run_whilea=2;
run_whileb=2;
Counter3a=0;
Counter3b=0;
U_new=10;

while run_whilea>1;
```

```
    Counter3a=Counter3a+1;
    %Temperature at cement-formation interface, F
    T_wb_13=(T_prev*f_t + (k_e/(r_to*U_prev)*T_g))/...
        (f_t + (k_e/(r_to*U_prev)));
    %Temperature inside of 13 3/8 casing surface, F
    T_ci_13=T_wb_13 + (r_to*U_prev*(log(r_wb_13/r_co_13)/k_cem +...
        log(r_co_13/r_ci_13)/k_csg)*(T_prev-T_wb_13));

%     %Assuming thermal conducitivty in tubing and casing is high;
%     %T_ti=T_to, T_ci_9=T_co_9 and T_ci_13=T_co_13
%     T_ci_13=T_wb_13 + (r_to*U_prev*(log(r_wb_13/r_co_13)/k_cem)*...
%         (T_prev-T_wb_13));


    %B Annulus calculations
    %View factor based on outside tubing and inside casing surfaces,
    %dimensionless
    F_tci=1/((1/e_co)+((r_co_9/r_ci_13)*(1/e_ci-1)));
    %Heat transfer for radiation in B-annulus, Btu/hr sq ft F
    %Temperatures i Rankin (T(R)=T(F)+460)
    h_r2=SB*F_tci*((T_co_prev+460).^2+(T_ci_13+460).^2)*...
        ((T_co_prev+460)+(T_ci_13+460));

    %Temp in Annulus B, F
    T_an2=(T_co_prev+T_ci_13)/2;
    %Betta,temp in R
    betta2=1/(T_an2+460);
    %Prandtl number, Pr, dim.less
    Pr2=(cp_an2*my_an2)/k_an2;
    %Grashof number, Gr, dim.less
    Gr2=((r_ci_13-r_co_9).^3*g_hr*rho_an2.^2*...
        betta2*abs(T_co_prev-T_ci_13))/my_an2.^2;
    %Heat transfet for natrual convection in B-annulus, Btu/hr sq ft F
    h_c2=((0.049*(Gr2*Pr2).^(1/3))*(Pr2.^0.074)*k_an2)/...
        (r_co_9*log(r_ci_13/r_co_9));
```

```
        %New temperature outside of 9 5/8 casing surface, F
    T_co_new=T_ci_13 + r_to*U_prev/(r_co_9*(h_r2+h_c2))*(T_prev-T_wb_13);

    %Margin of error in the iterative approach
    if abs(T_co_new-T_co_prev)<1e-10
        while run_whileb>1;
            Counter3b=Counter3b+1;
            %Temperature inside of 9 5/8 casing surface, F
            T_ci_9=T_co_new + r_to*U_prev*log(r_co_9/r_ci_9)/...
                k_csg*(T_prev-T_wb_13);

%             %For the assumption
%             T_ci_9=T_co_new;

            %A annulus calculations
            %View factor based on outside tubing and inside casing surfaces
            %dimensionless
            F_tci=1/((1/e_to)+((r_to/r_ci_9)*(1/e_ci-1)));
            %Heat transfer for radiation in A-annulus, Btu/hr sq ft F
            %Temperatures i Rankin (T(R)=T(F)+460)
            h_r=SB*F_tci*((T_prev+460).^2+(T_ci_9+460).^2)*...
                ((T_prev+460)+(T_ci_9+460));

            %Temp in Annulus A, F
            T_an=(T_prev+T_ci_9)/2;
            %Betta,temp in R
            betta=1/(T_an+460);
            %Prandtl number, Pr, dim.less
            Pr=(cp_an1*my_an1)/k_an1;
            %Grashof number, Gr, dim.less
            Gr=((r_ci_9-r_to).^3*g_hr*rho_an1.^2*...
                betta*abs(T_prev-T_ci_9))/my_an1.^2;
            %Heat transfet for natrual convection in A-annulus, Btu/hr sq
ft F
```

```
            h_c=((0.049*(Gr*Pr).^(1/3))*(Pr.^0.074)*k_an1)/...
                (r_to*log(r_ci_9/r_to));

            %Over-all heat transfer coefficient, Btu/hr sq ft F
            U_new=1/(1/(h_c+h_r)+r_to/((h_c2+h_r2)*r_co_9)+...
                (r_to*log(r_wb_13/r_co_13))/k_cem+(r_to*...
                log(r_co_13/r_ci_13))/k_csg+(r_to*log(r_co_9/r_ci_9))/...
                k_csg+(r_to*log(r_to/r_ti))/k_tub);

%             %For the assumption
%             %Over-all heat transfer coefficient, Btu/hr sq ft F
%             U_new=1/(1/(h_c+h_r)+r_to/((h_c2+h_r2)*r_co_9)+...
%                 (r_to*log(r_wb_13/r_co_13))/k_cem);

            if abs(U_new-U_prev)<1e-10
                %Inverse relaxation distance, ft
                A=cp_f*W/(2*pi)*((k_e+r_to*U_new*f_t)/(r_to*U_new*k_e));
                %Temperature of flowing fluid, F
                T_new =  T_g + A*(1-exp((-MD_prev+MD_i)/A))*...
                    (-g*sin(degtorad(hor))/(g_c*J*cp_f) +...
                    g_T*sin(degtorad(hor))) + exp((-MD_prev+MD_i)/A)*...
                    (T_prev-T_g_prev);
                break
            elseif  Counter3b==100;
                    Counter3b=0;
                    break
            else
                U_prev=U_new;

            end
        end

    else
        T_co_prev=T_co_new;
    end
```

```
        if abs(T_co_new-T_co_prev)<1e-10 && abs(U_new-U_prev)<1e-10
        break
    end
end
disp(['Counter for case 3a:' num2str(Counter3a(end))]);
disp(['Counter for case 3b:' num2str(Counter3b(end))]);
end
```

D.2.2.4 Function for Case 4

```
%%%-------------------------------------------------------------------------%%%
%%%------------------------Master Thesis 2015-------------------------------%%%
%%%---------------------------------Case 4----------------------------------%%%
%%%------------------------Knut Vegard Loebergsli---------------------------%%%
%%%---------Calculation of the overall heat transfer coefficient--------%%%
%%%-----------------and the wellbore fluid temperature-------------------%%%
%%%------------------------Last updated 05.06.15--------------------------%%%
%%%-------------------------------------------------------------------------%%%

% TUpred4 calculates the fluid temperature in case nr.2 by an iterative
% process until convergence is obtained with the guessed and calculated
% U_to.

%%%-------------------------------------------------------------------------%%%


function [U_new, T_new, T_co_new, T_wb_20] = TUpred4(T_prev,U_prev,...
    MD_prev,MD_i,T_g_prev,T_g,hor,T_co_prev,alpha,t,r_wb_20,r_to,...
    k_e,r_co_13,k_cem,r_ci_13,k_csg,r_co_9,e_co,e_ci,SB,cp_an2,my_an2,...
    k_an2,rho_an2,g_hr,e_to,r_ci_9,cp_an1,my_an1,k_an1,rho_an1,r_ti,...
    g,g_c,J,cp_f,g_T,k_tub,W,r_co_20,r_ci_20);

%Where:
%T_prev=T_f(i-1)
%T_new=T_f(i)
```

```
%U_prev=U_to(i-1)
%U_new=U_to(i)
%MD_prev=MD(i-1)
%MD_i=MD(i)
%T_g_prev=T_geo(i-1)
%T_g=T_geo(i))
%hor=HOR(i)
%T_co_new=T_co(i)
%T_co_pres=T_co(i-1)

%Transient time function, dimensionless. Devloped by Ramey (1962)
% f_t=log(2*sqrt(alpha*t)/r_wb_20)-0.29;

%Tranisent time function, dimensionless. Developed by Hasan and Kabir
%(1994)
t_D=alpha*t/r_wb_20;

if t_D>=1e-10 && t_D<=1.5
    f_t=1.1281*sqrt(t_D)*(1-0.3*sqrt(t_D));
else
    f_t=(0.4063+0.5*log(t_D))*(1+0.6/t_D);
end



run_whilea=2;
run_whileb=2;
Counter4a=0;
Counter4b=0;
U_new=10;

while run_whilea>1;
    Counter4a=Counter4a+1;
    %Temperature at cement-formation interface, F
    T_wb_20=(T_prev*f_t + (k_e/(r_to*U_prev)*T_g))/...
        (f_t + (k_e/(r_to*U_prev)));
```

```
        %Temperature inside of 13 3/8 casing surface, F
        T_ci_13=T_wb_20 + (r_to*U_prev*(log(r_wb_20/r_co_20)/k_cem +...
         log(r_co_20/r_ci_20)/k_csg + log(r_ci_20/r_co_13)/k_cem +...
         log(r_co_13/r_ci_13)/k_csg)*(T_prev-T_wb_20));

%      %Assuming thermal conducitivty in tubing and casing is high;
%      %T_ti=T_to, T_ci_9=T_co_9, T_ci_13=T_co_13 and T_ci_20=T_co_20
%      T_ci_13=T_wb_20 + (r_to*U_prev*(log(r_wb_20/r_co_20)/k_cem +...
%              log(r_ci_20/r_co_13)/k_cem)*(T_prev-T_wb_20));


    %B Annulus calculations
    %View factor based on outside tubing and inside casing surfaces,
    %dimensionless
    F_tci=1/((1/e_co)+((r_co_9/r_ci_13)*(1/e_ci-1)));
    %Heat transfer for radiation in B-annulus, Btu/hr sq ft F
    %Temperatures i Rankin (T(R)=T(F)+460)
    h_r2=SB*F_tci*((T_co_prev+460).^2+(T_ci_13+460).^2)*...
        ((T_co_prev+460)+(T_ci_13+460));

    %Temp in Annulus B, F
    T_an2=(T_co_prev+T_ci_13)/2;
    %Betta,temp in R
    betta2=1/(T_an2+460);
    %Prandtl number, Pr, dim.less
    Pr2=(cp_an2*my_an2)/k_an2;
    %Grashof number, Gr, dim.less
    Gr2=((r_ci_13-r_co_9).^3*g_hr*rho_an2.^2*...
        betta2*abs(T_co_prev-T_ci_13))/my_an2.^2;
    %Heat transfet for natrual convection in B-annulus, Btu/hr sq ft F
    h_c2=((0.049*(Gr2*Pr2).^(1/3))*(Pr2.^0.074)*k_an2)/...
        (r_co_9*log(r_ci_13/r_co_9));

    %New temperature outside of 9 5/8 casing surface, F
    T_co_new=T_ci_13 + r_to*U_prev/(r_co_9*(h_r2+h_c2))*(T_prev-T_wb_20);
```

```
    %Margin of error in the iterative approach
    if abs(T_co_new-T_co_prev)<1e-10
        while run_whileb>1;
            Counter4b=Counter4b+1;
            %Temperature inside of 9 5/8 casing surface, F
            T_ci_9=T_co_new + r_to*U_prev*log(r_co_9/r_ci_9)/...
                k_csg*(T_prev-T_wb_20);

%             %For the assumption
%             T_ci_9=T_co_new;

            %A annulus calculations
            %View factor based on outside tubing and inside casing
surfaces,
            %dimensionless
            F_tci=1/((1/e_to)+((r_to/r_ci_9)*(1/e_ci-1)));
            %Heat transfer for radiation in A-annulus, Btu/hr sq ft F
            %Temperatures i Rankin (T(R)=T(F)+460)
            h_r=SB*F_tci*((T_prev+460).^2+(T_ci_9+460).^2)*...
                ((T_prev+460)+(T_ci_9+460));

            %Temp in Annulus A, F
            T_an=(T_prev+T_ci_9)/2;
            %Betta,temp in R
            betta=1/(T_an+460);
            %Prandtl number, Pr, dim.less
            Pr=(cp_an1*my_an1)/k_an1;
            %Grashof number, Gr, dim.less
            Gr=((r_ci_9-r_to).^3*g_hr*rho_an1.^2*...
                betta*abs(T_prev-T_ci_9))/my_an1.^2;
            %Heat transfet for natrual convection in A-annulus, Btu/hr sq
ft F
            h_c=((0.049*(Gr*Pr).^(1/3))*(Pr.^0.074)*k_an1)/...
                (r_to*log(r_ci_9/r_to));
```

```
                %Over-all heat transfer coefficient, Btu/hr sq ft F
                U_new=1/(1/(h_c+h_r)+r_to/((h_c2+h_r2)*r_co_9) +...
                 (r_to*log(r_wb_20/r_co_20))/k_cem +...
                 (r_to*log(r_ci_20/r_co_13))/k_cem +...
                 (r_to*log(r_co_20/r_ci_20))/k_csg +...
                 (r_to*log(r_co_13/r_ci_13))/k_csg +...
                 (r_to*log(r_co_9/r_ci_9))/k_csg +...
                 (r_to*log(r_to/r_ti))/k_tub);

%               %For the assumption
%               %Over-all heat transfer coefficient, Btu/hr sq ft F
%               U_new=1/(1/(h_c+h_r)+r_to/((h_c2+h_r2)*r_co_9) +...
%                   (r_to*log(r_wb_20/r_co_20))/k_cem +...
%                   (r_to*log(r_ci_20/r_co_13))/k_cem);

            if abs(U_new-U_prev)<1e-10
                %Inverse relaxation distance, ft
                A=cp_f*W/(2*pi)*((k_e+r_to*U_new*f_t)/(r_to*U_new*k_e));
                %Temperature of flowing fluid, F
                T_new =  T_g + A*(1-exp((-MD_prev+MD_i)/A))*...
                    (-g*sin(degtorad(hor))/(g_c*J*cp_f) +...
                    g_T*sin(degtorad(hor))) + exp((-MD_prev+MD_i)/A)*...
                    (T_prev-T_g_prev);
                break
            elseif  Counter4b==100
                    Counter4b=0;
                    break
            else
                U_prev=U_new;
            end
        end

    else
        T_co_prev=T_co_new;
    end
```

```
    if abs(T_co_new-T_co_prev)<1e-10 && abs(U_new-U_prev)<1e-10
        break
    end
end
disp(['Counter for case 4a:' num2str(Counter4a(end))]);
disp(['Counter for case 4b:' num2str(Counter4b(end))]);
end
```

D.2.2.5 Function for Case 5

```
%%%-------------------------------------------------------------------------%%%
%%%------------------------Master Thesis 2015-------------------------------%%%
%%%---------------------------------Case 5----------------------------------%%%
%%%------------------------Knut Vegard Loebergsli---------------------------%%%
%%%---------Calculation of the overall heat transfer coefficient--------%%%
%%%-----------------and the wellbore fluid temperature-------------------%%%
%%%------------------------Last updated 05.06.15--------------------------%%%
%%%-------------------------------------------------------------------------%%%

% TUpred5 calculates the fluid temperature in case nr.2 by an iterative
% process until convergence is obtained with the guessed and calculated
% U_to.

%%%-------------------------------------------------------------------------%%%


function [U_new, T_new, T_co_new, T_wb_30] = TUpred5(T_prev,U_prev,...
    MD_prev,MD_i,T_g_prev,T_g,hor,T_co_prev,alpha,t,r_wb_30,r_to,k_e,...
    r_co_13,k_cem,r_ci_13,k_csg,r_co_9,e_co,e_ci,SB,cp_an2,my_an2,k_an2,...
    rho_an2,g_hr,e_to,r_ci_9,cp_an1,my_an1,k_an1,rho_an1,r_ti,g,g_c,J,...
    cp_f,g_T,k_tub,W,r_co_20,r_ci_20,r_co_30,r_ci_30);

%Where:
%T_prev=T_f(i-1)
%T_new=T_f(i)
```

```
    %U_prev=U_to(i-1)
    %U_new=U_to(i)
%MD_prev=MD(i-1)
%MD_i=MD(i)
%T_g_prev=T_geo(i-1)
%T_g=T_geo(i))
%hor=HOR(i)
%T_co_new=T_co(i)
%T_co_pres=T_co(i-1)

%Transient time function, dimensionless. Devloped by Ramey (1962)
% f_t=log(2*sqrt(alpha*t)/r_wb_30)-0.29;

%Tranisent time function, dimensionless. Developed by Hasan and Kabir
%(1994)
t_D=alpha*t/r_wb_30;

if t_D>=1e-10 && t_D<=1.5
    f_t=1.1281*sqrt(t_D)*(1-0.3*sqrt(t_D));
else
    f_t=(0.4063+0.5*log(t_D))*(1+0.6/t_D);
end

run_whilea=2;
run_whileb=2;
Counter5a=0;
Counter5b=0;
U_new=10;

while run_whilea>1;
    Counter5a=Counter5a+1;
    %Temperature at cement-formation interface, F
    T_wb_30=(T_prev*f_t + (k_e/(r_to*U_prev)*T_g))/...
        (f_t + (k_e/(r_to*U_prev)));
    %Temperature inside of 13 3/8 casing surface, F
```

```
T_ci_13=T_wb_30 + (r_to*U_prev*(log(r_wb_30/r_co_30)/k_cem +...
    log(r_co_30/r_ci_30)/k_csg + log(r_ci_30/r_co_20)/k_cem +...
    log(r_co_20/r_ci_20)/k_csg + log(r_ci_20/r_co_13)/k_cem +...
    log(r_co_13/r_ci_13)/k_csg)*(T_prev-T_wb_30));

%     %Assuming thermal conducitivty in tubing and casing is high;
%     %T_ti=T_to, T_ci_9=T_co_9, T_ci_13=T_co_13, T_ci_20=T_co_20 and
%     %T_ci_30=T_co_30
%     T_ci_13=T_wb_30 + (r_to*U_prev*(log(r_wb_30/r_co_30)/k_cem +...
%         log(r_ci_30/r_co_20)/k_cem + log(r_ci_20/r_co_13)/k_cem));

%B Annulus calculations
%View factor based on outside tubing and inside casing surfaces,
%dimensionless
F_tci=1/((1/e_co)+((r_co_9/r_ci_13)*(1/e_ci-1)));
%Heat transfer for radiation in B-annulus, Btu/hr sq ft F
%Temperatures i Rankin (T(R)=T(F)+460)
h_r2=SB*F_tci*((T_co_prev+460).^2+(T_ci_13+460).^2)*...
    ((T_co_prev+460)+(T_ci_13+460));

%Temp in Annulus B, F
T_an2=(T_co_prev+T_ci_13)/2;
%Betta,temp in R
betta2=1/(T_an2+460);
%Prandtl number, Pr, dim.less
Pr2=(cp_an2*my_an2)/k_an2;
%Grashof number, Gr, dim.less
Gr2=((r_ci_13-r_co_9).^3*g_hr*rho_an2.^2*...
    betta2*abs(T_co_prev-T_ci_13))/my_an2.^2;
%Heat transfet for natrual convection in B-annulus, Btu/hr sq ft F
h_c2=((0.049*(Gr2*Pr2).^(1/3))*(Pr2.^0.074)*k_an2)/...
    (r_co_9*log(r_ci_13/r_co_9));

%New temperature outside of 9 5/8 casing surface, F
T_co_new=T_ci_13 + r_to*U_prev/(r_co_9*(h_r2+h_c2))*(T_prev-T_wb_30);
```

```
        %Margin of error in the iterative approach
    if abs(T_co_new-T_co_prev)<1e-10
        while run_whileb>1;
            Counter5b=Counter5b+1;
            %Temperature inside of 9 5/8 casing surface, F
            T_ci_9=T_co_new + r_to*U_prev*log(r_co_9/r_ci_9)/k_csg*...
                (T_prev-T_wb_30);

%             %For the assumption
%             T_ci_9=T_co_new;

            %A annulus calculations
            %View factor based on outside tubing and inside casing surfaces
            %dimensionless
            F_tci=1/((1/e_to)+((r_to/r_ci_9)*(1/e_ci-1)));
            %Heat transfer for radiation in A-annulus, Btu/hr sq ft F
            %Temperatures i Rankin (T(R)=T(F)+460)
            h_r=SB*F_tci*((T_prev+460).^2+(T_ci_9+460).^2)*...
                ((T_prev+460)+(T_ci_9+460));

            %Temp in Annulus A, F
            T_an=(T_prev+T_ci_9)/2;
            %Betta,temp in R
            betta=1/(T_an+460);
            %Prandtl number, Pr, dim.less
            Pr=(cp_an1*my_an1)/k_an1;
            %Grashof number, Gr, dim.less
            Gr=((r_ci_9-r_to).^3*g_hr*rho_an1.^2*...
                betta*abs(T_prev-T_ci_9))/my_an1.^2;
            %Heat transfet for natrual convection in A-annulus, Btu/hr sq
ft F
            h_c=((0.049*(Gr*Pr).^(1/3))*(Pr.^0.074)*k_an1)/...
                (r_to*log(r_ci_9/r_to));
```

L

```
            %Over-all heat transfer coefficient, Btu/hr sq ft F
            U_new=1/(1/(h_c+h_r)+r_to/((h_c2+h_r2)*r_co_9) +...
                (r_to*log(r_wb_30/r_co_30))/k_cem +...
                (r_to*log(r_co_30/r_ci_30))/k_csg +...
                (r_to*log(r_ci_30/r_co_20))/k_cem +...
                (r_to*log(r_co_20/r_ci_20))/k_csg +...
                (r_to*log(r_ci_20/r_co_13))/k_cem +...
                (r_to*log(r_co_13/r_ci_13))/k_csg +...
                (r_to*log(r_co_9/r_ci_9))/k_csg +...
                (r_to*log(r_to/r_ti))/k_tub);

%             %For the assumption
%             %Over-all heat transfer coefficient, Btu/hr sq ft F
%             U_new=1/(1/(h_c+h_r)+r_to/((h_c2+h_r2)*r_co_9) +...
%                 (r_to*log(r_wb_30/r_co_30))/k_cem +...
%                 (r_to*log(r_ci_30/r_co_20))/k_cem +...
%                 (r_to*log(r_ci_20/r_co_13))/k_cem);

            if abs(U_new-U_prev)<1e-10
                %Inverse relaxation distance, ft
                A=cp_f*W/(2*pi)*((k_e+r_to*U_new*f_t)/(r_to*U_new*k_e));
                %Temperature of flowing fluid, F
                T_new =  T_g + A*(1-exp((-MD_prev+MD_i)/A))*...
                    (-g*sin(degtorad(hor))/(g_c*J*cp_f) +...
                    g_T*sin(degtorad(hor))) + exp((-MD_prev+MD_i)/A)*...
                    (T_prev-T_g_prev);
                break
            elseif  Counter5b==100
                    Counter5b=0;
                    break
            else
                U_prev=U_new;
            end
        end
```

```
        else
            T_co_prev=T_co_new;
    end

    if abs(T_co_new-T_co_prev)<1e-10 && abs(U_new-U_prev)<1e-10
        break
    end
end
disp(['Counter for case 5a:' num2str(Counter5a(end))]);
disp(['Counter for case 5b:' num2str(Counter5b(end))]);
end
```